INSTITUTO SUPERIOR TÉCNICO
Universidade Técnica de Lisboa

Synthesis and Chemiluminescence Studies of Luminol and Derivatives

Filipe Miguel Cardoso Menezes

Dissertação para obtenção do Grau de Mestre em

Química

Júri

Presidente: Profª Maria Matilde Duarte Marques

Orientador: Prof. Mário Nuno Berberan e Santos

Co-Orientador: Prof. Carlos Alberto Mateus Afonso

Vogal: Prof. Luís Filipe Coelho Veiros

Junho 2010

Acknowledgments

The work herein presented describes my first journey through Chemistry and Natural Sciences fields. The good moments were flavoured as the result of hard work having therefore an extremely special significance. The bad times were interpreted as a lack of knowledge on the system that clearly needed to be fulfilled, being therefore used to increase the desire to know more about luminol. Therefore, the overall result was a great enrichment not only at the professional level but also personally.

Of all people, there are not enough words to recognize the contributions, the scientific advices and all the commitment of my scientific supervisors: Professors Carlos Alberto Mateus Afonso and Mário Nuno Berberan-Santos. For that, for the good moments provided, for the ideas and most of all for their complete availability, I wish to thank both of them. For Professor Carlos Afonso I also wish to acknowledge the support he gave me to attend NMR training courses that without any doubt were essential for my scientific development but also to interpret NMR experiments indispensable to define the course of this work. His good mood in our laboratorial discussions and the enthusiasm he addressed to less satisfactory results were also extremely important to my progress as a future scientist but more importantly, as a person. To Professor Mário Nuno Berberan-Santos I wish to acknowledge all the support given to personally learn how to rationalize the bad results, but especially to the orientation given throughout the work. To both my supervisors I wish also to acknowledge the financial support given that allowed me to assist high quality scientific conferences and to expose my work to the scientific community.

Two other extremely important people in the course of this work were undoubtedly Dr. Carlos Miguel Calisto Baleizão and Professor Luís Filipe Coelho Veiros. To Dr. Carlos Baleizão I wish to acknowledge all his availability and attendance in all spectroscopic studies performed. His personal support and comprehension helped me to prepare myself to some hard situations and played also an extremely important role in my personal development. For Professor Luís Veiros I thank all the availability and promptness to answer all my doubts and questions. The scientific and personal discussions we had along with his good advices were undoubtedly crucial and contributed to the growth of what I believe to be a strong friendship.

These acknowledgments would also be incomplete without referring Graduate Andreia Rosatella for all her support in synthetic work, Undergraduate Pedro Franco Pinheiro for helping me in compound characterization (IR), Graduate Sofia Martins for helping me with some experimental details in spectroscopy studies and also to Graduate Tiago Fernandes that helped me in the characterization of luminol's derivatives chemiluminescence in aprotic media. Still regarding personal support I would also like refer the great contributions of Professor Margarida Salema and my laboratory co-workers (PhD Gema Marcelo, PhD Krassimira Guerra, PhD Nuno Lourenço, PhD Prashant Kulkarni, PhD Raquel Frade, PhD Zeljko Petrovsky, Graduate Alexandre Trindade, Graduate Bruno Martins, Graduate Carolina Carias, Graduate Jaime Coelho, Graduate Leila Moura

and Graduate Tânia Ribeiro), especially Graduate Carlos Monteiro, Master Luís Gomes and PhD Luís Frija.

To all my family (especially mother, father and sister), girlfriend and friends I deeply thank their emotional support and complete devotion during not only this work but also to the rest of my life.

Abstract

Since its synthesis in 1928, luminol has been the subject of several studies mainly due to the strong blue light emission upon specific oxidative conditions. That chemiluminescence property of luminol is so important to the field that this reaction has been widely applied in bio-analytical chemistry, namely biosensors and heavy metal identification. Of all applications, the most relevant one is the identification of haemic iron from cleaned blood-stains.

Even with that favourable background, the search for both more chemiluminescent derivatives and the search for structures with light emission with different colour has not ceased. Both aromaticity extent and introduction of well known chromophores are the most common derivatizations. In this work we have synthesized and analysed the effect of acylation of luminol in the absorption, fluorescence and chemiluminescence properties of the chromophore. The isolated derivatives were N-ethoxy carbonyl luminol, N-trifluoroacetyl luminol, N-benzoyl luminol and two still unidentified compounds obtained with dimethyl carbamic chloride in DMF at both high and room temperatures. The absorption spectra of these compounds were the most affected upon derivatization, appearing new patterns. Fluorescence was also changed but the overall aspect of the spectra was retained in almost all media. As for chemiluminescence, the only observed difference was on the relative intensity that decreased in all luminol derivatives, meaning that the induced substitution brought no chemiluminescence efficiency improvement or shift in emission wavelength.

Besides, luminol's reaction has also been the subject of several mechanistic studies owing to controversial reaction steps. We therefore performed basic photophysical property studies on luminol and on the assigned light emissive species in the chemiluminescence reaction (aminodiphthalate), using MP2 theoretical calculations as background. We concluded that luminol should exist as a mixture of two main tautomers and assigned the relative acidity of luminol's protons. In addition, we studied the nature of the transitions in several protic and aprotic media of which ethanol-methanol mixture is the most relevant one because it allowed us to have access to excitation anisotropies. Therefore, we observed that the experimental data seems not to disagree with the results from our calculations. The last study that we performed was a chemiluminescence decay analysis that showed that the oxidative conditions we used were consistent with a two step mechanism. In summary, besides synthesizing several luminol derivatives that decreased luminol's chemiluminescence and did not change the maximum emission wavelength, we performed basic photophysical properties of luminol and aminodiphthalate, corroborating the results with theoretical calculations.

Keywords: Luminol; Chemiluminescence; Acyl Luminols, MP2, Anisotropy, Chemiluminescence Decay.

Resumo

Desde que foi sintetizado em 1928, o luminol tem sido objecto de diversos estudos devido à sua intensa quimioluminescência azul em condições oxidantes adequadas. Tal propriedade do composto é tão relevante para as áreas envolventes que a reacção tem sido amplamente aplicada em química bio-analítica, nomeadamente em bio-sensores e doseamento de metais pesados. De todas as aplicações, a mais famosa é sem dúvida a identificação de ferro hémico em manchas de sangue limpas.

Mesmo com este panorama geral já de si bastante atractivo, a pesquisa por compostos mais quimioluminescentes e com máximos de emissão noutras regiões do espectro electromagnético visível não tem cessado. As derivatizações mais comuns consistem na extensão da aromaticidade e na introdução de grupos cromóforos já conhecidos. Neste trabalho relatamos assim o efeito da introdução de certos grupos acilo nos espectros de absorção, fluorescência e quimioluminescência do luminol. Os derivados isolados são o N-etóxi carbonil luminol, N-trifluoroacetil luminol, N-benzoil luminol e dois compostos ainda por identificar obtidos por reacção com o cloreto carbâmico de dimetilo em DMF por aquecimento e à temperatura ambiente. Observámos que com a derivatização a absorção era bastante afectada, criando novas distribuições energéticas dos estados excitados. A fluorescência também foi afectada muito embora a forma geral do espectro se mantivesse inalterada. Quanto à quimioluminescência, verificámos que a intensidade de emissão decresceu, indicando que os substituintes introduzidos não só não trouxeram melhoria no rendimento quântico de quimioluminescência como não desviaram o comprimento de onda de máximo de emissão.

Além de estudos de derivatização, por ainda existir controvérsia em alguns passos da reacção, a oxidação do luminol é também objecto de estudos mecanísticos. Neste trabalho abordámos este tema começando por estudos de propriedades fotofísicas do luminol e da espécie tida como responsável pela emissão observada (aminodiftalato), tendo como suporte cálculos teóricos *ab initio* MP2. Verificámos que o luminol deve existir como uma mistura de dois tautómeros preponderantes e atribuímos ainda a acidez relativa dos protões da molécula. Estudámos também a natureza das transições electrónicas em solventes próticos e apróticos dos quais se destaca uma mistura de etanol e metanol que nos permitiu aceder a anisotropias na excitação. No global, recolhemos dados experimentais que não discordam dos métodos teóricos por nós utilizados. Por fim estudámos o decaimento de quimioluminescência que mostrou que nas condições experimentais que utilizámos o luminol tinha cinética de oxidação concordante com um mecanismo de dois passos. Assim, além de termos sintetizado diversos derivados do luminol que não só decresceram o rendimento quântico de quimioluminescência como não alteraram o comprimento de onda de emissão máxima, estudámos algumas propriedades fotoquímicas do luminol e correspondente aminodiftalato comparando estes com os resultados de cálculos teóricos.

Palavras-Chave: Luminol; Quimioluminescência; Acil Luminóis, MP2, Anisotropia, Decaimento de Quimioluminescência.

Index

Tables Index

complexity of the reaction mixture (T for TLC and N for NMR). Whenever NMR spectra were collected, TLC analysis was also performed.

5. Computational Chemistry

Diagrams and Figures Index

1. Introduction

2. State of the Art

3. Experimental Section

4. Experimental Work

5. Computational Chemistry

6. Spectrocopic Studies

Abbreviations

Ac	Acetyl group;
ADP	AminoDiPhthalate;
AMP	AminoMonoPhthalate;
APA	AminoPhthalic Acid;
APT	Attached Proton Test;
Atm	Atmosphere (pressure unit);
a. u.	Arbitrary Units;
Bn	Benzoyl group;
BnLum	Luminol's benzoyl derivative;
^{n}Bu	Normal butyl group;
^{t}Bu	*Tert*-butyl group;
COSY	Correlation Spectroscopy. 2D NMR spectroscopy experience;
CPD	Composite-Pulse Decoupling;
d	Duplet;
DCM	Dichloromethane;
DMAP	DiMethyl Amino Pyridine;
DMF	N,N-DiMethylFormamide;
DMSO	DiMethyl SulfOxide;
DMU1Lum	First compound isolated with conditions to obtain dimethylamine-luminol urea;
DMU2Lum	Second compound isolated with conditions to obtain dimethylamine-luminol urea;
ECLum	Ethyl carbamate luminol derivative;
ES	Excited State;
Et	Ethyl group;

GC Gas Chromatography;

GS Ground State;

HF Hartree-Fock;

HOMO Highest Occupied Molecular Orbital;

HPLC High Performance Liquid Chromatography;

***i*Lum** Isoluminol;

IR InfraRed spectroscopy;

Lum Luminol;

LUMO Lowest Unoccupied Molecular Orbital;

m Multiplet;

M Molar;

Mmol millimol;

nM Nanomolar;

Me Methyl group;

MP2 Second order Möller-Plesset perturbation theory;

MS Mass Spectrometry;

NMR Nuclear Magnetic Resonance;

^{1}H NMR Proton's Nuclear Magnetic Resonance;

^{13}C NMR Carbon 13 Nuclear Magnetic Resonance;

^{19}F NMR Fluorine 19 Nuclear Magnetic Resonance;

PES Potential Energy Surface;

Ph Phenyl group;

Pr Propyl group;

^{i}Pr Isopropyl group;

Py Pyride;

q Quartet;

Rf	Retention factor;
ROS	Reactive Oxygen Species;
s	Singlet;
S_j	j^{th} electronic singlet state;
SPE	Single Point Energy calculations;
t	Triplet;
TEA	Triethylamine;
TFALum	Trifluoroacetyl luminol derivative;
THF	TetraHydroFuran;
TLC	Thin Layer Chromatography;
TMS	Trimethylsilyl;
UV/Vis	UltraViolet/Visible;
X-Ray	X-Ray Diffraction (Crystallography);

1 - Introduction

Since the beginning of mankind, light emission phenomena have been described and associated to mythological and cultural events. Luminol (Figure 1.1), synthesized in 1928 in the pioneering work of Albrecht,[1] is a strong chemiluminescent compound (the energy released as a photon comes directly from a strong exothermic reaction) characterized by blue light emission upon oxidative conditions. The process itself is quite useful and attractive, especially for analytical applications. Besides heavy metal quantification (for instance, copper can be detected in sub-nM concentrations),[2] *in vivo* analytical chemistry and biosensors, chemiluminescence analysis also account with simple instrumentation, low detection limits, large calibration range and short analysis time.[3] Therefore, chemiluminescence has been widely used in areas such as pharmaceutical, environmental or even life sciences.[4] It is worth reminding that luminol's most known application is in crime scene investigations, used to identify cleaned bloodstains from materials (residuals of haemic iron). This application is widely spread in television shows like "Crime Scene Investigation", commonly known as "CSI".

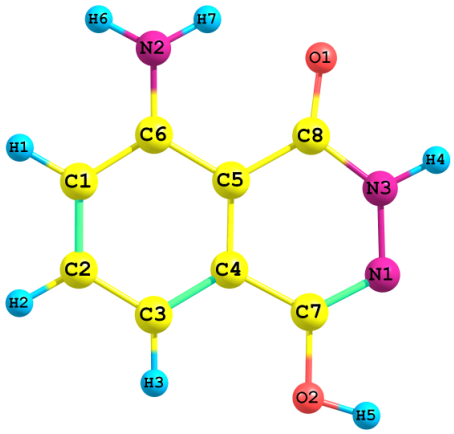

Figure 1.1: Luminol structure obtained by MP2/6-31G(d,p) optimization.

Due to the relevance of some of its applications, several groups have searched for some luminol derivatives trying not only to maximize the chemiluminescence quantum yield of this compound (in order to intensify the photon emission) but also to expand the range of emission wavelengths in the visible region of the electromagnetic spectrum. Even though some of the experiments have been quite successful, the study of this phenomenon is far from being exhausted, not only because there are no strong enough chemiluminescent structures for each specific region of visible wavelengths (green, yellow, red, ...) but also because the oxidation mechanism is not still completely understood and established.

In this work we have studied the effect of acylation of luminol into chemiluminescence parameters, namely maximum emission wavelength and chemiluminescence quantum yield, as well as in the photophysical properties of the chromophore. For this purpose, several acylating agents are

analysed, having each of these acyl substituents a specific stereoelectronic character to cover the widest range of effects in the compounds chemiluminescence. The main types of acylants used were saturated perfluorocarboxylic acid, an unsaturated acyl group (with aromatic ring), a carbamate and a urea. To achieve a better comprehension of the whole phenomenon, spectroscopic studies on luminol and its derivatives absorption and fluorescence are also performed. Besides, the effect of the position of the luminol aniline group (N2, H6 and H7 from Figure 1.1) is evaluated in absorption, fluorescence and chemiluminescence spectra. Finally, the properties of light emissive species in luminol's chemiluminescent reaction, aminodiphthalate, are studied. To aid the quest of obtaining a luminol derivative with stronger chemiluminescence and maximum emission wavelength in another spectral region (the optimal case would be in green), theoretical calculations results are compared to experimental results to evaluate their ability to predict some properties of these structures.

In summary, the work will be mainly divided into seven main sections. After this Introduction section 2 presents a global State of the Art; section 3 is an experimental section that deals not only with instrumental part (device description), experimental set ups and conditions but also with luminol's acyl derivatives preparation (synthetic work) and their spectroscopic characterization (structural analysis, *i.e.*, IR and NMR); the fourth section is an experimental synthetic work one, a collection of small texts that cover all the synthetic work performed not only to isolate the acyl derivatives of luminol whose synthesis are presented in section 3 but also others yet to be isolated; section 5 deals with computational calculations where several theoretical methods are evaluated in their ability to describe luminol's system, being then applied to study luminol's tautomerism and proton acidity; the sixth section deals with spectroscopic studies, namely absorption, fluorescence and chemiluminescence, of luminol, isoluminol and its acyl derivatives (whose synthesis are described in the first section). The aminodiphthalate absorption and fluorescence in water is also presented, being chemiluminescence decay analysis the last subject of the section, allowing the estimation of the chemiluminescence quantum yields for synthesized derivatives; the final section, seventh, presents a global set of conclusions. Besides this generic scheme, a small and more specific introduction is present along with a summary of conclusions, when necessary. In Figure 1.2 is the outline of the dissertation with arrows that establish the connection between sections (Introduction and Conclusions are not considered). The description provided in this figure does not have any relation with the selected presentation order.

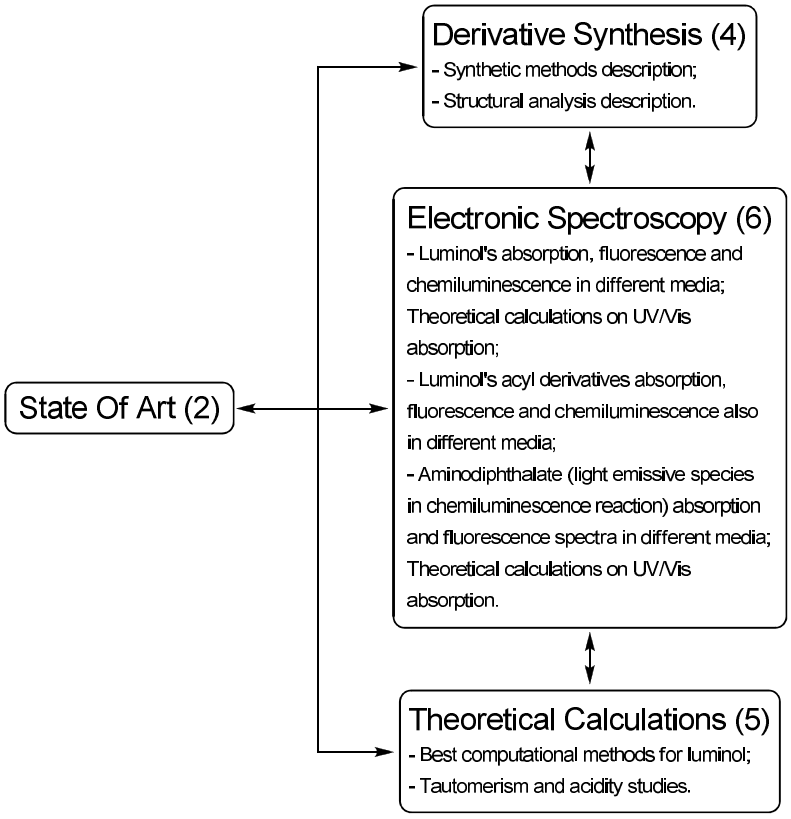

Figure 1.2: Dissertation outline. In brackets is the number attributed to each section.

With respect to the nomenclature used, we chose not to follow IUPAC's nomenclature for organic chemistry, last revision (1993).[5] The reason for this choice is because the substituents introduced in luminol are all in the same functional group. It is thus convenient to adapt a simpler way to identify compounds. Nevertheless, the IUPAC name of each isolated compound is written in the respective section.

2 - State of the Art

Luminol's oxidation reaction may proceed in several different conditions exhibiting, according to media's properties, particular features. Figure 2.1 presents a generic scheme for luminol's oxidation that is usually accepted to be valid for all known conditions.[3]

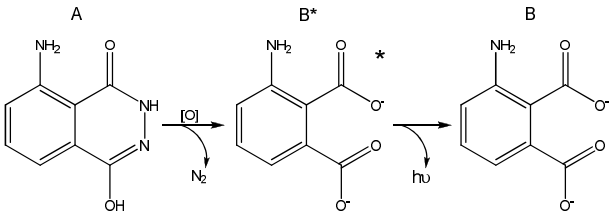

Figure 2.1: Generic scheme for luminol's oxidation reaction.

As Figure 2.1 shows, upon suitable conditions (that typically include an oxidant species and alkaline media), luminol (species A) is oxidized to aminodiphthalate (species B). The reaction pathways can be numerous but to have light emission, the reaction should proceed in such a way that when the aminodiphthalate is formed it is in an electronic excited state (B*) that will then return to its ground state, possibly accompanied with light emission. The formation of that excited state would therefore be a result from the accumulation of the energy from an extremely exothermic reaction step in one chemical species.[3]

Of all possible media, the most important one to study the oxidation of luminol is water, mainly because it's most relevant applications are biology related.[3] In this solvent, the maximum emission wavelength is typically around 430 nm (it depends slightly on the conditions). Besides water, several other conditions are known. Some results for maximum emission wavelengths of this oxidation reaction are presented in Table 2.1.

Table 2.1: Maximum emission wavelength for luminol's chemiluminescence in different media according to different authors with each solvent polarity. Chemiluminescence quantum yields (Φ_{CL}) are also presented for some media.

Solvent	λ_{max} (nm)	Φ_{CL}	Dielectric Constant[6]
H_2O	431 [3], 425 [6], 470 [8]	0.01 [6,9]	80
DMSO	502 [3], 480-502 [6]	0.05 [6,9]	47.2
DMF	499 [3]	---	38.3
MeCN	500 [3]	---	36.6
THF	496 [3]	---	7.52

From this table, we verify that the emissive species obtained by luminol's oxidation, aminodiphthalate (B in Figure 2.1), exhibits positive linear slope in the plot of wavelength for maximum emission with each solvent's polarity.[3] This means that, when enhancing the polarity of the media, the light emission is red shifted, being the excited state structure more stabilized than the correspondent ground state. Therefore, we can state that upon one electron excitation, the

aminodiphthalate species acquires such a molecular geometry and charge distribution that the dipole moment is slightly increased. The tenuous effect of solvent's polarity in the maximum emission wavelength and the observed trend in the shift are both in agreement with an electronic excited state from a $\pi\pi^*$ transition. The other result from this table is the fact that in water, instead of a red shift, an abnormal blue shift is verified. This shift can be rationalized by hydrogen bonding effect (this is the only polar protic solvent presented in the table). The critical change in light emission indicates that this parameter will play a central role in the stabilization (and therefore emission) of the excited state structure formed in this oxidation reaction. Because the emission is blue shifted in water, hydrogen bonding will destabilize the excited state's structure more than it affects (both stabilization and destabilization can occur) the electronic ground state for the same species, at least when compared to other solvents presented in the study. A hypothesis for this result is that with protic solvents, the intramolecular hydrogen bond in the amino moiety will be substituted (weakened) by hydrogen bonding with the solvent, leading to smaller stabilization of each molecule. Besides, the presence of intermolecular hydrogen bonding may also change the character of the electronic excited states of this compound. One possible example is the introduction of $n\pi^*$ character in the transition that would also account for all the observed events.

Another parameter quite important to this study is the chemiluminescence quantum yield (see also Table 2.1). By definition, the chemiluminescence quantum yield (Φ_{CL}) is the product of fluorescence quantum yield of the light emissive species (Φ_F) with the yield for the reaction (Φ_{RX}) that ends with formation of the excited state species (Φ_{ES}), *i.e.*,

$$\Phi_{CL} = \Phi_{RX}\Phi_{ES}\Phi_F \qquad (1)$$

The chemiluminescence quantum yield is therefore a measure for the light emission efficiency of the reaction itself. According to Table 2.1, luminol's light emission efficiency is only 1 % in water, being 5 times higher in DMSO. While some hypotheses to rationalize these results are related to the catalytic decomposition of the oxidant species by the metal ions present in aqueous media (that will allow other non-chemiluminescent, dark, reaction pathways)[11] it is also proposed that the intramolecular hydrogen bond (amino group and the closest carboxyl) is weakened in such a way in aqueous media that the conformations of the reaction intermediates along the reaction pathway are "negatively affected", decreasing therefore the efficiency for the formation of the excited state species (Φ_{ES}).[12] This conformational effect is assumed to influence the crossing for the excited state potential energy surface (PES).

From this same parameter, substituent effects can be partly studied. According to the literature, electron releasing substituents enhance the chemiluminescence quantum yield in luminol and related structures because the slope for the correspondent Hammet equation (chemiluminescence efficiency Vs. substituent electronic effect) is negative.[11] Thus, the chemiluminescence quantum yield can be predicted for monosubstituted luminols with some accuracy using physico-chemical methodologies (Figure 2.2 with R=NH_2 and two other R_j groups as protons).

For poly-substituted structures, the predictability is not accurate, *i.e.*, substituent effect additivity is not observed.[12] Table 2.2 presents schematically some of those results that will also be analyzed.

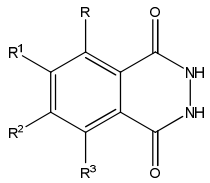

Figure 2.2: Generic structure for cyclic hydrazides subject to study in this work.

Table 2.2: Effect of some substitutions in luminol structure. A plus (+) in the chemiluminescence column (CL) stands for chemiluminescence increase while a minus (-) for a decrease. In this column, zero stands for complete loss of chemiluminescence. R in the maximum emission wavelength column (M.E.) stands for red shifting. In brackets may be (when quantified) the shifting value or the chemiluminescence colour. The signal of the shift is negative for blue shifting and positive for red shifting. Here zero will stand for no shift. When present, R_4 will stand for an alkyl group.

Substituents	CL	M.E.
$R=NH_2$; R_2,R_3=OMe; R_1=H/OMe [10]	+	
R,R_2,R_3=H; R_1=NEt_2/pyrrolidine [9]	+	
R,R_2,R_3=H; R_1=NH_2 [13]	- (1-10 %)	0
R_1,R_2,R_3=H; R=H/Me/NO_2/Cl [10]	0	
R_1,R_2,R_3=H; R=OH [10]		R (yellow)
$R=NH_2$; R_1,R_2=H; R_3=NH_2/OMe [10,15]	0	
R_1,R_2,R_3=H; R=R_4CONH [8,16]	- (5-10 %)	R
$R=NH_2$; R_1,R_2=H; R_3=^{i}Pr/CH_2OMe [12]	-	
R_1,R_3=H; R2=^{t}Bu; R=NH_2 [12]	-	

Perhaps some of the most interesting examples are, for instance, when $R=NH_2$, R_2, R_3=OMe and R_1=H or OMe.[10] The compounds get much more efficient than luminol in light emission. Other examples of luminol derivatives more chemiluminescent than luminol are with R, R_2, R_3=H and R_1=NEt_2, pyrrolidine[9] and $R=NH_2$, R_1, R_2=H and R_3=Me, Pr. The maximum emission wavelengths for the last two compounds (with methyl and propyl substituents) are blue shifted towards luminol.[12]

When R, R_2, R_3=H and R_1 is NH_2 (isoluminol) the chemiluminescence quantum yield decreases 10-100 times towards luminol itself.[13] In respect to luminol's isosters (according to Erlenmeyer's definition), when the amino group in position R is substituted by H (phthalic hydrazide), Me, NO_2 or Cl, the compounds lose completely their chemiluminescence.[10] In the first example of these non-chemiluminescent species, when in water and with typical chemiluminescence conditions, a yellow light emission is sometimes observed,[10] being those emitted photons assigned to an hydroxyl derivative formed within the reaction media. This is in agreement with the fact that in aprotic media the phthalic hydrazide itself does not yield any chemiluminescence.[14]

Other non-chemiluminescent species but rather curious examples are the luminol derivatives with $R=NH_2$, R_1, R_2=H and R_3=NH_2, OMe. According to what has been previously referred about the substituent electronic effect, these structures should exhibit at least luminol's chemiluminescence.

According to the authors, the aromatic moieties of these compounds are so electronically rich that the oxidant tends to react with these rings forming non-chemiluminescent quinone structures.[10,15] From this result we conclude that the electronic density in the aromatic ring of luminol and its derivatives will play a very special and specific role in the chemiluminescence reaction. Also from these examples can be concluded that light emission phenomena is related to the heterocyclic moiety of this family of compounds.

Another type of substitution that usually decreases the chemiluminescence quantum yield is luminol's aniline-N substitution.[17] Several examples are already known and worth denoting are acyl derivatives that show 5-10% of luminol's chemiluminescence, being the maximum emission wavelength slightly red shifted.[8,16] The so far known luminol acyl derivatives are all composed of saturated alkyl groups bonded to the carboxyl functionality (luminol's acetamide and propylamide)[8], fatty acid derivatives (luminol's undecenylamide)[8] and the succinyl derivative.[16] Alkylation of the aniline functionality also decreases the chemiluminescence quantum yield.[9,10] To account for it, both conformation and hydrogen bonding may be negatively affected by that type of substitution. Curiously, the same type of substitution in isoluminol (alkylation) enhances its chemiluminescence properties.[9,10] Besides, it is also known that some isoluminol derivatives whose aromaticity was extended or that have known chromophores attached to the main structure can reach chemiluminescence intensities 3100 times higher than the one exhibited by luminol.[18,19] Figure 2.3 B presents this last luminol derivative.

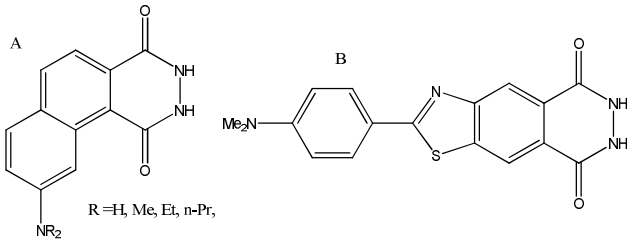

Figure 2.3: Some luminol derivatives whose aromaticity was extended or some known chromophores were attached. While A is a representative structure for aromaticity extent[10], B is the derivative with chemiluminescence intensity 41 higher than luminol.[18]

Other examples of luminol derivatives less efficient in chemiluminescence are the compounds with R=NH_2, R_1, R_2=H and R_3=^{i}Pr, CH_2OMe and the luminol derivative with ^{t}Bu substituent in the *meta* position to the amino functionality. These last examples seem to be evidence for the role of sterical hindrance and molecular conformation to the quantum yield for excited state formation (Φ_{ES}). All these structures have emission slightly blue shifted towards luminol.[12]

In respect to the heterocyclic moiety, its derivatives and substitutions usually render the compounds non-chemiluminescent.[10] Compounds like the ones presented in Figure 2.4 are just some examples. Plausible rationales for the loss of chemiluminescence are inhibition of nitrogen release and/or inhibition of any other step in this oxidation reaction mechanism.

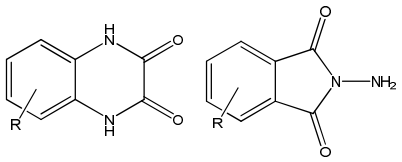

Figure 2.4: Non-chemiluminescent luminol isomers.

As for aromaticity, two main effects usually arise. The first is red shifting of the maximum emission wavelength.[9,10] The second is that with aromaticity extension the light emission efficiency of the compound is enhanced (several examples are provided in Figure 2.3 A).[10,17,20] The former result may be easily rationalized using simple arguments from molecular orbital theory and results from photophysics. It is well known that when electron delocalization is extended, the energy gap between the frontier molecular orbitals (especially the highest occupied molecular orbital, HOMO, and the lowest unoccupied molecular orbital, LUMO) tends to decrease. Because these molecular orbitals are usually the most relevant ones for this type of electronic transitions, at least the first two singlet electronic states will be energetically closer. When that happens, the potential energy surfaces for those states tend to be more entangled, *i.e.*, for more molecular geometries the energetic degeneracy of the two electronic states is enhanced, leading to enhanced probability of PES crossing. When that probability is enhanced, the yield for excited state formation is increased and globally, if the chemical reaction yield remains almost the same, the chemiluminescence quantum yield is also increased. Besides, aromaticity extension also increases the $\pi\pi^*$ character of electronic transitions. Due to the high oscillator strengths typically associated with the radiative transitions between $S_1 \xrightarrow{\pi\pi^*} S_0(\pi\pi^*)$ we can also rationalize the enhancement of chemiluminescence quantum yield of aromaticity extended luminols by increase in fluorescence quantum yield (Φ_F) of the light emissive species (the correspondent aminodiphthalates). So far, the most efficient luminol derivative was obtained by aromaticity extension (Figure 2.3 A).[20]

To account for the amino group position effect in the chemiluminescence quantum yield and the trends observed from phthalic hydrazide to luminol (and isoluminol) and from luminol to its methoxy derivatives, we need to look closer to luminol and its isomer. Because their chemiluminescence quantum yield is completely different, the effect, present in luminol but absent in phthalic hydrazide cannot be merely justified by mesomeric effect. Therefore, phthalic hydrazides need an *ortho* effect to exhibit chemiluminescence.[21] This result is in agreement with the proposal that phthalic hydrazide only exhibits chemiluminescence after hydroxyl radical oxidation (in *ortho* position). In respect to the latter compounds, luminol's methoxy derivatives, the effect may be merely mesomeric because the *ortho* amino group is present and several types of substitution yield similar results. In respect to the nature of the groups *ortho* to hydrazide moiety, some authors also refer that if they are ionisable, the *ortho* effect may be enhanced.[20]

As for the chemiluminescence reaction conditions, as previously referred, two classes may be recognized. The first is in protic polar solvents (like water). Typically the system needs peroxides as oxidants, a metal ion or one of its complexes as "catalyst" (*cf.* below for the discussion regarding the

role of metal ions and their complexes in luminol's oxidation in protic media) and alkaline media. In the second case, aprotic polar solvents, only base and molecular oxygen are needed.[10,22]

The hydroxyl anion (or any other alkaline species) effect is to enhance the chemiluminescence quantum yield. The chemiluminescence efficiency increases as the pH increases until it reaches the value of 11.5 in water. When the pH is higher than 12, the chemiluminescence quantum yield tends to decrease once again.[23] In DMSO, addition of two equivalents of base typically maximize the chemiluminescence light emission intensity.[6] As for reaction kinetics, the aqueous oxidation of luminol follows a first order kinetics on base if the pH of the medium is lower than 13.[24] In some conditions where the reaction's speed have been conveniently slowed down, the aqueous oxidation of luminol exhibits zero order kinetics in respect to base but the chemiluminescence quantum yield is increased when the concentration of those reagents is increased.[25] The latter observation is evidence for change in reaction's rate limiting step. For aprotic solvents the reaction rate follows a second order kinetics on base.[25] This leads directly to the next point of this review: the light emissive species.

Due to the secondary order kinetics in aprotic media for luminol's chemiluminescence, every author refer that the dicarboxylate of the aminophthalic acid (aminodiphthalate) is the light emissive species (Figure 2.1 B*).[22,24,26] In aqueous media, due to the first order kinetics in hydroxyl anion, some authors state that the light emissive species may be the aminomonophthalate (monoprotonation of the structure in Figure 2.1 B*).[23,27] In any case, luminol's chemiluminescence spectra are only consistent with the fluorescence spectra of the aminodiphthalate (dianion).[26]

To be consistent with the fluorescence data, the authors defend that the emission by the aminomonophthalate in photophysical conditions is subject to a hydrogen bonding effect inexistent in chemiluminescence conditions. This proton, in the former conditions, would be located between the two carboxyl groups from the ground state, structure therefore unachievable in the chemiluminescence media because the time necessary to form that 7 member ring species was much higher than the lifetime of the excited state species. The light emission of the aminomonophthalate would therefore be similar to the one exhibited by the aminodiphthalate.[27] In either case, it is well established that the electronic state responsible for the light emission is the first excited singlet.[10,26,28] Besides, it is also proposed that the light emission efficiency is directly related to the molecular geometry of the immediate precursor of the dicarboxylate in the excited state. Being that true, the proposed conformational effect of hydrogen bonding in luminol's chemiluminescence would be completely justified and, therefore, the closest that precursor species is to the first singlet excited state (S_1) equilibrium geometry of the aminodiphthalate, the highest is the expected chemiluminescence emission quantum yield.[10] This statement can be also rationalized by means of potential energy surfaces crossing, because the closer the geometries (and energies), the higher the superposition of those two PES.

In respect to the oxidants used in both systems, molecular oxygen (O_2) should be always present. In aprotic polar media this is the oxidant itself that turns luminol to reaction intermediates and

then these to the aminodiphthalate (ADP). It is also known that in DMSO one O_2 molecule is needed to oxidize each luminol dianion present in the media.[27] In order to prove the relevance of this oxidant in the referred media, White and co-workers prepared alkaline solutions of luminol in both DMSO and DMF showing that those solutions were stable for a long periods of time if molecular oxygen was completely absent from the media. The authors went even further stating that those same solutions would be indefinitely stable if those conditions were verified.[22] Moreover, luminol's dianionic conjugate bases salts (in solid state) exhibited chemiluminescence when exposed to molecular oxygen, being those same salts indefinitely stable in anoxic media.[10] On the other hand, the analogous monosodic luminol salts exhibited stability to molecular oxygen and only when one equivalent of alkaline substrate was added (in solution) they started exhibiting chemiluminescence (maximum emission was observed when one base equivalent was added). Those same authors have also shown that O_2 adds to luminol in the heterocyclic moiety by using $^{18}O_2$ in the oxidation process. The isotopic oxygen atoms corresponded to 50% of the oxygen atoms in the aminodiphthalate, product of the luminol oxidation (the species responsible for the light emission according to almost all authors).[22,25] Therefore, when in oxic media, luminol's dianions will tend to form an adduct with O_2 that will further rearrange and form the aminodiphthalate species, releasing during this chemical transformation one molecule of N_2 for each molecule of luminol's dianion oxidized.[28] The formation of a triplet species that will generate the excited structures was also proposed by those same authors. According to the literature, with molecular oxygen, luminol's oxidation in DMSO has a rate constant (rate limiting step) of 50 $M^{-1}.s^{-1}$.[6]

To clear which reactive oxygen species reacts with luminol in light emissive pathways, studies with singlet oxygen reacting with luminol, coined as the type II oxidation, were undertaken. According to those sources, this reaction is extremely fast but dark. In order to have light emission, luminol derivatives should react with triplet molecular oxygen or, when in water, with the superoxide anion. Reactions of luminol with superoxide and $^3O_2$ were therefore coined together as type I oxidation.[29] Also according to the same reference, the luminol species that is most reactive with superoxide is its monoradical anion. No more studies on this subject were performed both in DMSO and water. Therefore, whichever the reactive oxygen species that decomposes luminol in light emission pathways is, the general opinion is that in both protic and aprotic media, the rate of the reaction is first order on oxidant.[25] If only reactions of luminol (or one of its derivatives) with superoxide (or $^3O_2$) are able to yield the aminodiphthalate in an excited state then radicalar species should be present both in protic and aprotic luminol oxidation reactions. While in aqueous oxidations of luminol a strong EPR signal is typically observed, in aprotic solvents, base and molecular oxygen no EPR signal is observed even at -60 ^oC.[10]

As for the range of oxidants, in aqueous conditions, it can be extremely vast. This in part justifies the wide applicability of these conditions in analytical chemistry. The reagents include hydrogen peroxide (H_2O_2), oxygen, potassium permanganate, nitric oxide (NO) and oxygen free radicals such as the referred super oxide anion (O_2^-) and hydroxyl radicals (OH).[4] When peroxides and/or superoxides are used, typically metal ions are fundamental to observe chemiluminescence.[9] At

least one exception is known to that rule, being that Rauhut and co-workers conditions.[25] That system uses hydrogen peroxide and potassium persulphate as oxidants. This system is also an exception because allylic alcohol does not seem to inhibit the reaction's rate, being this evidence for two electron oxidations of luminol in that specific system.[25]

In respect to general systems that use peroxides as oxidants, the need for molecular oxygen is peroxide dependent. When a peracid is used, strong chemiluminescence is observed even in anoxic media. With other peroxides, especially aliphatic, removal of molecular oxygen decreases the chemiluminescence quantum yield or completely silences that light emissive process.[11]

In the same type of oxidation conditions (aqueous) the superoxide radical anions are usually formed and essential to observe light emission.[6] Its formation is usually assigned to molecular oxygen's monoelectronic reduction.[31]

The last ROS present in the aqueous media capable to oxidize luminol and its electronic/ionic derivatives worth mentioning is the hydroxyl radical. When irradiated, a luminol sample will show new peaks in the ^{1}H NMR spectrum, resultant from hydroxylation of the aromatic ring.[14] This is an indication that the hydroxylation of luminol is extremely favorable when the hydroxyl radical is present and in the aqueous oxidation of luminol it has been proved that this radical is present (scavenging studies).[11] In those conditions, the referred ROS tends to add to the aromatic moiety of luminol rendering non-luminescent species (the quinone structures referred previously in the substituent effects analysis).[11,14,23]

As for the metal ion role, in order to induce chemiluminescence, once again we have several species to choose from. Lists of several metal ions are published in the literature[3] being the most widely used the iron derivatives, either in the form of its cyano complexes (for instance K_3FeCN_6), metallic porphyrins or inserted in some enzyme.[11,30,32] Regarding the role of the heavy metal species, it is still not completely understood. Some authors refer that it has catalytic activity in monoelectronic oxidations of luminol and non-catalytic activity in two electronic oxidations[24] while others refer solely to its non-catalytic activity.[23] In any case it has been reported that the metal ion order in the reaction rate is smaller than one and that aqueous alkaline solutions of luminol and metal ions without O_2 are non-chemiluminescent. If O_2 is later introduced to those systems, no chemiluminescence is also observed, meaning that luminol was indeed consumed in non-radiative reaction pathways. Besides, it appears that the metal ion does not quench luminol's chemiluminescence.[24]

In respect to luminol itself in the oxidation conditions, the reaction is generally divided in two main parts. The first one, the slowest, starts from luminol to end up in a α-hydroxy-peroxide or the respective endoperoxide (Figure 2.5). The species formed is media dependent. While the endoperoxide is usually assigned to aprotic conditions (molecular oxygen addition), the other structure is assumed to be a key intermediary in protic solvents (addition of hydrogen peroxide or superoxide radical to some luminol degradation intermediary). Both are also assumed to be extremely reactive because their existence is still to be proved.[31] Therefore, due to the relative kinetics (towards

the second part of the oxidation), the first reaction steps are the most sensible to chemical conditions, namely pH, system composition and chemical nature of the involved species.[31] The second part of luminol's oxidation is the decomposition of these intermediates, a set of reaction steps that strictly depend on the system's pH.[31] This independence upon other composition parameters is directly related to the rate of this set of steps. It is reported in the literature that luminol's oxidation is extremely fast even at -60 °C.[3,22] Because the dependence of the chemiluminescence quantum yield with temperature is quite small, it has been proposed that the activation energies for each set of reaction steps should be approximately the same, being the activation energies for the second part of the mechanism much smaller than in the first part (no intermediates have been isolated or undoubtedly identified).[27] Whichever the conditions are, the chemiluminescent species (similar in both systems) is one the previously referred aminophthalic acid base conjugates, presented in Figure 2.1.[33]

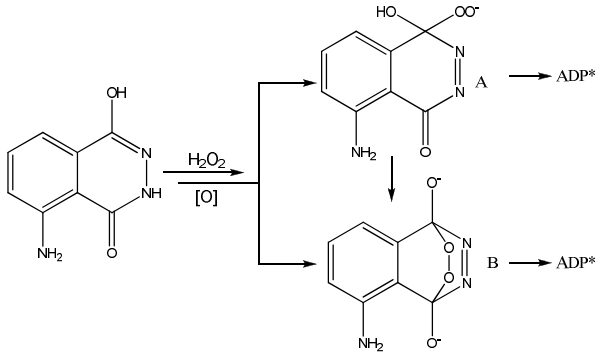

Figure 2.5: A α-hydroxy-Peroxide and B endoperoxide, intermediates in luminol's oxidation reaction.

In order to know how the system behaves to, starting from luminol, reach the key intermediates in Figure 2.5 and then to end up in the aminodiphthalate, several kinetic and synthetic studies have been performed.

The first to report were acid/base ones. Apparently some inconsistencies appear in the literature because several (distinct) pK_a values are reported for luminol (*cf.* Table 2.3).

Table 2.3: Luminol pK_a's.

pK_{a1}	pK_{a2}	pK_{a3}
1.46 [14]	6.35 [14]	15.21 [14]
6.3 [34]	10.4/~13 [34]	---
~6 [24]	~13 [22]	---

But not only the pK_a values are inconsistent. Lack of agreement is present in the acidity order of luminol's protons. The only thing in common is the general idea that the protons from the amine moiety are relatively stable and are the less acidic.[10] By ^1H NMR studies it has been observed that the hydrazide protons had variable width in their peak but also that the aniline moiety interacted strongly with water protons.[14] The same authors also refer that the lability of the hydrazide protons should be high enough to allow keto-enolic tautomerism in some solutions, result observed in some NMR

studies. It should be denoted here that the crystallographic structure of luminol exhibits the hydrazide functionality in the *meta* position to the amino group tautomerized in the enolic form, as shown in Figure 2.1, structure A.[35]

According to the literature, when two base equivalents are added to a solution of luminol in aprotic solvent, the chemiluminescence quantum yield is maximized. Assuming that the equilibrium situation is characterized by having luminol without its two most acidic protons, the most reactive luminol species in aprotic media should be the dianion derivative.[36] The oxidation of this dianionc species by molecular oxygen (or any other non-radicalar ROS formed in the media) to generate the most reactive intermediates is expected to be the rate limiting step for the whole process.[10] It should be denoted once again that the oxidation should be induced both by triplet or singlet molecular oxygen (the last one generated by quenching of some aminodiphthalate in an excited electronic state).[10] After this process, the previously referred endoperoxide intermediate should be formed, being its decomposition to aminodiphthalate extremely fast and "invisible" to current technology equipment. Like it is shown in Figure 2.5 B, this species has two extremely labile functionalities. One is the endoperoxide moiety, known to decompose rapidly to yield carbonyl (or, in this case, carboxyl) groups while the other is the endodiazo functionality. The decomposition of the formerly referred functionality in luminol can proceed in a concerted fashion with a six member ring transition state with aromatic character. To be more precise, the decomposition of the endoperoxide functionality can be considered as a retro [6π] electrocyclic reaction, extremely favorable. As for the other labile functionality, the endodiazo functionality, analogously to the endoperoxide moiety, it may release molecular nitrogen in a retro [4+2] cycloaddition reaction that also goes in a concerted fashion with cyclic and aromatic transition state. Whichever bond breaking controls the decomposition of this intermediate of luminol's oxidation, it is in this step that the excited state of the aminodiphthalate is proposed to be formed, right after the O-O bond cleavage.[3] Still regarding this step it is worth denoting that some authors propose a non-concerted release of molecular nitrogen with the peroxide bond cleavage. Therefore, these authors propose an extra intermediate in this process (with an extremely small lifetime) that would rapidly form the light emissive species.[25,27]

Regarding the aqueous oxidation, some authors consider that the α-hydroxy-peroxide intermediate can decompose immediately to the excited state species without forming the endoperoxide. According to them this is a direct consequence of the extremely low activation energy for the whole decomposition process.[27] According to Baldwin's ring closing rules[37] (from the α-hydroxy-peroxide to the endoperoxide the process should be a 6-exo-trig reaction that leads to a bicyclic structure), the ring closing reaction (to form the endoperoxide), is expected to be an extremely favorable and fast reaction, being a similar argument used to justify the formation of the endoperoxide intermediate. Because acyclic hydrazides show in the most favorable cases one third of luminol's chemiluminescence efficiency[22], we can argument favorably to the formation of endoperoxide prior to the generation of the excited state species in the media. Whichever the primary decomposition pathway is, the formation of both those key intermediates is quite different from aprotic to protic media. According to the literature, in aqueous media, the luminol reactive species is the monoanionic

derivative and due to the presence of the metal ion or any ROS in the media ($E^0_{Luminol} = 800\,mV$)[9] this species will rapidly form the monoelectronic oxidation derivative.[36] Because the superoxide anion is formed by the oxidant decomposition (catalyzed by the metal ion species) and because in the pH range for the oxidation process (in protic media) the superoxide anion disproportionation is inhibited[34], it will react with luminol's monoradical-anion derivative to yield two plausible intermediates (the superoxide anion is the strongest oxidant for luminol's monoradical-anion)[23]: the α-hydroxy-peroxide key intermediate[27] and a diazaquinone obtained by a second monoelectronic oxidation (*cf.* Figure 2.6). Besides, luminol's monoradical-anion can disproportionate extremely easily, leading to one molecule of luminol and another of the diazaquinone intermediate. It was also verified that this monoradical derived from luminol do not react directly with molecular oxygen and, according to what has been previously reported, molecular oxygen is necessary strictly to form superoxide anion.[27] If the formation of the diazaquinone species is one of the most favourable processes in this media we can start wondering about the influence of this species in the chemiluminescence quantum yield decrease from aprotic to protic media. To check the presence of this species in the media, it was synthesized and, when added to H_2O/H_2O_2/Metal ion systems, it exhibited chemiluminescence. It was also observed that the chemiluminescence spectrum was exactly the one shown by the related hydrazide, luminol,[37] being also shown that the oxidation product was also the aminodiphthalate.[10] Therefore, this diazo compound was assumed to be an intermediary in one light emissive pathway of luminol's chemiluminescence reaction in aqueous media.[36] To yield the excited state species, the diazaquinone in Figure 2.6 would require hydrogen peroxide in the media. The nucleophilic attack of the peroxide to this intermediate is consistent with the experimental data.[27] This would therefore be the rate limiting step in all systems that show unitary order kinetics in respect to peroxides. As for Rauhut and co-workers conditions, the zero order dependence on hydrogen peroxide is justified by change in rate limiting step.

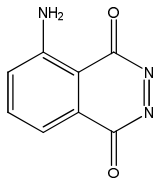

Figure 2.6: Diazaquinone intermediate proposed as intermediate in luminol's chemiluminescent oxidation reaction.

After concluding that the diazaquinone derivative of luminol obtained by two electrons oxidation is an effective intermediate in luminol's chemiluminescence in water, studies to verify the formation of this species in aprotic media were also undertaken. Adding butadiene to a chemiluminescent solution of phthalic hydrazide not only yielded no Diels-Alder adduct but also induced no decrease in the light emission intensity (Figure 2.7). The authors also verified that the chemiluminescence spectrum of the phthalic hydrazide diazaquinone derivative was different (in DMF) from the one exhibited by the parent hydrazide. The formation of the diazaquinone derivative in aprotic media was completely ruled out when the authors verified that butadiene reacted in an extremely fast fashion with the referred diazaquinone compound, even at -80 ^{o}C.[37]

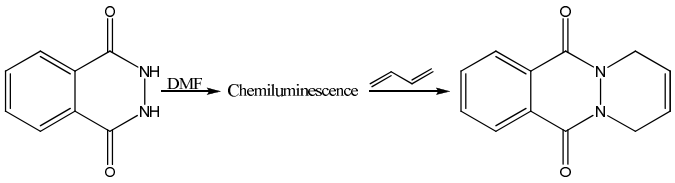

Figure 2.7: Diazaquinone intermediate proposed as intermediate in luminol's chemiluminescent oxidation reaction.

In summary, luminol's oxidation reaction may proceed in several media, of which water and DMSO are the most relevant ones. In water, where most of the reaction's applications were developed, the kinetics are in agreement with a two step mechanism where an extremely reactive intermediate is formed (in the reaction pathway that is accompanied by light emission). Only then the aminodiphthalate species in one of its electronic excited states (in principle S_1 or S_0) is formed, emitting light by fluorescence. It has also been suggested that the key reactive intermediate can be an endoperoxo-endodiazo tricyclic compound (Figure 2.5 B), a α-hydroxy-peroxide (Figure 2.5 A) or a diazaquinone (Figure 2.6). In respect to aprotic oxidation of luminol, it was proven that the diazaquinone species could not be a reaction intermediate. Regarding the nature of the transition, in aprotic media it seems to be $\pi\pi^*$. In water, an increase in $n\pi^*$character or a strong intermolecular hydrogen bonding effect seems to occur. Also in that solvent the concrete structure of the light emissive species is also still subject to some discussion. The uncertainty underlies in the presence or absence of a proton, *i.e.*, if the light emissive species is a dicarboxylate or its acid conjugate. Besides, the oxidation mechanism for luminol is still not completely known. Some possible reaction intermediates (for some conditions) were isolated and from them no more reaction intermediates can be identified. What is known is that the reaction should be first order in luminol, first order in oxidant and first order in base.

The hydrogen bonding between the aniline group from luminol and the closest carboxyl group is proposed to greatly influence the reaction's pathway determining mainly the quantum yield for the excited state formation. Relatively to substituent effects, typically, electron withdrawing substituents reduce the chemiluminescence quantum yield while electron releasing groups may increase the light emission efficiency, depending the effect on conformational restrictions and to relative electronic density in the two six member rings.

3 - Experimental Section

This section aims to describe the apparatus, the reagents and the solvents used throughout the work, either in synthetic and spectroscopic components.

3.1 - Solvent Purification and Reagents

All the solvents used in synthetic experimental procedures were distilled (Acetone, Dichloromethane, Diethyl Ether, Ethanol, Ethyl Acetate, *n*-Hexane, Methanol, Toluene, Triethylamine) and, in the case of DMF, it was also distilled over CaH_2 under reduced pressure according standard procedures[39]:

Due to the extensiveness it would cause to the list, reagents and solvents used in synthetic work will be omitted. What can be said is that those compounds were all commercially available and in reagent grade purity. As for solvents and other compounds for spectroscopic studies, the main information is resumed in Table 3.1.

Table 3.1: Origin and purity grade of reagents and solvents used in spectroscopic studies.

Reagent/Solvent	Supplier	Purity
Aminodiphthalate	Sigma Aldrich	90 %
DMF	Sigma Aldrich	Spectrophotometric Grade, ≥ 99.8 %
DMSO	Riedel-de-Haën	Puriss p.a., ≥ 99.9 % (GC)
Ethanol (absolute)	Panreac	UV-IR-HPLC PAI, ≥ 99.9 % (GC)
HCl (37%)	Panreac	p.a.
H_2O_2 (35%)	Riedel-de-Haën	Puriss
Isoluminol	Sigma Aldrich	98 %
KBr	Merck	UVsol for IR Spectroscopy
KOH	Riedel-de-Haën	Puriss p.a.
$K_2S_2O_8$	Merck	p.a., 99 %
Luminol	Fluka	≥ 98.0 % (HPLC)
Methanol	Riedel-de-Haën	Spectranal, ≥ 99.9 % (GC)

As for aqueous absorption, fluorescence and chemiluminescence essays, distilled water available in the laboratory was used. The same source of this solvent was used during synthetic work.

3.2 - Apparatus and Chemiluminescence

Infrared spectra (IR) were recorded in a Jasco Canvas FT/IR 4100 using KBr disks containing around 1 ppm of the desired solute. All IR spectra collected were performed in these conditions. In the spectral description of each purified compound, the widest list of significant signals and functional groups characteristic signals is presented in wavenumber (cm^{-1}).

NMR spectra were recorded in an Ultrashield Bruker Avance III 300 or Bruker Avance III 400 using DMSO-D_6 as solvent. All ^{1}H and ^{13}C NMR chemical shifts are reported in ppm relative to $(CH_3)_4Si$ (external standard). ^{19}F NMR shifts are also reported in ppm but relative to $CFCl_3$ (external standard). Coupling constants are expressed in Hz. Some products were also subject to COSY experiments to confirm the assigned identification.

For fluorescence, excitation spectra and for chemiluminescence essays (both spectra acquisition and emission decay) a Spex Fluorolog F112A fluorimeter was used. Luminol's solid state spectra were also recorded with this equipment using an adapter for solids. Measures were performed close to the Magic Angle.

UV/Vis spectra were all recorded in a Shimadzu UV-3101PC UV-Vis-NIR spectrophotometer.

Regarding measures of aqueous solutions pH, they were performed in a Crison micro pH 2001.

In respect to acquisition of chemiluminescence spectra, to have practically time independent spectra, conditions that slowed down the reaction rates were needed. For that, Rauhut and co-workers reaction conditions were reproduced.[25] Those consisted on 6.0×10^{-2} M of potassium persulphate ($K_2S_2O_8$) and 3.0×10^{-2} M of hydrogen peroxide (H_2O_2). Luminol's concentration range was extremely wide but it was chosen to have concentrations (for luminol and its derivatives) of 5.0×10^{-5} M. To control the reaction start, to a solution of luminol with hydrogen peroxide (with the double of the concentrations, *i.e.*, 1.0×10^{-4} M of luminol and 6.0×10^{-2} M of H_2O_2) was added a potassium peroxide solution (with concentration of 12×10^{-2} M). The additions were therefore performed in such way that when potassium persulphate was added the concentration of all species in the media was reduced to half of the initial values. Thus, half of the total final volume came from luminol and hydrogen peroxide solution while the other half came from potassium persulphate's solution, obtaining therefore the experimental conditions reported in the literature.

3.3 - Synthetic Procedures

The synthetic procedures exhibited below are the result of an optimization process, being the most favourable reaction, workup and purification conditions presented. Eventually, alternative experimental procedures may also be presented but those must exhibit alternative properties (for instance, in crystallizations, the alternative procedure would produce less amount of product but the recovered one in a purest form). The procedures will be divided by compound. It should be noticed that even though several compounds synthetic procedures are presented, not all were subject to spectroscopic studies. That is, for instance, the case of compound DMU2Lum. The reasoning underlying is that the isolated compound's purity is still unsatisfactory. So far, only mixtures of DMU2Lum and luminol have been obtained (contamination closer to 50 %) and therefore, no

chemiluminescence analysis is worth performing because we would not know if the observed properties would be from luminol or from its derivative.

In respect to the presentation mode, each derivative section will be named with the compound's IUPAC name, followed by its abbreviated designation inside brackets. For simplicity, it was assumed that luminol only exists in the most stable tautomeric form from solid state and therefore, the IUPAC names should reflect that. In the cases of DMU1Lum and DMU2Lum, because no structure is yet assigned to the compounds, only the abbreviated name (without brackets) is presented. Afterwards is presented the reaction scheme. If the structure for the product is still not conveniently assigned, only its abbreviated name will be presented. The reaction procedure, the workup procedure and the purification procedure, all properly identified, will come next. In the procedure description, the number of mol of each reagent along with the number of equivalents towards luminol is presented inside brackets. In the end of each compound section, structural analysis data is presented. Examples are IR data (only peaks are presented, in cm^{-1}), ^{1}H NMR data, that it is presented peak by peak, being those identified by their chemical shift (in ppm), ^{13}C NMR and eventually ^{19}F NMR spectrum. Regarding ^{1}H NMR data, for each presented peak is, inside brackets, the number of protons (integration relations), the splitting (*cf.* abbreviations for meaning of symbols used) and the coupling constant (in Hz if necessary). When peaks are superimposed, the non-curve brackets give specific information only regarding each peak, being outside those brackets the common information. In respect to ^{13}C NMR data, it is presented in the same way but this time inside curve brackets may be a reference for the peak signal in the APT spectrum (identified by + or -) and its presence in the DEPT 135 experiment (marked with a D). In the case of trifluoroacetyl luminol derivative (TFALum), due to heteronuclear coupling, multiplicity of the carbon peak is also inside brackets. For ^{19}F NMR spectrum, the exact same scheme was used. For all NMR experiments, brackets before the first peak description state experimental conditions, namely the frequency of the apparatus in the experience, the solvent and the reference.

3.3.1 - 2,2,2-trifluoro-N-(1-hydroxy-4-oxo-3,4-dihydrophthalazin-5-yl) acetamide (TFALum)

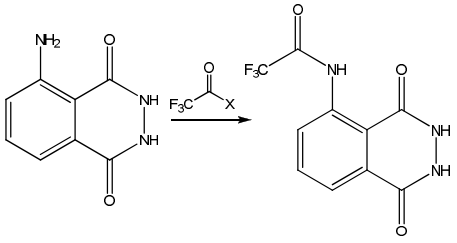

Figure 3.1: Generic scheme for the synthetic method used to obtain selectively trifluoroacetyl luminol. X represents a trifluoroacetic moiety.

Reaction

To 100 mg of Luminol (0.564 mmol) were added 2 mL of DMF until complete dissolution was observed (Note: when luminol was not completely dissolved, an extra millilitre of solvent was used to completely dissolve it). The system was purged with argon (or nitrogen) and 90 µL of triethylamine (0.646 mmol, 1.14 eq.) were added. After completion of the purge, 88 µL (0.628 mmol, 1.11 eq.) of trifluoroacetic anhydride were added directly and slowly. The temperature slightly rose and the solution achieved a yellow tonality immediately. White smoke was also observed. After one hour, a white dispersion substituted the yellow colour indicating the end of the reaction.

Workup

50 mL of water were rapidly added and the precipitate amount increased. It was also filtered.

Purification

20 to 30 mL of ethanol were added to the solid and the mixture heated until the boiling point was achieved. The solid was completely dissolved. Cold distilled water was added until turbidity appeared. The mixture was heated again until the solvent started to boil and the mixture left to rest. Within one to two days crystals were collected and dried. This crystallization procedure was applied several times to retrieve a larger amount of product. The yield after the first crystallization (using this procedure) was 70 % (107.9 mg of product). Alternatively, water-acetone mixtures can be used to crystallize higher amounts of product but at the cost of getting less pure compound. The isolated crystals were white, cotton like and melted at 335 ºC (when they also decomposed).

The product obtained by this procedure exhibited the following structural analysis data:

^{1}H NMR (400 MHz, DMSO-D_6, TMS): 14.46 ppm (1H, s); 12.13 ppm (2H, large s); 8.67 ppm (1H, d, 8.1); 7.90 ppm (1H, t, 8.1); 7.72 ppm (1H, d, 8.0).

^{13}C NMR (100 MHz, DMSO-D_6, TMS): 161.27 ppm (s, -); 154.54 ppm (q, 74.6, -); 152.04 ppm (s, -); 138.17 ppm (s, -); 135.23 ppm (s, +, D); 126.305 ppm (s, -); 121.67 ppm (s, +, D); 120.65 ppm, (s, +, D); 120.21 ppm (s); 115.87 ppm (t, 147.3 + 141.3, -).

^{19}F NMR (376 MHz, DMSO-D_6, $CFCl_3$): 75.47 ppm (3F, s).

IR (KBr Disk): 3213, 1725, 1679, 1620, 1572, 1534, 1425, 1401, 1353, 1295, 1162, 1107, 1065, 1048, 898, 813, 782, 750, 703, 662, 642, 535, 514, 500, 464, 454, 437, 430, 419, 415, 403.

3.3.2 – N-(1-hydroxy-4-oxo-3,4-dihydrophthalazin-5-yl) benzamide (BnLum)

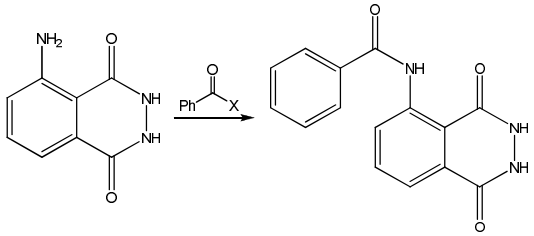

Figure 3.2: Generic scheme for the synthetic method used to obtain selectively benzoyl luminol. X represents a chlorine atom.

Reaction

To 200 mg of Luminol (1.13 mmol) were added 4 mL of DMF until complete dissolution was observed (Note: when luminol was not completely dissolved, an extra millilitre of solvent was used to completely dissolve it). The system was purged with argon (or nitrogen) and 150 µL of triethylamine (1.08 mmol, 0.953 eq.) were added. After completion of the purge, 200 µL of benzoyl chloride (1.72 mmol, 1.52 eq.) were directly and slowly added. The solution acquired a yellow tonality after the addition of the electrophile (benzoyl chloride) and a white dispersion appeared within the reaction media. The reaction evolution was checked by TLC analysis. When the reaction ended (at least 60 minutes after benzoyl chloride addition), it was stopped.

Workup

50 mL of water were rapidly added and the precipitate amount increased. It was filtered.

Purification

20 to 30 mL of ethanol were added to the solid and the mixture was heated until the boiling point was achieved. The solid was completely dissolved and cold distilled water was added until turbidity appeared. The mixture was once again heated until the solvent started to boil. It was then left to rest. Within one to two days crystals were collected and dried. This crystallization procedure may be applied several times to retrieve a larger amount of product. The yield after the first crystallization (using this procedure) was 34 % (108.3 mg of product). Crystallization just in ethanol can also be performed yielding product with similar composition. The isolated product was a white powder that decomposed at 206 ºC and exhibited the following structural analysis data:

^{1}H NMR (300 MHz, DMSO-D_6, TMS): 12.20 ppm (1H, s); 7.30-8.30 ppm (nH, m); 6.96 ppm (1H, d, 8.2); 6.63 ppm (1H, d, 7.6).

^{13}C NMR (75 MHz, DMSO-D_6, TMS): 164.64 ppm; 162.915 ppm; 162.31 ppm; 151.55 ppm; 146.295 ppm; 136.10 ppm; 135.325 ppm; 130.655 ppm; 130.51 ppm; 129.74 ppm; 129.54 ppm; 127.84 ppm; 127.60 ppm; 126.72 ppm; 117.48 ppm; 110.43 ppm; 108.47 ppm.

IR (KBr Disk): 3461, 3344, 3166, 3016, 2965, 2915, 1745, 1658, 1622, 1599, 1565, 1540, 1492, 1449, 1418, 1324, 1259, 1227, 1178, 1102, 1078, 1061, 1022, 1001, 938, 819, 778, 703, 649, 630, 555, 534, 502, 473, 438, 428, 420, 414.

3.3.3 - Ethyl 1-hydroxy-4-oxo-3,4-dihydrophthalazin-5-yl carbamate (ECLum)

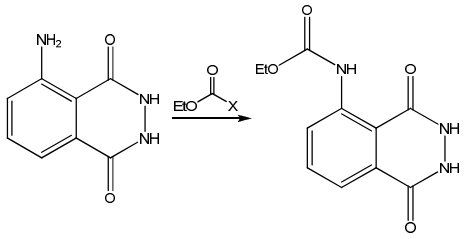

Figure 3.3: Generic scheme for the synthetic method used to try to obtain selectively ECLuminol. X represents a chlorine atom.

Reaction

To 200 mg of Luminol (1.13 mmol) were added 4 mL of DMF until complete dissolution was observed (Note: when luminol was not completely dissolved, an extra millilitre of solvent was used to completely dissolve it). The system was purged with argon (or nitrogen) and 150 µL of triethylamine (1.08 mmol, 0.953 eq.) were added. Then, 200 µL of ethyl chloroformate (2.10 mmol, 1.86 eq.) were directly and slowly added. The temperature slightly rose and the solution achieved a yellow tonality that after 30 to 60 minutes was completely gone. A white dispersion substituted the yellow colour indicating the end of the reaction.

Workup

50 mL of distilled water were rapidly added and the precipitate amount increased. The solid was filtered and ethyl acetate used to extract more product from the aqueous phase. After extraction, the ethyl acetate phase was added to the previously collected solid. The solvent was then evaporated and a solid or a yellow liquid were obtained.

Purification

10 to 15 mL of ethanol were added to the solid (or yellow liquid) and the mixture heated until the boiling point was achieved. The mixture was left to rest and within one to two days crystals were collected and dried. This crystallization procedure may be applied several times to retrieve a larger amount of product. The yield after crystallization (using this procedure) was 28 % (80 mg of product). The product obtained was pale yellow with rod form that melted at 150 ºC and exhibited the following structural analysis data:

^{1}H NMR (400 MHz, DMSO-D_6, TMS): 12.12 ppm (1H, s); 7.535 ppm (1H, t, 6.6 and 7.4); 7.42 ppm (2H, s); 6.98 ppm (1H, d, 7.4); 6.69 ppm (1H, d, 6.6); 4.31 ppm (2H); 1.315 ppm (3H).

^{13}C NMR (100 MHz, DMSO-D_6, TMS): 162.85 ppm; 152.46 ppm; 151.58 ppm; 145.68 ppm; 135.37 ppm; 126.42 ppm; 117.56 ppm; 110.43 ppm; 108.20 ppm; 66.095 ppm; 14.35 ppm.

IR (KBr disk): 3442; 3329; 3172; 3116; 2968; 2910; 2873; 1760; 1661; 1595; 1549; 1494; 1472; 1446; 1393; 1368; 1325; 1259; 1228; 1188; 1166; 1119; 1077; 1046; 1005; 932; 892; 878; 849; 815; 804; 782; 706; 686; 666; 639; 576; 528; 516; 477; 459; 446; 438; 430; 420; 410.

3.3.4 - DMU1Luminol

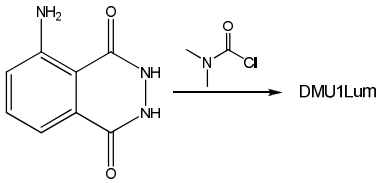

Figure 3.4: Scheme for the synthetic method used to try to obtain DMU1Luminol.

Reaction

To 200 mg of Luminol (1.13 mmol) were added 4 mL of DMF until complete dissolution was observed (Note: when luminol was not completely dissolved, an extra millilitre of solvent was used to completely dissolve it). The system was purged with argon (or nitrogen) and 200 µL of dimethyl carbamic chloride (2.17 mmol, 1.92 eq.) were directly and slowly added. The temperature slightly rose and the solution achieved a pale yellow tonality. The system was heated and kept for one day at 60 ºC. A white dispersion substituted the yellow colour indicating the end of the reaction.

Workup

Rapidly were added 50 mL of water and the precipitate dissolved. The solvent was evaporated.

Purification

10 to 15 mL of ethanol were added to the solid and the mixture heated until the boiling point was achieved. The mixture was left to rest and within one week good and large crystals were collected and dried. This crystallization procedure may be applied several times to retrieve a larger amount of product. The amount of product obtained by this procedure (after crystallization) was 104.3 mg. Alternatively, methanol can be used as crystallization solvent yielding much bigger crystals. The isolated product was always white but when the crystallization was performed in methanol, 1 mm edge crystals are obtained. On the ethanol crystallization a granulated powder was obtained.

The product obtained by this procedure exhibited the following structural analysis data:

^{1}H NMR (400 MHz, DMSO-D_6, TMS): 12.67 ppm (1H, s); 9.02 ppm (1H, d, 6.7); 7.90 ppm and 7.85 ppm (2H, [t, 8.1] and [d, 6.8]); 7.65 ppm (1H, d, 7.8); 7.49 ppm and 7.45 ppm (2.5H, m); 2.51 ppm (0.5H, s); 1.06 ppm (2.5H, t, 7.0).

^{13}C NMR (100 MHz, DMSO-D_6, TMS): 168.51 ppm; 160.92 ppm; 152.02 ppm; 145.11 ppm; 135.61 ppm; 134.78 ppm; 129.68 ppm; 129.56 ppm; 127.92 ppm; 127.60 ppm; 126.37 ppm; 121.80 ppm; 118.34 ppm; 115.27 ppm.

IR (KBr Disk): 3315, 3227, 3112, 2981, 2967, 2925, 2895, 1676, 1652, 1623, 1566, 1520, 1481, 1432, 1417, 1330, 1255, 1238, 1193, 1175, 1143, 1134, 1109, 1080, 1043, 1023, 936, 900, 890, 876, 822, 811, 774, 753, 715, 687, 643, 626, 617, 572, 554, 515, 497, 481, 447, 437, 427, 420, 411.

3.3.5 - DMU2Luminol

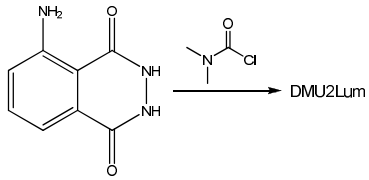

Figure 3.5: Scheme for the synthetic method used to try to obtain DMU2Luminol.

Reaction

To 200 mg of Luminol (1.13 mmol) were added 4 mL of DMF until complete dissolution was observed (Note: when luminol was not completely dissolved, an extra millilitre of solvent was used to completely dissolve it). The system was purged with argon (or nitrogen) and 200 µL of dimethyl carbamic chloride (2.17 mmol, 1.92 eq.) were directly and slowly added. The temperature slightly rose and the solution achieved a pale yellow tonality. After four days, a white dispersion substituted the yellow colour indicating the end of the reaction.

Workup

50 mL of water were rapidly added and the precipitate dissolved. The solvent was evaporated.

Purification

10 to 15 mL of distilled water were added to the solid and the mixture heated until the boiling point was achieved. Ethanol was added until turbidity appeared and the mixture heated once again until the solvent's boiling point was achieved. The mixture was then left to rest and within one to two days crystals were collected and dried. This crystallization procedure may be applied several times to retrieve a larger amount of product. The amount of product obtained by this procedure (after

crystallization) was 212.7 mg, being this product contaminated with luminol (excess estimate of 50 %). The isolated product was a pale yellow granulated powder.

The product obtained by this procedure exhibited the following structural analysis data. Peaks that matched luminol's were marked with the letter L inside brackets.

^{1}H NMR (400 MHz, DMSO-D_6, TMS): 13.77 ppm (1H, d, 10.8); 11.32 ppm (3H, large s); 9.28 ppm (1H, d, 10.8); 7.99 ppm (1H, d, 8.1); 7.83 ppm (1H, t, 7.6 and 8.1); 7.63 ppm (1H, d, 7.6); 7.30 ppm (L); 6.79 ppm (L); 6.74 ppm (L); 3.12 ppm (s).

^{13}C NMR (100 MHz, DMSO-D_6, TMS): 161.73 ppm (L); 161.14 ppm; 152.89 ppm; 151.90 ppm (L); 151.14 ppm (L); 138.93 ppm; 135.34 ppm; 134.30 ppm (L); 126.90 ppm (L); 126.74 ppm; 120.80 ppm; 118.04 ppm; 116.86 ppm (L); 115.27 ppm; 110.82 ppm (L); 109.93 ppm (L); 43.83 ppm; 37.19 ppm.

4 - Experimental Work

This next section of the work deals mainly with synthetic work developed in the laboratory to obtain luminol acyl derivatives for fluorescence, absorption and chemiluminescence essays. The section will present in detail the laboratorial work to attempt compound isolation and is thus a description of the well succeeded and unsuccessful experiments. Because the text will be divided by derivative, it will not reflect the time evolution of the work. The experimental work presentation will be backed up with at least TLC (thin layer chromatography) analysis and eventually NMR information. These will be used to evaluate the success (or unsuccess) of the experiments. For isolated compounds, a more detailed structural analysis (analysis of NMR experiment results) is performed to show how conclusions were achieved.

Regarding the presentation mode, because not all the presented compounds were isolated (only those whose synthetic procedure was described in section 3.3), each section will be named with a convenient designation related with the generic substituent whose experiments described here attempted to introduce. Like previously performed, inside brackets will be the assigned abbreviation for isolated compounds. For non-isolated compounds, a generic scheme that represents the main reactions will be presented (for other species, Figures 3.1-3.5 were already presented). Regarding the way the experiments are described, Table 4.1 will act as backup. This extensive table will have in each numbered entrance a set of reaction descriptors, like the amount of luminol, which electrophile was used, its amount, reaction solvents, temperature, base and other relevant information to describe the experiment. For convenience, Table 4.1 will be presented before the first compound section, right after this short introduction. For simplicity, each entry of this table will be called during the text by a number inside square brackets. In respect to the presentation of TLC results, curve brackets indicate the eluent used and whenever needed, Rf's are included. It should be stated here that even though not all TLC analysis results are reported, all reactions were followed by this technique and no workup procedure was ever applied before knowing those results. Besides, all reactions proceeded under argon atmosphere and the workups consisted in water addition to destroy the excess of electrophile. Regarding isolated species, because peak chemical shift and integration were previously reported (*cf.* Section 3.3), the annexed spectra will be free from any supplementary information.

Regarding the generic procedures that can be used to obtain luminol derivatives (including here mainly aniline or hydrazide derivatization), Figure 4.1 presents a schematic resume.

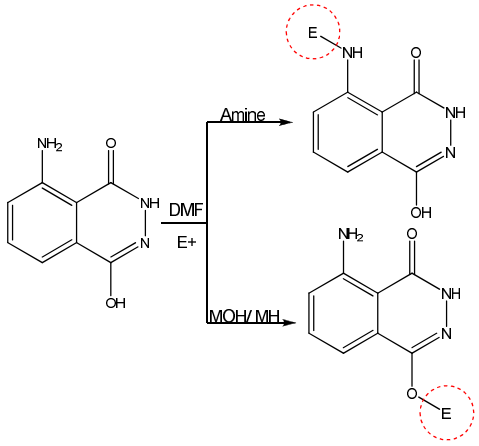

Figure 4.1: Main synthetic procedures to obtain luminol derivatives.

As we can verify, when softer and weaker bases (like pyridine) are used, the main effect of the alkaline species is to increase the nucleophilicity of the aniline moiety, possibly by acid-base equilibria. On the other hand, when harder bases are used (the typical case is alkaline metal hydroxides or hydrides) the protons to be removed are majorly the most acidic ones, *i.e.*, from the hydrazide functionality. Therefore, this dicarboxylic functionality of luminol will have the highest electronic density of the whole structure and will thus be the most nucleophilic one.[8,16,40]

Table 4.1: Main information regarding experiments performed to synthesize luminol's derivatives. Atm. stands for atmosphere while Succ. Anh. stands for succinic anhydride and TFAc Anh. for trifluoroacetic anhydride. SO_2Bn Anh. stands for 2-sulfonyl benzoic anhydride cyclic anhydride. In bold are the experiments that gave origin to experimental procedures in section 3.3. In results, P stands for isolated product being inside brackets the yield of pure product, NR for no reaction obtained (towards luminol, *i.e.*, luminol did not react), CM for complex mixture obtained, LP for product in extremely low yield and NIP stands for non-isolated product. Inside brackets may be the procedure yield, or the method used to prove that no derivative was isolated or that support the complexity of the reaction mixture (T for TLC and N for NMR). Whenever NMR spectra were collected, TLC analysis was also performed.

#		1	2	3	4	5
Luminol	mass (mg)	100	100	100	100	100
	n (mol)	5.64×10^{-4}	5.64×10^{-4}	5.64×10^{-4}	5.64×10^{-4}	5.64×10^{-4}
Electrophile	Name	AcCl	AcCl	AcCl	AcCl	AcCl
	Vol (µL)	50	45	45	45	45
	n (mol)	7.03×10^{-4}	7.03×10^{-4}	7.03×10^{-4}	7.03×10^{-4}	7.03×10^{-4}
Base	Name	TEA	Py	Py	Py	Py
	Vol (µL)	100	45	2000+500	2000+500	2000+500
	n (mol)	7.17×10^{-4}	5.59×10^{-4}	3.10×10^{-2}	3.10×10^{-2}	3.10×10^{-2}
Solvent (mL)		1+2	2+0.41	2+0.5	2+0.5	2+0.5
Temperature (ºC)		RT	RT	RT	Reflux	Reflux
Time		4 days	1 day	4 days	4 days	1 day
Comments		Ar Atm.	Ar Atm.	Ar Atm.	Ar Atm.	Ar Atm.; Cat. $ZnCl_2$
Results		NR (T)	NR (N)	NR (T)	NR (T)	NR (T)

#		6	7	8	9	10
Luminol	mass (mg)	100	100	100	100	100
	n (mol)	5.64×10^{-4}	5.64×10^{-4}	5.64×10^{-4}	5.64×10^{-4}	5.64×10^{-4}
Electrophile	Name	Ac_2O	Ac_2O	BnCl	BnCl	BnCl
	Vol (µL) / Mass* (mg)	2000	2000	90	90	90
	n (mol)	1.92×10^{-2}	1.92×10^{-2}	7.75×10^{-4}	7.75×10^{-4}	$7.75E\times10^{-4}$
Base	Name	NaOAc	K_2CO_3	TEA	TEA	TEA
	Vol (µL) / Mass* (mg)	0.5487 *	1.0771 *	100	2000+500	2000+501
	n (mol)	6.69×10^{-3}	7.79×10^{-3}	7.17×10^{-4}	1.79×10^{-2}	1.79×10^{-2}
Solvent (mL)		2	2	1+2	2.5	2.5
Temperature (°C)		130	130	RT	RT	Reflux
Time		1.5 hour	1.5 hour	4 days	4 days	1 day
Comments		Ar Atm.	Ar Atm.	Ar Atm.	Ar Atm.; Cat. DMAP	Ar Atm.; Cat. DMAP
Results		CM (T)	CM (T)	NR (T)	CM (N)	NR (N)

#		11	12	13	14	**15**
Luminol	mass (mg)	100	90	200	200	**200**
	n (mol)	5.64×10^{-4}	5.08×10^{-4}	1.13×10^{-3}	1.13×10^{-3}	**1.13×10^{-3}**
Electrophile	Name	BnCl	BnCl	BnCl	BnCl	**BnCl**
	Vol (µL)	145	80	145+145	145+146	**200**
	n (mol)	1.25×10^{-3}	6.89×10^{-4}	2.50×10^{-3}	2.50×10^{-3}	**1.72×10^{-3}**
Base	Name	Py	TEA	TEA	TEA	**TEA**
	Vol (µL)	45	1000	160	160	**160**
	n (mol)	5.59×10^{-4}	7.17×10^{-3}	1.15×10^{-3}	1.15×10^{-3}	**1.15×10^{-3}**
Solvent (mL)		2.4	2	4	4	**4**
Temperature (ºC)		RT	RT	RT	RT	**RT**
Time		4 days	1 day	2 days	1 day	**1 day**
Comments		Ar Atm.	Ar Atm.; 1.45×10^{-3} mol $AgNO_3$	Ar Atm.	Ar Atm.	**Ar Atm.**
Results		NR (N)	CM (N)	CM (T)	CM (N)	**P (34 %)**

#		16	**17**	18	19	20
Luminol	mass (mg)	100	**200**	100	200	200
	n (mol)	5.64×10^{-4}	**1.13×10^{-3}**	5.64×10^{-4}	1.13×10^{-3}	1.13×10^{-3}
Electrophile	Name	EtOCOCl	**EtOCOCl**	PhNCO	PhNCO	PhNCO
	Vol (µL)	60	**200**	70	140	200
	n (mol)	6.30×10^{-4}	**2.10×10^{-3}**	6.44×10^{-4}	1.29×10^{-3}	1.84×10^{-3}
Base	Name	Py	**TEA**	---	---	---
	Vol (µL)	45	**150**	---	---	---
	n (mol)	5.59×10^{-4}	**1.08×10^{-3}**	---	---	---
Solvent (mL)		2+0.4	**4+1**	2	4	4+1
Temperature (ºC)		RT	**RT**	RT	RT	RT
Time		3 days	**2 hours**	2 hours	12 hours	12 hours
Comments		Ar Atm.	**Ar Atm.**	Ar Atm.	Ar Atm.	Ar Atm.
Results		NR (N)	**P (28 %)**	CM (N)	CM (T)	NR (N)

#		21	22	23	24	25
Luminol	mass (mg)	200	100	100	200	100
	n (mol)	1.13×10^{-3}	5.64×10^{-4}	5.64×10^{-4}	1.13×10^{-3}	5.64×10^{-4}
Electrophile	Name	PhNCO	Succ. Anh.	Succ. Anh.	Succ. Anh.	TFAc Anh.
	Vol (µL) / Mass* (mg)	1500	Excess *	Excess *	214 *	87
	n (mol)	1.38×10^{-2}	Excess	Excess	2.14×10^{-3}	6.21×10^{-4}
Base	Name	---	---	---	Py	Py
	Vol (µL)	---	---	---	100	45
	n (mol)	---	---	---	7.17×10^{-4}	5.59×10^{-4}
Solvent (mL)		1.5	---	---	2	2
Temperature (ºC)		RT	200	200	60	RT
Time		2 hours	5 hours	5 hours	1 day	1 day
Comments		Ar Atm.	Ar Atm.	Ar Atm.; Cat. $ZnCl_2$	Ar Atm.	Ar Atm.
Results		NR (T)	NR (T)	LP (<6 %)	NIP	P (65 %)

#		**26**	27	28	**29**	30
Luminol	mass (mg)	**100**	200	200	**200**	200
	n (mol)	**5.64×10^{-4}**	1.13×10^{-3}	1.13×10^{-3}	**1.13×10^{-3}**	1.13×10^{-3}
Electrophile	Name	**TFAc Anh.**	TMSCl | BnCl	SO_2Bn Anh.	**Me_2NCOCl**	Me_2NCOCl
	Vol (µL) / Mass* (mg)	**87**	2000 | 150	323.5 *	**200**	200
	n (mol)	**6.21×10^{-4}**	1.58×10^{-2} | 1.29×10^{-3}	1.76×10^{-3}	**2.17×10^{-3}**	2.17×10^{-3}
Base	Name	**TEA**	TEA	TEA	**TEA**	TEA
	Vol (µL)	**90**	1000	150	**150**	150
	n (mol)	**6.46×10^{-4}**	7.17×10^{-3}	1.08×10^{-3}	**1.08×10^{-3}**	1.08×10^{-3}
Solvent (mL)		**2**	1 DCM + 0.9 DMF	4	**4**	4
Temperature (ºC)		**RT**	60	60	**60**	RT
Time		**1 day**	4 days	5 days	**1 day**	4 days
Comments		**Ar Atm.**	Ar Atm.; Cat. KI	Ar Atm.; Cat. DMAP	**Ar Atm.**	Ar Atm.
Results		**P (70 %)**	NIP	NR (T)	**P (104 mg)**	NR (T)

#		**31**
Luminol	mass (mg)	**200**
	n (mol)	**1.13×10^{-3}**
Electrophile	Name	**Me_2NCOCl**
	Vol (µL)/Mass* (mg)	**200**
	n (mol)	**2.17×10^{-3}**
Base	Name	**---**
	Vol (µL)/Mass* (mg)	**---**
	n (mol)	**---**
Solvent (mL)		**4**
Temperature (oC)		**RT**
Time		**4 days**
Comments		**Ar Atm.**
Results		**P (213 mg)**

4.1 - Acetyl Luminol

This was the first luminol derivative that was tried to isolate through reaction of luminol with an acetylating agent (acetic anhydride and acetyl chloride). Therefore, several reaction media were tested. The experiments initially described tried not to use DMF to avoid the Vilsmeyer reagent formation. Besides, lower boiling point solvents would be more convenient for workup procedures. Although several conditions were tested, some directly from the literature,[8] the desired species was never isolated.

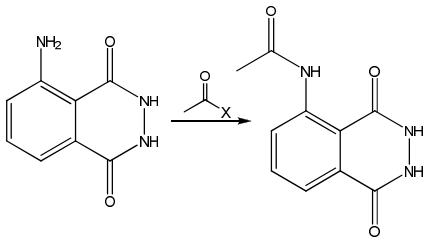

Figure 4.2: Generic scheme for the synthetic method used to try to obtain selectively acetyl luminol. X represents an adequate leaving group in order to make CH3COX a good acetylating agent.

[1] The first of all attempts was with luminol in dichloromethane (DCM) and triethylamine (TEA). The selected acetylating agent was acetyl chloride. Because luminol did not dissolve in the solvent and because it was spread all over the reaction vessel's walls, more solvent was added. After that, we performed the addition of the acetylating agent with the reaction vessel in an ice bath. Right after that, smoke appeared (indicating that acetyl chloride had reacted with something) and in the end of 4 days the reaction crude adopted a rose tonality (it was previously completely white). The first TLC analysis (MeOH; AcOEt) showed only two spots. The spot with lowest Rf was proved to be luminol. The other spot (Rf of 0.6 in MeOH and 0.8 in AcOEt) was not identified. The reaction mixture was then washed with an aqueous solution of HCl (10%) being the organic layer diluted with DCM. An emulsion formed and in the end nothing but luminol was isolated. The use of DCM as solvent was to try to play with relative solubility of luminol and the product in the solvent used. We expected that even if an extremely small amount of luminol got solubilized, it would be enough to react with the electrophile. Due to the expected different polarity of the reagent and the product, the dissolution equilibrium would dislocate and all luminol would therefore react.

[2] The next attempt was already performed in DMF. The base used was this time dried pyridine (dried according to standard procedures)[39]. Separately, an acetyl chloride solution in DMF was also prepared, purged and added to luminol's solution. The mixing of DMF solutions was once again performed in an ice bath and the electrophile was added to the nucleophile (to avoid eventual polyacylation reactions). Physical changes of the contents of the reaction's vessel were only observed one day after the beginning of the reaction, when the reaction crude became yellow. Water was then added and a precipitate was formed. After isolation of the solid, TLC analysis (9AcOEt:1hexane) showed just one spot with Rf similar to the one shown by luminol in that eluent (0.3). Besides, that spot showed the exact same fluorescence colour in the UV lamp used to reveal the result of the analysis. Even so, NMR experiments were performed to this sample and both ^{13}CCPD and ^{1}HNMR experiments gave spectra in agreement with the ones exhibited by luminol

[3] [4] After those first two experiments, removal of DMF was tested. To luminol and pyridine, acetyl chloride was added. Once again, a previous solution of the electrophile (in pyridine) was prepared and added to luminol's solution in an ice bath. In the end, no product was obtained. [5] Based on these previous conditions, an experiment with a catalytic amount of zinc chloride ($ZnCl_2$) was tested. After one day of reaction, the crude adopted a dirty white colour. TLC analysis

(3AcOEt:1EtOH) showed just a dragged spot. After removing pyridine by distillation, a solid was obtained. This was dissolved in ethanol and shown to be luminol by TLC (3AcOEt:1EtOH).

[6] [7] The last two experiments performed on acetyl luminol were with acetic anhydride. An excess of base (NaOAc and K_2CO_3) was added to luminol in both systems and acetic anhydride was used both as reagent and solvent. A yellow colour appeared in system [7] (with K_2CO_3) right after the addition of the electrophile. Both reaction vessels showed dispersed solids in the liquid and a TLC (3AcOEt:1EtOH) showed that the system was mainly composed by luminol. Therefore, we decided to heat the sample. One hour and half after starting heating, the potassium carbonate sample turned black while the other sample (NaOAc) turned red. Ethanol was added and TLC analysis (3AcOEt:1EtOH) performed. Reaction [7] (K_2CO_3) exhibited a spot right on top of the luminol's while the other sample showed a spot with Rf of 0.05. No isolation was attempted in these samples but after a few days in ethanol we noticed some luminol needling crystals in those two vessels.

4.2 - Benzoyl Luminol (BnLum)

[8] The first attempt to isolate this luminol derivative was performed simultaneously with the first attempt to obtain acetyl luminol. Therefore, reaction conditions were extremely similar. The solvent was DCM but now the electrophile was benzoyl chloride. TEA was once again used as base. When luminol and the electrophile were mixed, the solution got a yellow colour. By TLC analysis (MeOH) it was proved that after four days no luminol reacted. It was also verified by that analysis that benzoyl chloride partly hydrolyzed to benzoic acid.

[9] Similarly to what has been previously performed with acetyl chloride, the use of base as solvent was tested for this type of derivatization. Instead of pyridine, triethylamine was used. DMAP (dimethyl amino pyridine) was also added (before the electrophile) in a catalytic amount. After the benzoyl chloride addition, the solution got once again yellow but luminol remained undissolved. A TLC (DCM) showed four distinct spots. Benzoyl chloride, luminol and benzoic acid were identified but the nature of the other spot remained unknown. Therefore, an aqueous solution of Na_2CO_3 was added, being the system under stirring for 2 hours (pH=8). After pH neutralization, the aqueous solution was washed with diethyl ether and the organic layer dried with magnesium sulphate. It was verified that the aqueous phase contained luminol and benzoic acid. The ^{13}C NMR performed to the solid (obtained after ether low pressure evaporation) showed that benzoic acid had been isolated. [10] Right after this unsuccessful attempt to isolate BnLum, the same system was tested but this time in reflux. An analogous workup was applied but the NMR spectra were too complex to take any other conclusion besides the inexistence of luminol in the isolated sample. Therefore, a chromatographic column using AcOEt as eluent was performed and, once again, benzoic acid was isolated but this time contaminated with several solvents.

[11] The next experiment consisted again in benzoyl chloride addition to a luminol's solution, this time in DMF. Pyridine was once again the selected amine base. After one day, the solution in the

system was pink. Four days after starting the reaction water was added and a thin precipitate formed. The isolated solid was then completely dissolved in DCM and after solvent removal a mixture of white and yellow solids was obtained. The TLC analysis (AcOEt) showed distinctively three spots from compounds less polar than luminol. By adding once again dichloromethane, the two colour solid was washed being obtained a white solid. Proton and carbon NMR to that sample showed that once again benzoic acid was the isolated species. Regarding the yellow compound, its colour was consistent with benzoyl chloride.

[12] Due to the negativity of the last reported results, benzoyl chloride activation was tested. Instead of adding DMAP like previously, silver nitrate was used. Thus, to a luminol, triethylamine and $AgNO_3$ solution in DMF, benzoyl chloride was added. A white/silvered solid appeared inside the reaction vessel and a few minutes later the system turned red. Because there are several reports[3] on the use of luminol to identify metal ions in water, it was assumed by correspondence that the silvered solid was silver (after recovery, it was verified that it was insoluble in any common laboratory solvent). TLC analysis (3AcOEt:1EtOH) to the sample showed 3 different spots (Rf's of 0.11, 0.54 and 0.77) and therefore we decided to add water, forming immediately a precipitate. By TLC (in 3AcOEt:1EtOH) we verified that the aqueous phase retained only the most polar compound. Because the water solution exhibited the same coloration obtained after luminol's chemiluminescence reaction (in water) and due to formation of silver, it was assumed that the most polar compound in TLC was luminol's oxidation product, aminodiphatalate (ADP). After filtration, the precipitate was dissolved in acetone (became yellow) and residues of silver that were still in the acetone solution were (practically) completely removed by centrifugation. After crystallization (boiling acetone-water), NMR experiments showed an aromatic region too complex to perform any concrete conclusion regarding the effectiveness of the methods employed in this reaction.

[13] Due to this inconclusive result the reaction was repeated. In order to avoid the redox reaction of silver cations with luminol, the addition of silver nitrate was programmed to occur only after the electrophile addition. For that purpose, to a luminol and TEA solution in DMF, benzoyl chloride was added. Surprisingly, immediately after the addition of the latter species, the reaction crude got yellow and a few minutes later a solid formed. The TLC (3AcOEt:1EtOH) showed that besides luminol and benzoyl chloride two other unknown species were in the media (Rf's of 0.11 and 0.57) and, therefore, silver was not added. The benzoyl chloride amount was doubled and the reaction continued for one more day. After adding water, a pale yellow solid formed along with some smoke. The sample was left under water and stirring for two hours and afterwards the solid was filtered and dissolved in acetone with a small amount of supersaturated Na_2CO_3 aqueous solution (this method was employed to remove benzoyl chloride and benzoic acid). No pure enough samples were obtained.

[14] [15] The two next experiments related to benzoyl luminol reproduced experiment [13] but with a large excess of acylating agent from the start. The systems behaved exactly the same way and after one day, water was added to both. In this point, the treatment of those samples differed significantly. While one stayed in water for 2 weeks, the other was subject to several operations. The first one was washing with diethyl ether. The solid became drier and a crystallization system

(acetone-ether) was attempted. Because the solid amount obtained was unsatisfactory, chromatographic purification was performed (3AcOEt:3Hexane:3Toluene). The product thus isolated was contaminated only with benzoyl chloride, being luminol residues completely removed. Both TLC (3AcOEt:1EtOH) and NMR showed that the product was purer. In the meanwhile, a completely white solid was collected from the other sample. The obtained solid was dissolved in ethanol and in one day 57.5 mg of a solid crystallized. After that process, another crystallization system (boiling ethanol-water) was attempted. More 50 mg of product were isolated.

The ^{1}H NMR spectrum showed a quite complex aromatic region but two distinct duplets were present at 6.96 ppm and 6.63 ppm. These were assigned to derivatized luminol (luminol shows those two duplets at 6.95 ppm and 6.89 ppm). These peaks were completely free (no other peaks in a certain vicinity) being the benzoyl protons in the region of 7.3-8.3 ppm (by peak assignment in spectra from similar compounds)[41,42]. The ^{1}H NMR spectrum of this sample seemed to be evidence to state that luminol reacted with benzoyl chloride. A peak at 12.20 ppm was assigned to the N2's proton (of substituted luminol). The integration of this peak indicated that only one proton was present, being this evidence for aniline substitution in luminol.

As for the ^{13}C NMR spectrum, in the lowest field region of the spectrum (chemical shifts higher than 150 ppm) we observed four peaks: 151.55 ppm, 162.31 ppm, 162.915 ppm and 164.64 ppm. Because luminol's peak at 151 ppm disappeared, because peaks at 162 and 164 ppm appeared and due to proton NMR evidence, it was concluded that luminol's structure was efficiently changed.

From these results, it was concluded that benzoyl luminol (BnLum) had been isolated. Annex 1 presents benzoyl luminol's ^{1}H and ^{13}C NMR spectra.

4.3 - Ethoxy Carbonyl Luminol (ECLum)

[16] The first experiment performed to obtain ethoxy carbonyl luminol was already with a luminol's solution in DMF. Dried pyridine[39] was added to luminol and DMF and then the solution was subject to an ice bath. Meanwhile, a DMF solution of ethyl chloroformate was prepared, being posteriorly added to the luminol solution. Unfortunately, a loss of ethyl chloroformate occurred during the addition and much less than one equivalent was added. Three days after the beginning of the reaction, no difference was observable in TLC analysis (dichloromethane). Even though the analysis seemed to be unfavourable for luminol derivatization, water was added and a white powder was filtered. TLC analysis (1AcOEt:1EtOH) showed that the powder consisted solely on luminol. ^{1}H NMR experiment led to the exact same conclusion.

[17] Due to the technical problem that occurred during reagent mixing, the reaction was repeated. In this new reaction the scale was also increased. After the addition of the chloroformate, a yellow colour appeared in the reaction vessel. The yellow tone got stronger after a few minutes and disappeared within half an hour to yield a white solid. TLC analysis (6EtOAc:1Hexane) showed one

spot with null Rf as well as three other spots, respectively with Rf's of 0.29, 0.44 and 0.59. After water addition, the less polar compounds precipitated. Because it was verified that the precipitation was incomplete and because it was possible to dissolve the precipitate in AcOEt, this solvent was used to extract the desired solute from the aqueous phase (note that luminol's solubility in ethyl acetate is extremely low). After completing the extraction, the organic phase was mixed with the previously filtered solid and the solvent evaporated. Instead of a pure solid, a yellow liquid with solid was obtained (ethyl acetate shows some miscibility with water). Because water previously helped to precipitate the supposed product, no precautions were taken to completely remove it. Afterwards, a small amount of ethanol was added (10 mL) and heated to its boiling point. The amount of water was adjusted for the system to exhibit early crystallization and the vessel with the solution was once again heated to its boiling point. In one day crystals were obtained and this purification methodology was applied one more time to recover the maximum amount of product. Besides these attempts, crystallization in ethanol-water was also tested but this time only black crystals were obtained, completely different from the pale yellow ones previously obtained. This product was therefore neglected.

To the latter sample isolated, both ^{1}H and ^{13}C NMR studies were performed. Like what has been observed for BnLum, the characteristic signals from luminol's aromatic protons were changed (6.98 ppm and 6.69 ppm instead of 6.95 ppm and 6.89 ppm). Because luminol was the only aromatic compound used in the reported experimental procedure, evidence for its derivatization was gathered. Besides, the peak from N2's protons exhibited total integration correspondent to one proton. Other differences from pure luminol spectrum consisted on peaks at 4.32 ppm and 1.32 ppm. Because these peaks were superimposed with others at 4.20 ppm and at 1.06 ppm, no perfectly reliable integration was possible. Regarding assignment to those peaks, due to the nature of reagents in the system, they must come undoubtedly from ethoxy functionalities, one possibly from the product and the other from ethanol. In that hypothesis, the two less intense peaks (of each set) can be assigned to the solvent and a qualitative integration (based on the total integration) led us to conclude that the desired substitution was achieved. Besides, it is also concluded that the isolated solid was highly contaminated with ethanol (an excess estimative indicates that one ethanol molecule is present for each luminol derivative molecule).

Regarding ^{13}C NMR spectrum, the derivative exhibited extra peaks at 145.68 ppm (carbamate's carboxyl carbon), 66.095 ppm (from carbon directly bonded to the oxygen atom in the ethoxy group) and at 14.35 ppm (from the methyl group's carbon in the ethoxy moiety). Besides, all luminol peaks were also present but all shifted.

From these evidences, it was concluded that ethoxy carbonyl luminol derivative was obtained. The collected NMR spectra are presented in the second annex, Annex 2.

4.4 - Phenylamine-Luminol Urea

The derivative supposedly obtained with this set of reactions would be the first with an urea functionality. Even though the electrophile chosen in this system was extremely reactive, no product was ever isolated due to secondary effects on the reaction crude. The generic reaction scheme is presented in Figure 4.3.

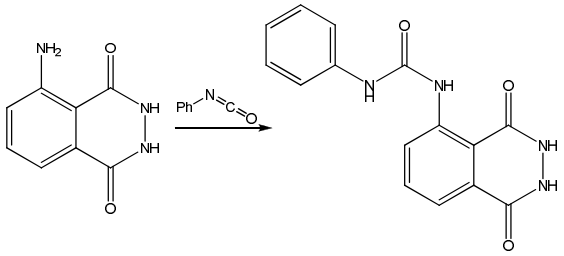

Figure 4.3: Generic scheme for the synthetic method used to try to obtain selectively phenylamine-luminol urea.

[18] The first experiment for this type of substitution used a DMF solution of luminol. Phenyl isocyanate was then added and the solution changed from uncoloured to yellow. By means of TLC analysis (3AcOEt:1EtOH) a slightly less polar species than luminol was identified in the reaction crude. Water was added 2 hours later and a pallid yellow precipitate was immediately formed and filtered. By addition of acetone, the solid completely dissolved and a TLC analysis proved that the desired species was in this phase. After evaporation of acetone, boiling ethanol was added along with cold water to induce crystallization (several systems were tested and this seemed to be the best). A grey wet solid was filtered but the NMR analysis showed an extremely impure sample (^{13}C NMR revealed duplication of almost all peaks).

[19] The next attempt performed just increased the reaction scale. Once again, after addition of the electrophile the reaction crude turned yellow but this time a precipitate formed. Twelve hours later the solid redissolved and the TLC analysis (3AcOEt:1EtOH) showed similar composition to the previously obtained. Water was added and another precipitate formed. After filtration and dissolution in acetone, crystallization in that solvent was attempted. The TLC analysis (3AcOEt:1EtOH) proved that the applied process had no selectivity. [20] It was therefore chosen to repeat the reaction with more phenyl isocyanate and stop it practically after the electrophile addition. The reaction crude evolved the same way as reported in [19] but this time acidified water (pH around 1 by addition of hydrogen chloride) was added (the amount of solid qualitatively appeared to have increased). After filtration, a TLC analysis (3AcOEt:1EtOH) allowed us to verify that the aqueous phase only contained luminol. Because the products obtained were all much less polar than luminol, toluene was added (several solvents and mixtures were tested) to clean the isolated solid from luminol. After heating, only a white solid remained undissolved (proved to be luminol). After toluene's evaporation and after drying the sample with the vacuum bomb, the ethanol-water crystallization system was tested. A grey solid was obtained (similar to the previously obtained one) and a TLC showed that the desired product crystallized in high purity. Proton and carbon NMR experiments were performed and allowed us to conclude that the symmetric urea of aniline was isolated.

[21] Given this extremely demotivating result, the reaction was once again repeated but this time using phenyl isocyanate as solvent. After the addition of the solvent, no apparent dissolution of luminol occurred but, a yellowish coloration also started to appear inside the reaction vessel. A few minutes later, a yellow precipitate formed once again but this time it completely stopped the reaction. The TLC analysis (3AcOEt:1EtOH) showed a spot from luminol and another one similar in colour to the previously obtained product upon UV light exposition. After destroying the excess of solvent with water and after evaporation to dryness, ethyl acetate was added and a TLC analysis showed that the product obtained was the same obtained in reaction [20].

4.5 - Succinyl Luminol

Another luminol derivative searched was its succinyl. Even though derivatization has been achieved, further studies on this species were not performed because this compound's chemiluminescent properties were already known.[16] The electrophile used in all experiments was succinic anhydride.

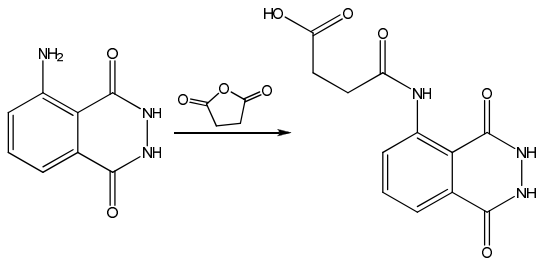

Figure 4.4: Generic scheme for the synthetic method used to try to obtain selectively luminol's succinyl derivative.

[22] [23] The first two experiences performed with succinic anhydride consisted on mixing luminol and an excess of solid succinic anhydride (no mass was measured). The main difference between those first two systems consisted on one having zinc chloride ($ZnCl_2$) added in a catalytic amount ([23]). In order to create a suitable media for the reactions, both vessels were subject to heat. The reaction was programmed to proceed slightly above 393.15 K (120 ºC), succinic anhydride's melting point.[43] At 383.15 K, sublimation was observed in both reaction vessels, being formed huge needling crystals in the top of the reaction vessel. When the thermometer reached 473.15 K (200 ºC), succinic anhydride melted and due to the high temperature discrepancies in the bottom and the top of the reaction vessel, succinic anhydride started to solidify in the top of the reaction vessel and the reactions were both stopped. TLC analysis (AcOEt; 3AcOEt:1EtOH) showed that the needle crystals were merely succinic anhydride and also that the reaction mixture with catalytic amount of zinc had a compound with higher polarity than luminol (besides being composed by luminol). These same TLC's also showed that the other compound was not the water neither the ethanol derivative of succinic anhydride. This compound's Rf was 0.51 in the second eluent. The sample was then dissolved in acetone and left to rest (water and EtOH were also tested not giving promising results). Crystals were

obtained within one day and were therefore subject to NMR experiments. These showed a aromatic region from the one obtained with luminol's protons. Unfortunately, it only corresponded to 5.5 % of the whole sample.

[24] The last experiment performed with this compound reproduced exactly literature's conditions.[16] Therefore, luminol and succinic anhydride were dissolved in DMF, being dried pyridine[39] also added. Afterwards, the reaction mixture was heated and after one day, the TLC analysis (3AcOEt:1EtOH) showed two spots, luminol and, with lower Rf, the supposed reaction product. Unlike luminol, this spot was dark blue fluorescent (luminol's light blue fluorescent). It must also be reported that the reaction crude was slightly rose. A hydrochloric acid aqueous solution (pH=1) was added to induce precipitation and the filtered solid was washed with water and methanol. NMR spectra proved that the solid contained predominantly the desired product,[16] *i.e.*, luminol's succinyl derivative. The solid was then dissolved in a sodium bicarbonate aqueous solution and then hydrochloric acid was added until complete precipitation was observed (ethanol-water, acetone-water and water were tested as crystallization media). Due to non-crystallinity of the isolated solid and to the fact that all its chemiluminescent properties were already known,[16] no further studies were performed.

4.6 - Trifluoroacetyl Luminol (TFALum)

This luminol derivative was obtained readily in the first attempt. The reaction conditions tested used all trifluoroacetic anhydride as electrophile and DMF as solvent. Regarding amine bases used, two were tested: pyridine (from literature's conditions reproduction) and TEA.

[25] The first experiment started with a DMF solution of luminol and pyridine. Trifluoroacetic anhydride was added and spontaneous change in reaction crude occurred: the media turned yellow and smoke was released (the addition was performed in an ice bath). Even though the TLC analysis (3AcOEt:1EtOH) showed solely one spot (with the same Rf as luminol), water was added to the system. After filtration, the solid was dissolved in ethanol and the mixture heated to the solvent boiling point. Cold water was then added and within one day crystals were grown (acetone-water crystallization system was also tested, yielding more but less clear crystals). The crystals were afterwards filtered, dried and subject to NMR studies.

The proton NMR spectrum before crystallization showed that besides being shifted, aniline's protons integration was reduced to half, meaning that the N2 substitution was achieved. Hydrazide's protons retained the same relative integration (2 protons). Besides, the derivative showed different aromatic peak arrangement. The spectrum from the sample also showed 9 mol % of luminol as impurity, that, after crystallization, completely disappeared from the spectra (carbon NMR also).

Regarding ^{13}C NMR spectra, it was composed by 10 peaks. APT spectrum showed that only three of these carbons were tertiary being all the others quaternary (theoretically those peaks can also be from secondary carbons, but the expected structure has no such carbon substitution). DEPT

135 yielded the same conclusions. In respect to ^{19}F NMR spectrum, it showed only a singlet at 75.47 ppm, indicating monosubstitution (along with ^{1}H and ^{13}C NMR data).

Proton and carbon spectra are presented in Annex 3 – NMR Spectra of TFALum. ^{19}F NMR spectrum is omitted because only a singlet peak is observed.

[26] The second reaction tested exactly the same conditions but with TEA instead of pyridine (several advantages come along with that substitution, namely toxicity and easier access to distilled samples of the amine). Besides, the addition of the electrophile was also performed without the ice bath. The same changes were observed during the addition but now a white solid formed within one day. Along with this precipitation process the reaction crude became transparent. By addition of an aqueous hydrochloric acid solution (pH close to one) more solid (white) precipitated in the reaction vessel. Note that due to previous results from TLC analysis this analytical technique would not be useful to determine reaction's end point. That white solid was subject to the crystallization procedure reported above and similar crystals were obtained. NMR data proved that these new crystals had the same composition has the ones obtained with pyridine and with ice bath during electrophile addition.

4.7 - Trimethylsilyl Luminol

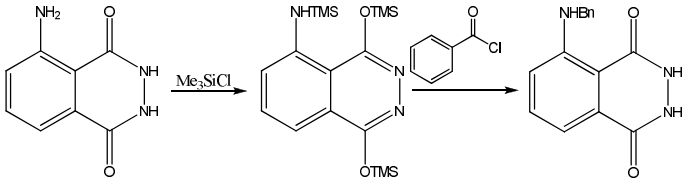

Figure 4.5: Scheme for the synthetic method used to try to obtain selectively a trimethylsilyl luminol derivative that was supposed to act as synthetic intermediate. Because an excess of the silicon compound was used (much more than three equivalents) the predominant product should be the exhibited one.

Regarding this derivatization of luminol, it was investigated not to get an isolatable derivative for chemiluminescence studies but to act as a synthetic intermediate to prepare other species. This was an extreme act because no successful results were being obtained, even when literature conditions were reproduced (by this time only studies on acetyl electrophiles and negative results with benzoyl chloride were performed). Because the TMS protecting group is quite unstable in water, the workup procedures so far documented would also remove the protective group. To induce complete trimethylsilylation of luminol, the reaction accounted with a great excess of trimethylsilyl chloride that acted also as solvent. This was an attempt to completely destroy the hydrogen bond between the carboxyl and the aniline functionalities, increasing therefore aniline's nucleophilicity.

[27] The reaction started with heating until reflux of a TMSCl luminol solution. Because even after ten minutes on reflux luminol remained practically undissolved, a catalytic amount of potassium iodide was added. Twenty minutes after, dichloromethane was added and once again no noticeable changes were observed. The situation remained like that for twelve hours and therefore, DMF was

added. Immediately after the addition, the reaction crude turned more viscous and changed its tonality to yellow, then orange and pink in the end. When the reaction mixture colour was strongly pink, the solvent was removed and both TEA and benzoyl chloride were added. The reaction mixture turned yellow, being a precipitate also formed. Therefore, water was added and a light orange precipitate was formed. After filtration, the solid was dissolved in acetone (became orange) and the solid crystallized. Even though that was a selective process, because simultaneously promising results were obtained in simpler reaction systems, studies on these conditions were abandoned.

4.8 - Benzoyl-Ortho-(Sulphonic Acid) Luminol

In respect to this luminol derivative only one experiment was performed, being this resumed in the scheme presented in Figure 4.6.

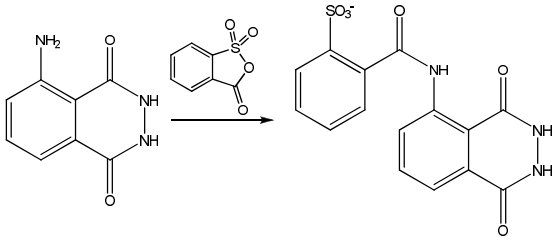

Figure 4.6: Scheme for the synthetic method used to attempt isolation of Benzoyl-Ortho-(Sulphonic Acid) Luminol.

[28] The reaction system consisted on TEA, 2-sulfobenzoic cyclic anhydride and luminol in a DMF solution. A yellow coloration seized the reaction crude when the latter was added but the TLC analysis (AcOEt) showed that no great develop from isolated reagents occurred. DMAP was therefore added to the reaction mixture but once again no further development was observed. We then decided to heat the reaction mixture leaving it under strong (but not turbulent) stirring. Twelve hours later a new spot appeared in the TLC plaque (EtOAc) but unfortunately no further development occurred within four days. No species isolation as well as other analyses were performed and therefore this luminol derivative was never obtained.

4.9 - Dimethylamine-Luminol Ureas

In respect to this section, it deals not with one but apparently with two distinct luminol derivatives obtained within similar reaction conditions. The experiments with dimethyl carbamic chloride were supposed to yield a luminol derivative that replaced phenylamine-luminol urea species, whose synthesis had recently turned out to be unsuccessful.

[29] The first experiment to report consisted simply in the direct addition of the electrophile to a luminol solution in DMF. A slight temperature rise was observed and the system acquired a pale

yellow coloration. Ninety minutes after the beginning of the reaction, TEA was added and afterwards a small spot below luminol's started to grow in the TLC analyses (AcOEt). After one night at 60 ºC and strong (but not turbulent) stirring, a pale yellow solid appeared inside the reaction vessel. Water was added but instead of precipitating, the solid dissolved completely, yielding a yellowish liquid. Both acidification and alkalinisation of that solution yielded no significant change and therefore we decided to completely evaporate the solvents and extract the desired species with hot (boiling) AcOEt. Ethanol was added to attempt a first crystallization procedure but because no crystals were isolated, both solvents were substituted by boiling ethanol and the solution left for crystallization. The NMR spectrum of the isolated crystals showed a singlet peak at 12.67 ppm with unitary integration, being this evidence for N (or O) substitution in luminol's structure. Besides, a duplet at 9.02 ppm, also with unitary integration, was present (due to chemical shift exhibited, this proton was assigned to be from an aldehyde like functionality). Regarding now pure aromatic peaks, the region was completely changed from luminol's fingerprint: a triplet at 7.90 ppm was superimposed with a duplet at 7.85 ppm, (with joint integration for two protons); a duplet at 7.65 ppm (one proton); a triplet at 7.49 ppm superimposed with singlet (7.45 ppm) with total integration for 2.5 protons. In the non-aromatic region, a singlet at 2.51 ppm (0.5 protons) and a triplet at 1.06 ppm (2.5 protons) were characteristic from the sample. A quartet superimposed with water's was also observed but no integration could be performed. 2D COSY experiment was also performed. This showed that the peak at 9 ppm was correlated with the aromatic peaks with higher chemical shift (7.90 ppm and 7.85 ppm). The quartet superimposed with water's peak also interacted with the triplet with lowest chemical shift (1.06 ppm). The spectrum composition clearly showed that a luminol derivative was obtained. Unfortunately, due to the presence of the peak at 9 ppm and also due to relative integration of saturated aliphatic protons, the desired substitution (urea) was not in principle obtained. To justify the peak at 9 ppm, the formation of the Vilsmeyer reagent with posterior reaction with luminol was evoked. Relatively to the other referred peaks, no plausible hypotheses were so far performed.

Regarding now the ^{13}C NMR spectrum of this sample, besides carbonyl and aromatics, two peaks at 56.52 ppm and 18.96 ppm were present being these possible evidence for the methyl groups. The odd result is the great difference observed in their chemical shifts, more common in ethyl groups.

Due to the cloudy results obtained in NMR experiments, the sample was dissolved in hot methanol and within one week, 1 mm edge crystals were collected. These are now waiting for X-ray analysis and the compound was named DMU1Lum.

[30] [31] In order to understand the behaviour of the system, two more experiences were performed. Those consisted of reproductions of the previous system but one had TEA right from the start while the other proceeded always without the amine. Both reaction systems were also at room temperature throughout time. By TLC analysis (AcOEt) it was verified that the system with TEA retained the exact same composition for four days. On the other hand, after that same period of time the other system (no TEA) presented a spot of a more polar compound. This species was isolated by the procedure reported for DMU1Lum but no pure sample was obtained yet (there is always a

contamination with luminol). Due to high solubility in methanol of both species, it's now being tested as crystallization solvent to isolate one of those species. NMR experiences performed to the impure sample showed that the most polar species possessed not only a different composition from luminol but also from DMU1Lum (aromatic peak disposition in ^{1}H NMR as well as ^{13}C NMR spectrum). Therefore, this sample was named DMU2Lum.

^{1}H NMR spectrum of this sample also presented a duplet at 13.77 ppm integrating for one proton and a large singlet at 11.32 ppm integrating for 3 protons. In respect to the duplet at lower field, it may be assigned to N2's proton, meaning that on the basis of this hypothesis, the desired type of substitution was achieved. According to COSY experiment this proton interacts with the proton at 9.28 ppm. With this chemical shift, the latter proton must also be assigned to an aldehyde like one. For that to be true, once again the Vilsmeyer reagent must be evoked in these reaction conditions. Regarding the large singlet at 11.32 ppm, it can be due to the hydrazide protons of the derivative as well as hydrazide protons (or aniline) from luminol. Regarding the aromatic region, a total of six protons are observed. An extremely intense singlet at 3.12 ppm (superimposed with water's) is also to be reported because it might be assigned to methyl groups. The presence of 6 aromatic protons appears to support the presence of two luminol aromatic nucleus in the media, proving the result from TLC analyses.

As for ^{13}C NMR spectra, both CPD and APT experiments were performed. The peaks from the reaction product were at 161.14 ppm, 152.89 ppm, 138.93 ppm, 135.34 ppm, 126.74 ppm, 120.80 ppm, 118.04 ppm, 115.27 ppm, 43.83 ppm and 37.19 ppm. The APT experience showed that peaks at 152.89 ppm, 135.34 ppm, 120.80 and 118.04 ppm correspond to quaternary or secondary carbons. From these data, either we assume that one carbon is somehow silenced in the spectrum (any product would have eleven and not ten carbons, five of those quaternary) or the substitution with Vilsmeyer reagent cannot be possibly verified. It is thus necessary to collect more information but prior to that, a purer sample must be obtained.

Spectra for both these derivatives are presented in Annex 4 – NMR spectra of DMULum's.

4.10 - Conclusions

Due to global results obtained, it is concluded that to synthesize a luminol derivative, not only luminol must be completely dissolved but also the electrophiles (and the media) must fulfil certain requisites. Latter results obtained seem to indicate that weak electrophiles do not reacted with luminol. That is for instance the case of 2-sulfo-benzoic cyclic anhydride. On the other hand, having an extremely strong electrophile is not a sufficient condition to achieve the desired goal. It is also necessary that after the first chemical attacks (or hydrolysis), the secondary product (nucleophilic) is not able to compete with luminol. When that condition is not fulfilled (phenyl isocyanate example), luminol proves its inability to act as a nucleophile and no product is isolatable, especially if other

variables act negatively on the system. Cases like trifluoroacetyl luminol derivative were successful because the secondary product, trifluoroacetate, was much less nucleophilic than luminol.

Regarding the results from benzoyl and acetyl luminol derivatives, they seem to be somewhat contradictory. It is known that benzoyl chloride is much less reactive than acetyl chloride, not only due to stereochemical hindrance but also because the aromatic ring reduces the electronegativity of the carboxyl group. Therefore, it would be expectable to isolate acetyl luminol and not benzoyl luminol. Therefore, to account for the inability to isolate acetyl luminol we rely on the inadequacy of the analytical methods applied. On the basis of this hypothesis is also TFALum. During its synthesis, we verified that no TLC was able to distinguish the product from luminol, not only due to similarity in Rf but also due to the same tonality presented during TLC plaque revelation. Transposing those results to acetyl luminol, we assume that at least in some systems the product was achieved but it was indiscernible from the reagent in the performed analyses. Because the chemiluminescence properties of acetyl luminol have already been previously described,[8] no great efforts regarding this product's isolation were performed. The aim of this derivatization was merely to tune up and to study the spectrum of available reaction media.

Still regarding the nucleophilicity subject, activation of luminol with TMSCl (in DMF) seemed to be an efficient process when no other methodologies work. As an act of desperation, these reaction conditions should be carefully explored. Another hypothesis is the use of silver nitrate for chlorine electrophiles activation. Apparently, this procedure worked well but at the cost of releasing silver (that is hard to remove from solids) and partly oxidizing luminol.

Also, from the TFALum system, we verified that both pyridine and TEA were equally efficient bases to promote the reaction. Perhaps because when TEA was used the product started to precipitate, this amine presents some advantages towards pyridine at the laboratorial level. Unfortunately, this statement is based only on few observations and more results are needed to prove its veracity. Besides its nature, the amount of base is also an important factor. When comparing all studied systems (*cf.* reaction yields in section 3.3) we have verified that when TEA is not in excess, the reaction yield significantly decreases. The addition of a smaller amount of base came from an error that propagated throughout the whole synthetic work. From the last two examples reported, we verify that the system must at least be slightly alkaline. If that is not observed, then the Vilsmeyer reagent is quite probably formed and "strange" reactions occur (unknown products). Besides, if the base amount is not sufficient, luminol may start to act as base and the reaction yield is significantly decreased. On the other hand, the base addition should not be in extreme excess because when sufficient amount of base is added in aprotic media, luminol starts to react with molecular oxygen in a luminescent fashion.[10,22] For that light emission to be observed, high amounts of base must be added but from our laboratorial experience, high amounts of base are not necessary for luminol to decompose in dark reaction pathways. In neutral solution of luminol in DMSO, significant decomposition occurs after two weeks if the flask is closed and base catalyses that decomposition process.

5 - Computational Chemistry

Luminol can exist in several tautomeric forms. Even though the crystallographic data shows that one of those structures is preponderant (tautomer B),[35] calculations on each tautomeric form should be performed to determine the relative stability in both vacuum (gas phase) and solution phases. Figure 5.1 shows six tautomeric forms of luminol in different conformations. Calculations to determine the stability of those structures were performed right after determination of the best method and basis set for both geometry optimizations and single point energy (SPE) calculations.

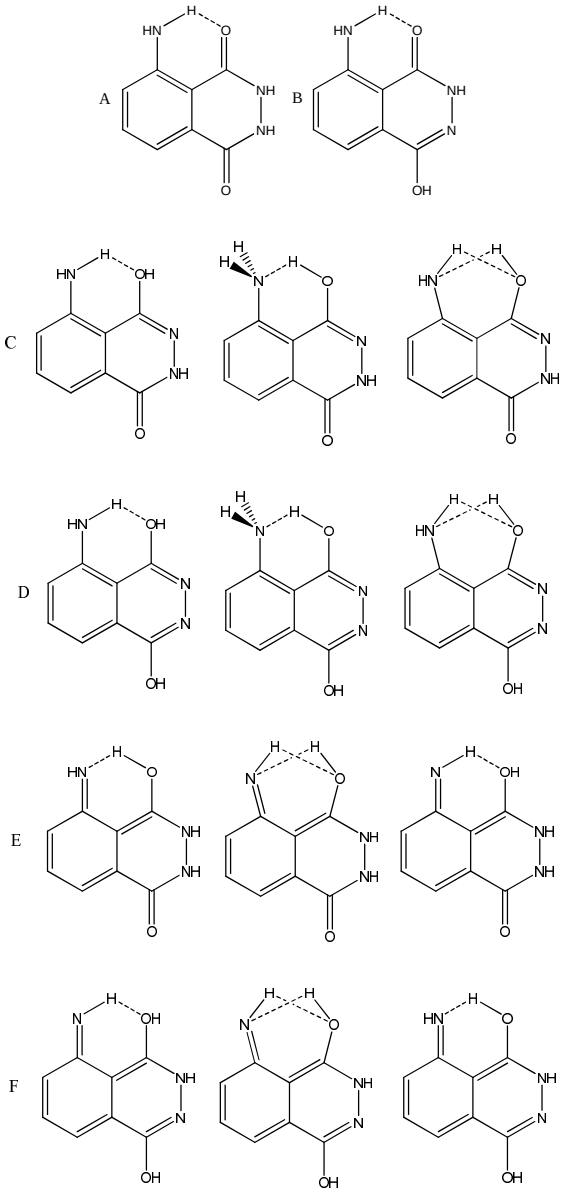

Figure 5.1: Considered tautomeric and conformational forms for luminol. When one tautomer exists in more than one conformation the nomenclature adapted was 1, 2 and 3 from left to right. As a title of example, tautomer C exists in forms C1 (the one from the left), C2 (middle structure) and C3 (right). If hydrogen bonding should be present it was represented by dashed line.

5.1 - Computational Details

All geometry optimizations in this work were performed using Gaussian 03 Revision C.02 program package.[44]

To determine the best computational methods for structure optimization we used as reference luminol's solid state structure.[35] Optimizations were performed with the 1996 one parameter exchange functional of Perdew, Burke and Ernzerhof combined with the 1996 gradient-corrected correlation functional of the same authors (PBE1PBE hybrid functional),[45] Becke's three parameter exchange functional with gradient-corrected correlation functional of Lee, Yang, and Parr, Density Functional Theory (DFT)/Hartree-Fock (HF) hybrid functional (B3LYP),[46,47] HF and Möller-Plesset second order perturbation theory.[48] In all these methods both Pople's (6-31G**, 6-311++G**) and Dunning's (cc-pVTZ) basis sets were used.[48] The augmented version of Dunning's basis set (aug-cc-pVTZ) were also tested for PBE1PBE method but no result was obtained within 2.5 days (structure optimizations would be too slow to get results in useful time).

For tautomer and acid-base analysis, HF (6-31G** and cc-pVTZ), PBE1PBE (6-31G**) and MP2 (6-31G**) levels of theory were used in geometry optimizations. Only the latter results are presented.

MP2 with diffuse basis set calculations (6-311++G** and aug-cc-pVTZ) and MP4/6-311++G** calculations were tested for SPE. Due to time expensiveness of the last method, no result was obtained within useful time. Therefore, only MP2 (with different basis sets) is evaluated. In these SPE calculations geometries from MP2/6-31G** calculations were used. Charges are analysed using natural bond orbital population analysis for the most refined basis sets.

Solvent effects were taken into account in SPE calculations on the basis of the vacuum MP2/6-31G** geometries. Both polarisable continuum model (PCM)[49] and continuous polarisable continuum model (CPCM)[50] methods were tested for MP2/aug-cc-pVTZ level of theory during method determination. For the rest of calculations in this work only the PCM model was used. The solvents used in calculations were DMSO and water. Gibbs free energy differences were calculated neglecting the solute dissolution entropy, *i.e.*, according to equation (1).

$$\Delta_{solution}G = \Delta_{gas}G + \left(\Delta E_{solution} - \Delta E_{gas}\right) \quad (1)$$

In equation (1), $\Delta_{solution}G$ stands for the Gibbs free energy difference between two tautomeric species in solution phase, $\Delta_{gas}G$ for Gibbs free energy difference between two tautomers in gas phase. $\Delta E_{solution}$ is the difference between the electronic energies of the two tautomers in solution and ΔE_{gas} the electronic energy difference between two tautomers in gas phase. The latter term (in parenthesis) consists on the dissolution Gibbs free energy of both tautomers. The same equation was applied to acid-base equilibria with the necessary adjustments.

All calculations were performed using restricted approximations for closed electron shells.

The Hessian matrix was calculated analytically for the optimized structures at all levels of theory in order to prove the exact location of correct minima in potential energy surfaces (only positive frequencies) and to estimate thermodynamic parameters, the latter calculated at 298.15 K and 1 atm.

Regarding time dependent (TD) calculations to determine absorption spectra, two main methods were employed: DFT using PBE1PBE hybrid functional and *ab initio* with Hartree-Fock. In both sets of calculations, both vacuum and solvent's dielectric calculations were performed. In all cases, augmented version of Dunning's triple zeta wavefunctions was used. These calculations were performed on previously optimized MP2/6-31G** geometries and are only presented in section 6.1.4.

5.2 - Method and Basis Set Determination

The first part of this computational work was the determination of the best computational method for both geometry optimizations and single point energy calculations.

As previously referred, the best method for geometry optimizations was determined by comparison of calculated bond distances and the geometry determined by X-Ray crystallography.[35] Geometry optimizations were performed with both PBE1PBE and B3LYP DFT/HF hybrid methods and with HF and MP2 *ab initio* methodologies. The basis set tested for geometry optimizations were 6-31G**, 6-311++G** and cc-pVTZ. The augmented version of Dunning's basis set (aug-cc-pVTZ) was tested for PBE1PBE functional but due to time expensiveness of the calculation, no result was obtained. The MP2/cc-pVTZ calculation was also stopped due to the same inconvenient. Table 5.1 resumes the information concerning geometry optimizations with all the different methods. When a negative vibrational frequency was obtained, the usual procedure to remove it was by perturbation of the optimized geometry with a fraction of the negative vibration vector, typically 10-20%.

Table 5.1: Resume of all the information concerning geometry optimizations. HF calculations had as starting geometry the one optimized with PBE1PBE/6-31G** calculation. MP2 calculations were performed using optimized PBE1PBE/6-31G** and B3LYP/cc-pVTZ geometries. N in the penultimate column is the number of steps, for the calculation to converge. All calculations were performed using 1000 MB in 2 processors.

Method		Δt (s)	Comment	N	Energy (a. u.)
PBE1PBE	6-31G**	4.5×10^3	Negative Frequency Aniline	8	-623.110939
		4.5×10^3	---	11	-623.110939
	6-311++G**	16.6×10^3	Negative Frequency Aniline	8	-623.261578
		17.3×10^3	---	19	-623.261586
	cc-pVTZ	57.2×10^3	Negative Frequency Aniline	8	-623.311549
		56.6×10^3	Sum 10% Negative Frequency. Converged to same structure as subtraction	9	-623.311554
		53.6×10^3	Subtraction 10% Negative Frequency	4	-623.311553
B3LYP	6-31G**	4.5×10^3	Negative Frequency Aniline	8	-623.796394
		4.5×10^3	Sum 10% Negative Frequency. Converged to same structure as subtraction	10	-623.796409
		4.5×10^3	Subtraction 10% Negative Frequency	10	-623.796409
	6-311++G**	16.1×10^3	Negative Frequency Aniline	7	-623.962312
		16.1×10^3	Sum 10% Negative Frequency. Converged exactly to same structure as subtraction	6	-623.962326
		16.0×10^3	Subtraction 10% Negative Frequency	5	-623.962326
	cc-pVTZ	54.3×10^3	Negative Frequency Aniline	9	-624.011969
		57.5×10^3	Sum 10% Negative Frequency. Converged exactly to same structure as subtraction	6	-624.011978
		55.1×10^3	Subtraction 10% Negative Frequency	4	-624.011978
HF	6-31G**	1.4×10^3	---	20	-620.123382
	6-311++G**	7.0×10^3	---	14	-620.264336
	cc-pVTZ	40.5×10^3	---	15	-620.324854
MP2	6-31G**	91.2×10^3	---	12	-622.008653
	6-311++G**	35.6×10^3	---	16	-622.269179

Table 5.2 compiles the relevant data for SPE calculations. Optimized MP2/6-31G** geometry was used in these calculations. Table 4 includes single points in solution with both PCM and CPCM methods.

Table 5.2: Resume of SPE calculations on luminol's tautomer B. Geometry for these calculations was the optimized in MP2/6-31G** method. All calculations were performed using 1000 MB in 2 processors.

Method		Δt (s)	Energy (a. u.)
MP2	6-311++G**	2.5×10^3	-622.268863
	aug-cc-pVTZ	101.8×10^3	-622.686500
MP2/aug-cc-pVTZ	PCM (H_2O)	102.3×10^3	-622.713630
	CPCM (H_2O)	100.8×10^3	-622.7138795
MP2/aug-cc-pVTZ	PCM (DMSO)	102.4×10^3	-622.713009
	CPCM (DMSO)	99.7×10^3	-622.713428

From the first table it is verifiable that both DFT methods are practically equivalent in terms of time and number of steps (N) to convergence. In these examples, B3LYP was able to remove easier the negative frequency obtained in the first calculation than PBE1PBE functional. From the available data, time and iteration efficiency is the same for both DFT methods applied.

In respect to *ab initio* calculations, MP2 calculations were much slower than HF ones. Even with that drawback, the number of steps to converge with MP2 was smaller. Because the energy for each structure obtained with MP2 calculations should be better (closer to reality) than the one obtained using HF calculations, the former method was preferred. It should also be referred that in *ab initio* geometry optimizations no negative frequency was obtained. Its appearance was related with amino (more specifically, aniline) functionality isomerisation.

As for single point energy calculations, only MP2 methods were tested. From Table 5.2 results, it is verifiable that Dunning's diffuse basis set led to a much more time expensive calculation when compared to Pople's basis set. Because the computational cost for the former basis set was affordable and due to its higher accuracy, Dunning's basis set was preferred. Regarding solution calculations, CPCM model was slightly slower than PCM (expected due to higher simplicity of the latter) but yielded no great difference in the energy of the system from the latter model (the energetic difference between luminol's tautomer B using CPCM and PCM models is less than 0.3 $kcal.mol^{-1}$). Another curious result is that CPCM model had more effect in DMSO calculation than in water. This would then mean that consideration of charges within the spheres around atoms or functionalities would not be significant to describe luminol's behaviour in solvent's dielectric constant.

Regarding geometry accuracy of the methods, Table 5.3 presents five geometrical parameters that will allow comparison between optimized geometries and experimental (crystallographic) results. For optimized geometries bond distances please check Annex 5 – Tautomer B optimized geometries. Figure 5.2 gives atomic labelling that will allow Table 5.3 interpretation. This figure also defines two parameters given in the referred table, distance d (hydrogen bonding distance) and dihedral angle θ.

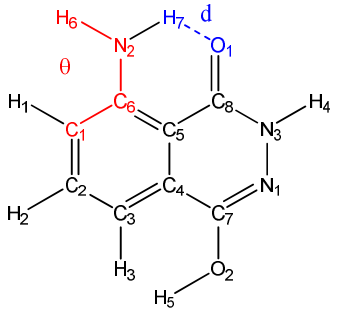

Figure 5.2: Atom labelling for luminol's tautomer B that allow Table 5.3 interpretation. Definition of distance d and dihedral angle θ.

Table 5.3: Resume of all the information concerning SPE calculations on luminol's tautomer B. Atom labelling that allows interpretation is in Figure 5.2. M. D. Is the Maximum Deviation between calculated and experimental bond distance. m. D. Is the minimal Deviation between calculated and experimental bond distances. Below each deviation value is the correspondent bond distance (*cf.* Figure 5.2). Av. is the averaged value for absolute bond distance deviation (all bonds in Annex 5 table excluding the ones with hydrogen atoms). d and θ are both defined in Figure 5.2.

Method		M. D. (Å)	m. D. (Å)	Av. (Å)	d (Å)	θ (degree)
PBE1PBE	6-31G**	3.13×10^{-2} (N3-C8)	-1.33×10^{-3} (C7-N1)	1.11×10^{-2}	1.870	3.219
	6-311++G**	-3.03×10^{-2} (N3-C8)	3.00×10^{-3} (C4-C7)	1.11×10^{-2}	1.894	7.827
	cc-pVTZ	3.13×10^{-2} (C8-O1)	1.00×10^{-3} (C4-C7)	1.07×10^{-2}	1.869	5.223
B3LYP	6-31G**	3.93×10^{-2} (N3-C8)	2.33×10^{-3} (C3-C4)	1.21×10^{-2}	1.895	10.627
	6-311++G**	3.83×10^{-2} (N3-C8)	3.33×10^{-4} (C3-C4)	1.17×10^{-2}	1.923	8.350
	cc-pVTZ	3.33×10^{-2} (N3-C8)	-2.00×10^{-3} (C4-C5)	1.09×10^{-2}	1.905	8.409
HF	6-31G**	-5.03×10^{-2} (C8-O1)	-1.67×10^{-3} (C5-C6)	1.38×10^{-2}	1.982	15.899
	6-311++G**	-5.53×10^{-2} (C8-O1)	2.33×10^{-3} (C1-C6)	1.44×10^{-2}	1.996	17.841
	cc-pVTZ	-5.53×10^{-2} (C8-O1)	-6.67×10^{-4} (C1-C6)	$1.44\text{x}10^{-2}$	1.984	17.838
MP2	6-31G**	3.73×10^{-2} (N3-C8)	1.00×10^{-3} (C4-C5) -1.00×10^{-3} (C4-C7)	1.20×10^{-2}	1.920	26.299
	6-311++G**	3.93×10^{-2} (N3-C8)	0.00 (C4-C7)	1.42×10^{-2}	1.928	25.593

From Table 5.3 we can easily verify that for DFT methods, whichever basis set is chosen, PBE1PBE calculation yields molecular geometry closer to the experimental one. In every calculation, hydrogen bonding and dihedral angle θ are always higher in B3LYP calculations. Because the experimental results are (unit cell has three luminol molecules with distinct d and θ values) d=1.872, 1.936, 1.846 Å and θ=32.2, 32.3, 1.4 º,[35] once again PBE1PBE calculation yields better estimations to

hydrogen bonding bond distance. Unfortunately, that functional has higher error in the dihedral angle estimation. Because the tendency to optimize the transition state for aniline isomerisation is directly related to the dihedral angle of that functionality, we can justify the fact that B3LYP removed the negative vibrational frequency in an easier fashion (even though both calculations have first optimized a transition state structure). Because the global time and iteration efficiency are similar in both B3LYP and PBE1PBE, the method selected for DFT calculations in luminol system was the latter. As for basis set in DFT calculations, the latter table also shows that in averaged terms both Pople basis sets are equally equivalent being the Dunning basis set slightly better. As for maximum deviation in bond distances, Dunning's basis set was better than Pople's. Because (maybe by chance) PBE1PBE/6-31G** calculation yielded the best prediction to hydrogen bonding bond distance and because none of these DFT calculations predicted correctly the dihedral angle, for initial studies in luminol, PBE1PBE/6-31G** calculations should be used.

In HF calculations, maximum and minimum deviations are typically worse than in other calculations (better than DFT calculations in minimum deviation). As for MP2, we verified that it was the best of all methods applied in respect to bond distances deviation (towards the experimental value). Regarding the hydrogen bond, MP2 calculation is at the same level as B3LYP being HF calculations between PBE1PBE calculations and MP2. In the dihedral angle, MP2 yielded the best result in averaged terms, being this result completely different from the results from any other theoretical calculation. HF calculations yielded angles smaller than MP2 by 10º being also better than DFT predictions. Regarding the basis set effect in HF method, we verified that non-diffused basis sets yield globally better results than the diffuse basis set tested. 6-31G** and cc-pVTZ geometry optimizations were curiously equivalent. As for MP2 calculations, even though the minimum deviation is given by the best value possible, due to other parameters, we can state that MP2/6-31G** calculation yielded the best result.

Given all these results, initial studies in this system may be performed with PBE1PBE/6-31G** calculation. MP2/6-31G** geometry optimization should be performed using as starting geometry (if available) the one obtained from DFT calculation. Eventually, both HF/6-31G** and HF/cc-pVTZ calculations can be performed but the energy values are expected to be extremely inaccurate. From all these methods, it was chosen to present just MP2 geometry optimization parameters. To refine theoretical results, single point energy calculations for vacuum and solution using MP2/aug-cc-pVTZ method should be performed. As for solvation model, Tomasi's PCM was selected because it gives slightly less computational time cost and yields the same result as CPCM.

5.3 - Tautomer Stability

After defining the best methods to study luminol's system, calculations on Figure's 5.1 structures could be performed. All tautomers in their conformations were optimized using PBE1PBE/6-31G**, HF/6-31G**, HF/cc-pVTZ and MP2/6-31G** methods but only MP2 results are

presented. When the MP2/6-31G** geometry was found, SPE calculations using the previously referred methods (MP2/aug-cc-pVTZ and PCM solvation) were employed. Only information regarding the most stable conformer for each tautomer will be presented.

Table 5.4 gives the Gibbs free energy (in kcal.mol^{-1}) between all luminol's tautomers. Tables comprising electronic energy, enthalpy and entropy relations between these structures are presented in Annex 6 – Energetic parameters between luminol's tautomers.

Table 5.4: Gibbs free energy difference between all luminol's tautomers in their respective conformations (when the conformer was computationally stable). The notation used in this table was $\Delta G_{X\rightarrow Y} = G_Y - G_X$. Therefore $\Delta G_{X\rightarrow Y}$ stands for the transformation of species Y to species X. Geometry optimizations performed in 6-31G** and SPE's with aug-cc-pVTZ basis sets. Energies in kcal/mol.

	MP2 OPT	Gas (SPE)	DMSO (SPE)	H_2O (SPE)
B→A	5.31	7.24	5.25	5.16
C1→A	1.73	3.39	3.21	3.29
D1→A	-5.06	-2.34	-3.33	-3.22
E2→A	-44.74	-42.35	-40.21	-39.69
F2→A	-39.18	-34.20	-33.45	-33.01
C1→B	-3.58	-3.85	-2.04	-1.86
D1→B	-10.37	-9.58	-8.58	-8.38
E2→B	-50.05	-49.59	-45.46	-44.84
F2→B	-44.49	-41.44	-38.70	-38.16
D1→C1	-6.79	-5.73	-6.54	-6.52
E2→C1	-46.48	-45.74	-43.42	-42.98
F2→C1	-40.91	-37.59	-36.66	-36.30
E2→D1	-39.69	-40.01	-36.88	-36.47
F2→D1	-34.12	-31.86	-30.12	-29.78
F2→E2	5.56	8.15	6.76	6.68

From the latter table, the first result to take is the fact that luminol's tautomers E and F (with higher imine character) are the less stable ones. The difference in Gibbs free energy towards tautomer B (the most stable in both gas and solution phases) is at least 38 kcal.mol^{-1}. For SPE calculations, towards gas phase, luminol's tautomers E and F are more stabilized by each solvent's dielectric than tautomer B. Because in all those phases the energetic gap (in Gibbs free energy) between tautomer B and those imine tautomers is extremely high, they can be completely neglected. At the equilibrium situation at 298 K, luminol's tautomer B will be at least 8.28x10^{32} times more concentrated than E (water dielectric's constant calculation) and 1.03x10^{28} times more concentrated than tautomer F, proving that point.

With respect to other tautomers, A, B, C and D, as referred, in gas phase the most stable tautomer is B, according to all theoretical models. When in solvent's dielectric the stability order of those species is maintained changing just the absolute energy values (and their differences). In

solution, tautomer A (structure usually assigned to luminol) is six thousand times less abundant than tautomer B and therefore can be completely neglected in further studies. In respect to tautomer C, completely analogous to B but with the enol group closer to the aniline functionality, it is 3.58 kcal/mol less stable in gas phase. In solution, the energetic gap decreases to 2 kcal.mol^{-1} in both solvents, meaning that at 298 K, tautomer C should be 422 times less concentrated than tautomer B in gas phase. In solution, it should only be 23 times less concentrated (value from SPE in water). Due to the usual error associated in theoretical calculations (1 kcal/mol), tautomer C can be relevant enough to describe the ground state of luminol systems. Regarding the aromatic tautomer of luminol, D, it appears that the aromatic driving force is not strong enough to beat the two carbonyl or even the one carbonyl (and one enol) functionality stabilization. D is therefore completely neglectable when compared to tautomers B, C or even A. Curiously, the energetic discrepancy between tautomer D and the others referred appears to decrease from gas to solution phases (except towards A).

To resume the last paragraph, Diagrams 5.1 and 5.2 are presented with SPE calculation results. G values presented in these diagrams are relative to the G for the most stable species in analysis (B), being therefore ΔG's.

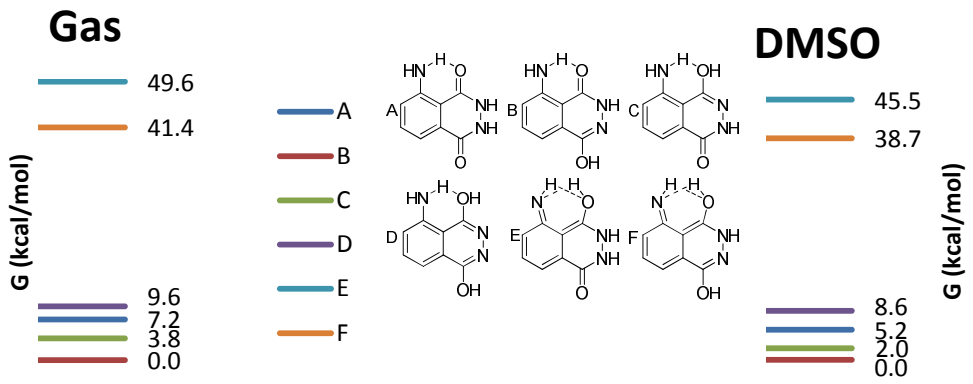

Diagram 5.1: Energetic relationship between luminol's tautomers in gas phase and DMSO according to MP2/aug-cc-pVTZ calculations.

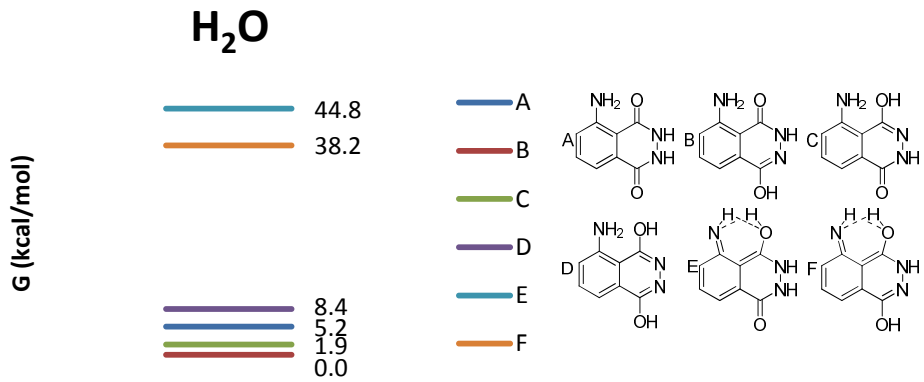

Diagram 5.2: Energetic relationship between luminol's tautomers in water according to MP2/aug-cc-pVTZ calculations with PCM solvation model.

According to the theoretical models applied, the dissolution behaviour of luminol in both DMSO and water should be approximately the same (the discrepancy in total energy is almost the same for the interaction of the structure with both solvent's dielectric). Therefore, the results in those two distinct media should be the same and only one will be analysed. We chose to follow DMSO's dissolution of luminol

To give a better insight in the system that will allow us an understanding of the relative stability of luminol's tautomers, a series of geometrical and electronic data will be presented. While Figure 5.3 gives a scheme of a generic luminol structure (with different atom labelling from the one in Figure 5.2), Table 5.5 will provide geometrical parameters regarding all tautomers (interpretation of Table 5.5 is dependent of Figure 5.3). Table 5.6 gives both CO and CN bond distances regarding functionalities in heterocyclic ring of luminol, ring 2. Finally, Table 5.7 provides the charge density in each luminol's atom in all its tautomers also according to Figure's 5.3 atom labelling. Proton charges were deliberately omitted. Charges given, result from SPE calculations (MP2/aug-cc-pVTZ both in vacuum and DMSO) on the optimized MP2/6-31G** geometry using NBO population analysis.

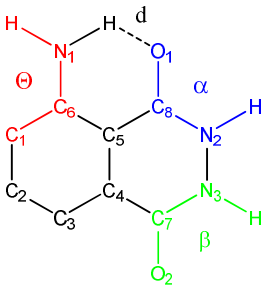

Figure 5.3: Luminol's skeleton with definition of α, β and θ angles. This figure acts as Table 5.5 support.

Table 5.5: Geometrical parameters regarding luminol's tautomers in (when applicable) some of their conformations for MP2/6-31G** level of theory. If α or β are in red it's because the respective oxygen atom is bonded to a proton. It should be denoted that due to sterical hindrance, hydrazide protons are in different sides of the heterocycle plan (only positive values for every angle are presented).

Tautomer	D	α	β	Θ
A	1.929	24.762	25.967	24.759
B	1.920	1.189	0.523	26.299
C1	1.982	0.769	0.527	27.192
D1	1.989	0.74	0.457	26.776
E2	2.139 | 2.393	35.013 | 13.066	26.815	14.052
F2	2.087 | 2.381	0.610 | 12.476	0.58	28.217

Table 5.6: Bond distances for C8-O1, C8-N2, C7-O2 and C7-N3 according to Figure's 5.3 atom labelling for MP3/6-31G** level of theory.

Tautomer	C8-O1	C8-N2	C7-O2	C7-N3
A	1.242	1.383	1.233	1.385
B	1.246	1.376	1.360	1.304
C1	1.370	1.302	1.236	1.380
D1	1.368	1.316	1.357	1.318
E2	1.345	1.364	1.229	1.398
F2	1.344	1.345	1.352	1.312

Table 5.7a: Charges in atomic units for each luminol atom for tautomers A, B and C in their most stable conformations. To get the values in Coulomb (C), multiply the value in the table by $e = 1.60217653(14) \times 10^{-19} C$. Charge densities were obtained with MP2/aug-cc-pVTZ SPE calculations on the optimized MP2/6-31G** geometry and with NBO population analysis.

	A		B		C	
	Vacuum	DMSO	Vacuum	DMSO	Vacuum	DMSO
C1	-0.602	-0.613	-0.617	-0.61	-0.692	-0.678
C2	-0.226	-0.183	-0.241	-0.23	-0.179	-0.165
C3	-0.93	-0.962	-1.045	-1.046	-0.942	-0.954
C4	1.162	1.231	1.639	1.649	1.134	1.168
C5	0.968	0.924	0.832	0.831	1.291	1.28
C6	0.591	0.603	0.729	0.697	0.7	0.67
C7	0.152	0.266	-0.036	-0.019	-0.058	-0.083
C8	-0.064	0.039	-0.241	-0.264	-0.254	-0.232
N1	-0.741	-0.771	-0.762	-0.773	-0.748	-0.755
N2	-0.015	-0.038	0.493	0.48	-0.798	-0.826
N3	-0.04	-0.061	-0.862	-0.889	0.388	0.377
O1	-0.844	-0.995	-0.94	-0.983	-0.507	-0.53
O2	-0.869	-1.017	-0.543	-0.571	-0.968	-1.028

Table 5.7b: Charges in atomic units for each luminol atom for tautomers D, E and F in their most stable conformations. To get the values in Coulomb (C), multiply the value in the table by $e = 1.60217653(14) \times 10^{-19} C$.Charge densities were obtained with MP2/aug-cc-pVTZ SPE calculations on the optimized MP2/6-31G** geometry with NBO population analysis.

	D		E2		F2	
	Vacuum	DMSO	Vacuum	DMSO	Vacuum	DMSO
C1	-0.674	-0.66	-0.57	-0.573	-0.553	-0.563
C2	-0.244	-0.23	-0.354	-0.35	-0.384	-0.381
C3	-0.839	-0.842	-0.998	-1.008	-0.971	-0.987
C4	1.257	1.268	1.412	1.438	1.53	1.546
C5	1.04	1.031	1.166	1.12	1.15	1.129
C6	0.71	0.68	0.968	0.925	0.963	0.909
C7	-0.044	-0.046	-0.05	-0.04	0.098	0.124
C8	-0.229	-0.225	-0.255	-0.188	-0.545	-0.507
N1	-0.746	-0.754	-1.191	-1.234	-1.199	-1.245
N2	-0.457	-0.51	-0.072	-0.072	0.406	0.392
N3	-0.507	-0.556	0.034	0.033	-0.882	-0.895
O1	-0.513	-0.534	-0.642	-0.647	-0.581	-0.589
O2	-0.552	-0.576	-0.883	-0.94	-0.549	-0.581

The parameters that more closely should be related to the relative stability of each species should be electronic delocalization, aromaticity, (intramolecular) hydrogen bonding between the aniline/imine group and the carboxyl/enol functionality closest and carboxyl Vs. enol stabilizations (namely comparison between CO and CN bond orders and the relative presence of OH Vs. NH groups, regarding functionalities in luminol's heterocycle).

To justify the energetic discrepancy between tautomers E and F towards tautomers A, B, C and D we can easily argue with the aromaticity stabilization. Due to their high imine character in the carbonated ring (ring 1), the aromatic character should decrease. From charge analysis it is verifiable that the global charge in the atoms directly in ring 1 is positive and at least 0.23 a. u. higher than in other tautomers (case of tautomer E in DMSO towards tautomer D also in DMSO). Another important and related parameter is the decrease in N1's electronic density from tautomers A, B, C and D to tautomers E and F, *i.e.*, acquisition of higher anionic character by this nitrogen atom. This indicates a reduction of the electronic delocalization and therefore an increase of the total energy for the species. These three factors in conjugation should account for the high energetic discrepancy. Besides, hydrogen bonding in these species is also weaker than in the rest of tautomers. To energetically distinguish tautomers E and F we may use for instance the electronic density in ring 2. From table 5.7, the global charge of atoms directly in ring 2 is higher in tautomer E than in F. Because ring 2 concentrates most of luminol's electronegative atoms, lower charge means higher structure stability. The relative stabilization of tautomer E towards F from vacuum to DMSO is justified by the fact that the solvent provides dipole-dipole interactions that stabilize the polar structure of E. In respect to

electronic delocalization (by analysis of angles provided in Table 5.5) it is expected to decrease in ring 2 from tautomer F to E being another factor that may account for the relative stability between those two species.

The relative stability of tautomer D towards the others can be accounted by the weakening of the hydrogen bond and the high single CO bond character. Plus, the fact that oxygen atoms have electronic density closer to zero means that the most electronegative atoms are not the ones with higher electronic population. The aromaticity extent in tautomer D can be verified by the fact that CN bond distance ("hydrazide" moiety) is in the middle of pure CN single and double bonds.[51] By comparison, we verify that the electronic delocalization should be similar in D, B and C leading to no great distinction between the species. Therefore, hydrogen bonding is the main factor affecting tautomer D. To account for the relative energetic discrepancy between tautomers D and B from gas to DMSO phases we use the relative charge on nitrogen's N1. This can also be the justification for the observed decrease in ΔG from gas to DMSO between tautomer B and tautomers A and C. In tautomer B, this nitrogen atom (naturally electronegative) acquires less amount of electronic density from gas to solution phase, being also in B where that atom has positive charge.

Comparing now C and B, in terms of C=O Vs. C=N and OH Vs. NH, no great distinction can be provided. Both species have the same functionalities but in distinct regions of the molecule. Charge analysis shows that in both media, tautomer B has less electronic density in ring 1, being that electronic population more localized in ring 2. Due to the relative electronegativity of the atoms involved, tautomer B should therefore be more stable than C. The fact that from gas phase to DMSO dielectric's constant tautomer B ring 2 loses more electronic density than tautomer C may account for the observed decrease of the energetic gap between those two species. Besides, hydrogen bonding can also be used to account for the energetic difference between those species. Table 5.5 shows that in tautomer C, hydrogen bonding between O1 and the aniline's proton is weaker than in B. This should be preponderant for the relative stability of that structure (note that tautomer A has stronger hydrogen bonding than C and even so it is not as stable).

To justify the relative stabilities of A and B in both gas and DMSO phases we need several factors. The slightly stronger hydrogen bond in B and the higher electronic delocalization in B should play important roles. The fact that species A has higher positive charge in ring 2 shows once again that electronic densities should be quite localized, avoiding stabilization of the whole structure. The C=O Vs. C=N bond factor should not be preponderant in this case because B (with only one carboxyl group) is more stable than A (two carboxyl functionalities). When passing from gas to DMSO the global electronic density in ring 2 is enhanced in tautomer A while in tautomer B it is decreased. This would mean that from Gas to DMSO, A allows higher electronic delocalization by its two rings and the most electronegative atoms will receive more electronic density (in both cases, oxygen atoms negative charge is increased). Due to the presence of a proton in tautomer's B O2, the charge density enhancement in that functionality is much less pronounced avoiding the interaction of a plausible dipole with the solvent's dielectric.

Regarding other studies, the relative stability of luminol's tautomers has recently been studied in the literature but without considering the two less stable species.[52] It was also performed in quite different conditions, namely the optimization methodology employed (B3LYP with Pople's diffused triple zeta basis set, 6-311++G**) and in water using specifically three water molecules (and less) without considering the "solvent's dielectric constant". Each water molecule was positioned next to the amino group and the hydrazide moieties. The results therein obtained indicate that luminol's tautomer A is 1.8 kcal.mol^{-1} less stable than tautomer B, being C 3.5 kcal.mol^{-1} less stable than B. Tautomer D, according to the literature, is 10.6 kcal.mol^{-1} less stable than B. Comparing to our results, significant differences arise in the middle term stability species, A and C. Because the differences in theoretical methods are mainly related to the description of the π system and the hydrogen bond, then a tenuous game between those two parameters determine the relative stability of those two tautomers.

5.4 - Acid-Base Studies

After determining the most stable neutral structures of luminol, acidity studies should be performed because the first two steps occurring in the oxidation mechanism of these systems are, at least in DMSO, acid-base ones. Therefore, ten conjugated bases of luminol were optimized, being those mono-, di- and one trianionic. These species came from luminol's tautomers A, B and C. In Figure 5.4 we present the acid-base equilibria studied and we assign a plausible origin for the base conjugates. The selected acids for this figure are luminol's tautomers A and B because A is the structure commonly assigned to luminol and B is its most stable tautomer.

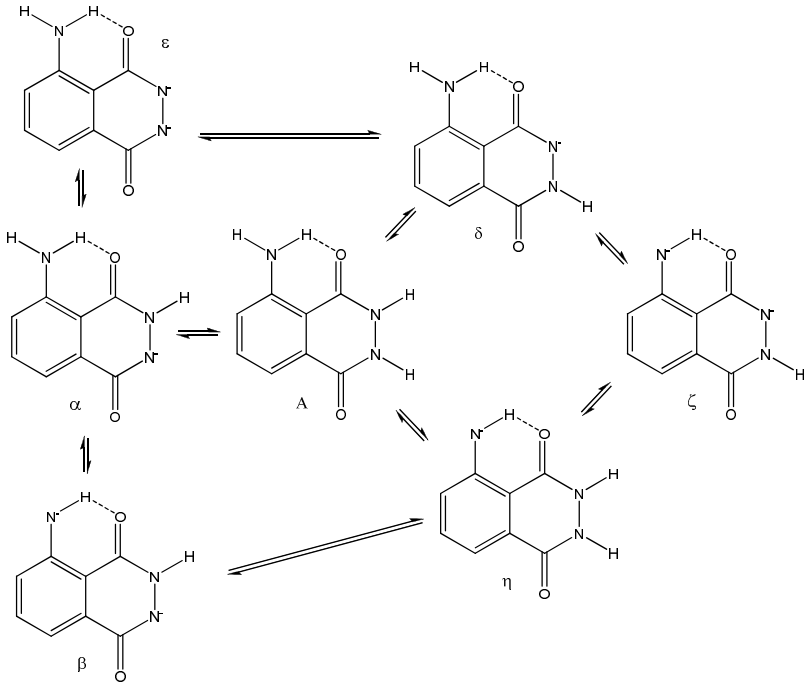

Figure 5.4a: Mono- and dianionic acid-base derivatives of luminol's tautomer A.

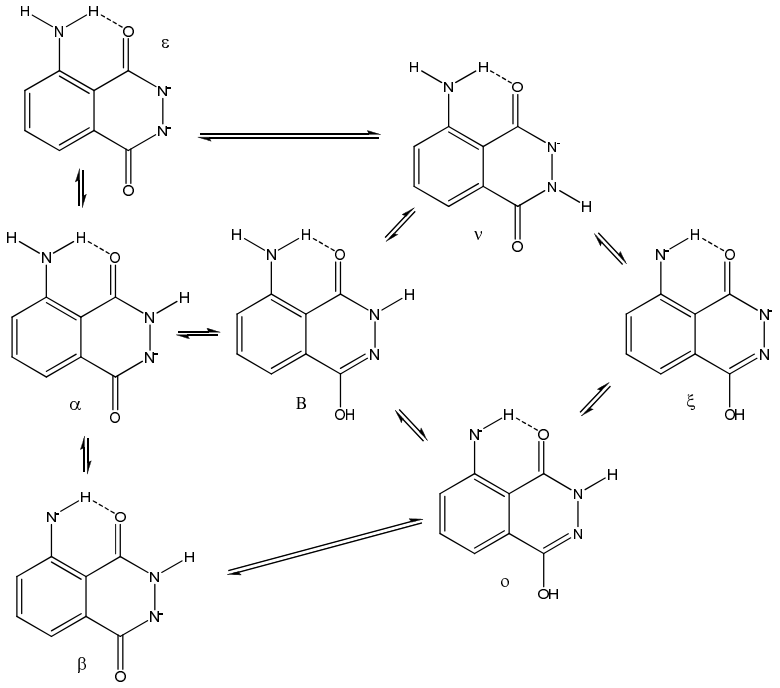

Figure 5.4b: Mono- and dianionic acid-base derivatives of luminol's tautomer B.

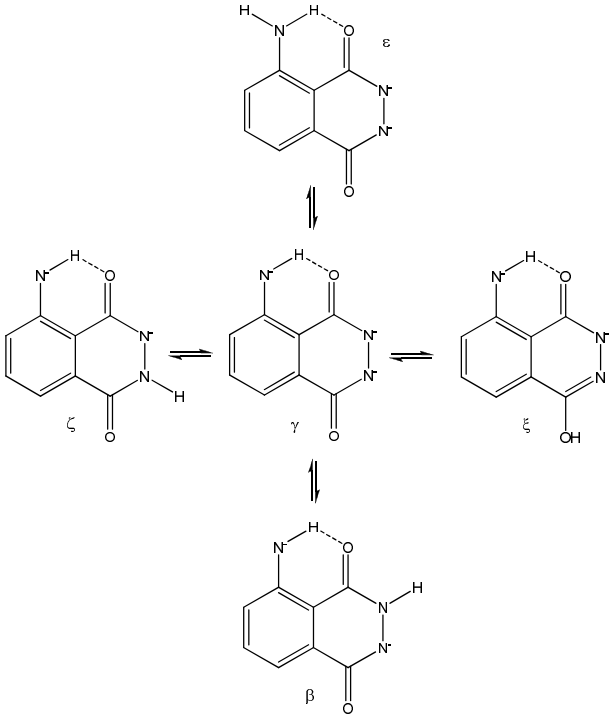

Figure 5.4c: Formation of luminol's trianionic acid-base derivative from its dianionic species.

Table 5.8 presents the Gibbs energy difference for the equilibrium equations on Figure 5.4 for two bases (hydroxyl anion and tert-butoxide) as well as the pK values only for SPE calculations (MP2/aug-cc-pVTZ level of theory). The equation used to relate the ΔG with pK is deduced in Annex 7 - Luminol Acidity. This annex also presents results obtained by MP2 calculations using 6-31G** as

basis set. These results were merely annexed to the report because they gave exactly the same qualitative result as the single point energy calculation with more accurate basis sets.

Prior to luminol's acid-base behaviour analysis it should be stated here that ε was not optimized in a geometry similar to the one presented in Figure 5.4. We selected an initial geometry close to the one from Figure 5.4 but during the structure optimization one of aniline's protons was removed by the oxygen atom in the closest carboxyl group. Thus, ε has high imine character. Figure 5.5 shows those results

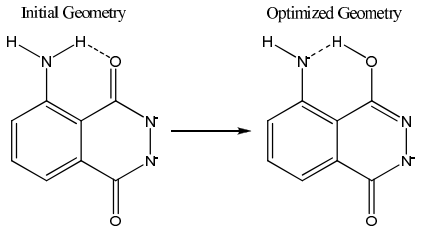

Figure 5.5: Epsilon optimized structure.

Table 5.8a: ΔG and pK values for luminol's acid-base behaviour in gas phase at MP2/aug-cc-pVTZ level of theory. Two bases were used to predict those values, hydroxide and tert-butoxide. Values predicted for equilibrium structures given in Figure 5.4.

MP2/aug-cc-pVTZ				
Structures In Equilibrium	$\Delta G_{tbutoxide}$ (kcal.mol^{-1})	$\Delta G_{hydroxide}$ (kcal.mol^{-1})	$pK_{hydroxide}$	$pK_{t\text{-}butoxide}$
Aα	-45.20	-59.18	-43.38	-33.13
Aδ	-47.72	-61.70	-45.22	-34.98
αε	57.24	43.26	31.71	41.96
αβ	57.86	43.88	32.16	42.41
βγ	142.89	128.91	94.49	104.74
δε	60.37	46.39	34.00	44.25
εγ	142.28	128.29	94.04	104.29
δζ	62.82	48.84	35.80	46.05
ζγ	139.82	125.84	92.24	102.49
Aη	-23.89	-37.87	-27.76	-17.51
ηβ	35.93	21.94	16.09	26.33
ηζ	38.99	25.01	18.33	28.58
Bα	-37.96	-51.94	-38.07	-27.82
βν	49.79	35.81	26.25	36.49
νε	50.41	36.42	26.70	36.95
νξ	63.51	49.53	36.31	46.56
ξγ	129.17	115.19	84.43	94.68
Bο	-20.04	-34.02	-24.93	-14.69
οβ	39.32	25.34	18.57	28.82
οξ	53.04	39.06	28.63	38.88

Table 5.8b: ΔG and pK values for luminol's acid-base behaviour in DMSO at MP2/aug-cc-pVTZ level of theory. Two bases were used to predict those values, hydroxide and *tert*-butoxide. Values predicted for equilibrium structures given in Figure 5.4.

Structures In Equilibrium	MP2/aug-cc-pVTZ/SCRF			
	$\Delta G_{tbutoxide}$ (kcal.mol^{-1})	$\Delta G_{hydroxide}$ (kcal.mol^{-1})	$pK_{hydroxide}$	$pK_{tbutoxide}$
Aα	-41.01	-35.92	-26.33	-30.06
Aδ	-41.89	-36.79	-26.97	-30.70
αε	-11.54	-6.44	-4.72	-8.46
αβ	-12.49	-7.39	-5.42	-9.15
βγ	-13.11	-8.01	-5.87	-9.61
δε	-11.61	-6.52	-4.78	-8.51
εγ	-12.16	-7.06	-5.18	-8.91
δζ	-9.01	-3.92	-2.87	-6.61
ζγ	-14.76	-9.66	-7.08	-10.82
Aη	-15.84	-10.75	-7.88	-11.61
ηβ	-36.71	-31.61	-23.17	-26.91
ηζ	-35.06	-29.96	-21.96	-25.70
Bα	-35.76	-30.66	-22.48	-26.21
βν	-18.58	-13.48	-9.88	-13.62
νε	-19.52	-14.43	-10.58	-14.31
νξ	-8.16	-3.06	-2.25	-5.98
ξγ	-23.52	-18.43	-13.51	-17.24
Bο	-15.18	-10.09	-7.39	-11.13
οβ	-32.12	-27.02	-19.81	-23.54
οξ	-21.70	-16.60	-12.17	-15.91

Table 5.9: Structural parameters obtained for luminol's base conjugates in geometry optimization. Parameters shown here are also defined in Figure 5.3.

Compound	D	α	β	Θ	Comment
Alpha (α)	1.857	0.566	---	40.433	Totally Planar
Beta (β)	2.042	1.290	---	---	High Imine Character
Gamma (γ)	1.9215	---	---	---	Totally Planar
Delta (δ)	1.715	---	0.362	38.113	Totally Planar
Epsilon (ε)	1.008	1.593	---	2.866	Totally Planar
Zêta (ζ)	1.925	---	1.087	---	Totally Planar
Êta (η)	2.037	35.341	26.812	---	High Imine Character
Nu (ν)	1.731	---	0.296	37.776	Totally Planar
Xi (ξ)	1.930	---	0.496	---	Totally Planar
Omikron (ο)	2.056	9.074	1.498	---	Slightly Aplanar

Diagrams 5.3 to 5.4 present the relative order of stability for the mono- and dianionic acid/base derivatives of luminol in both gas, MP2/aug-cc-pVTZ, and in DMSO's dielectric,

MP2/aug-cc-pVTZ/SCRF. These diagrams were built exactly the same way as Diagrams 5.1-5.2, by taking as zero the G value of the most stable species in analysis. Values presented are thus Gibbs energy differences between acid-base isomers.

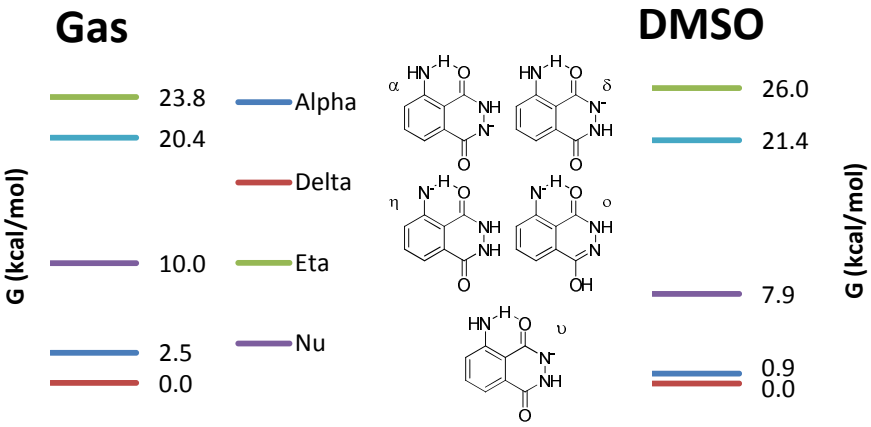

Diagram 5.3: Energetic relationship between luminol's monoanionic conjugate bases in gas phase and DMSO according to MP2/aug-cc-pVTZ calculations.

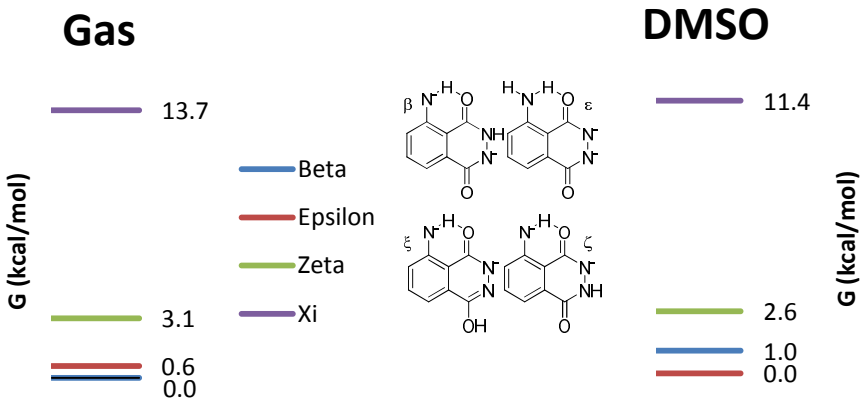

Diagram 5.4: Energetic relationship between luminol's dianionic conjugate bases in gas phase and DMSO according to MP2/aug-cc-pVTZ calculations.

From Table 5.8 we verify that the only reactions plausible in the gas phase system are abstraction of luminol's protons to yield species α, δ, η and ο. ν is the only conjugate base of luminol that should not be formed in gas phase acid-base equilibrium. It can also be concluded that in gas phase only monoanionic species can be possibly formed. The formation of the monoanionic species in luminol is justified by the fact that the negative charge in the alkaline species used should be much less stabilized (those are, by definition, strong bases). The non-formation of dianionic species is justifiable by the fact that luminol would acquire a second negative charge, extremely unstable in gas phase, even for the strongest base used. Because previous results from the literature indicate that two protons of luminol can be easily abstracted using $tBuO^-$ as a base (*cf.* section 2 – State of the Art), then the conditions of these calculations are not good enough to predict the system's behaviour

and only solution calculations will be analyzed in detail. Presentation of results concerning gas phase acid-base equilibrium serves only comparison purposes.

Of all the protons to remove, hydrazide's are the preferred ones, being δ the most stable luminol conjugate base. Even though that is the conclusion, the energetic difference between δ and α is within the experimental error, meaning that they should be equally stable. Diagram 5.3 shows graphically those statements. To account for the stability order we can verify that by mesomeric effect, abstraction of aniline's proton could not possibly be the preferred process due to higher perturbation on the aromatic ring. Thus, with ring 1 perturbation we are able to account for ο and η relative stabilities towards other monoanionic conjugate bases. It should be pointed out that this statement is confirmed by the high imine character in those species (*cf.* Table 5.9). The fact that omicron is more stable than eta can be justified by the same arguments used to justify the relative stability of E and F. Therefore, compared to tautomer stability, ο and η are like tautomers E and F towards A, B, C and D (α, δ and ν).

For the relative position of ν towards α and δ we can also rationalize it by means of the previous study, comparing the former species with tautomer D. Even though not performed, charge analysis should go along this rationale. As for the relative energy of α and δ we can simply argue with the relative strength of the hydrogen bond (*cf.* Table 5.9). The fact that the energetic difference is so small also goes along with the relative influence of hydrogen bonding towards the stabilization of the species.

Also from Table 5.8 and Diagram 5.4, comes that β and ε are the most stable luminol's conjugate bases after two protons abstraction. Even though not so favourable, formation of ζ and ξ should also be plausible using the studied bases in DMSO. Regarding the relative stability, to justify the relative position of ζ and ξ we use the hydrogen bond parameter as well as relative geometrical position of the electronic density. As for β and ε, we verify that the charge position should not be a good parameter to justify the relative stability due to their similarity but hydrogen bonding, on the other side, could explain the 1 kcal.mol^{-1} difference between those species. According to structures optimized, ε has the hydrogen bond between a negatively charged nitrogen and a neutral oxygen, being the latter atom the one that acts as hydrogen bond donor. In β, the charge distribution in the atoms should be similar but now the hydrogen donor is the negatively charged nitrogen. This should therefore justify the relative stability of those species. In respect to the rationale for the observed proton acidity, we must reinforce the fact that during ε optimization, an intramolecular proton abstraction occurred, meaning therefore that the intramolecular hydrogen bonding and higher charge separation should be essential to define the relative stability of these dianionic bases.

As for γ, all we can conclude is that when sufficient base is added, luminol can favourably yield a trianionic species.

Comparing experimental results with theoretical calculations we verify that the stability of aniline's protons is not as high as supposed to be from the literature,[10] *i.e.*, those two protons should remain untouched throughout luminol's oxidation. Because all performed calculations stated that aniline's protons should be the second most labile ones, then the literature argument should be rechecked. This result comes directly from the fact that aromaticity extension is not the preponderant factor for the relative stability of luminol's derivatives. On the other hand, these same theoretical results may also give another meaning to another literature statement that an ionisable group in ring 1 should be relevant to observe chemiluminescence in luminol and its derivatives.[10,20]

5.5 - Conclusions

To accurately study luminol and its derivatives oxidation, the most appropriate methods are MP2 and PBE1PBE with non-diffused basis sets. The observed accuracy of DFT calculations was somewhat independent of the basis set quality and due to computational cost, Pople's basis set was the preferred one, at least in this work. Between DFT methods, B3LYP gave slightly better aniline dihedral angles but the bond distances were slightly worse. On MP2 calculations, the introduction of diffuse basis set appears to decrease the calculation accuracy being therefore the preferred basis set 6-31G**.

As for single point energy calculations, because MP4, CC,... calculations were not possible to apply using the current machinery (lack of physical and processor memory in our computers). Therefore, MP2/aug-cc-pVTZ was selected.

Regarding luminol's tautomers, six were studied in several conditions and four of them tested in three conformations. The most stable tautomers in both gas and solvent dielectric were the ones with high aromatic character in ring 1. Of these, tautomers with more favourable charge distribution and stronger intramolecular hydrogen bonding between NH_2 and carboxyl functionalities are the most stable ones, being these statements valid for all conditions (gas and solvent dielectric). Combining all information from the discussion, we conclude that the main parameters affecting luminol's tautomers relative stability should be (i) aromaticity and (ii) electronic delocalization, (iii) hydrogen bonding and then (iv) charge distribution. The fact that aromaticity is the less relevant parameter can be understood by a decrease in the mesomeric effect of aniline functionality to ring 2.

Regarding luminol in alkaline media, if one equivalent of a strong base is added then α and δ should be both formed. These come directly from abstraction of a hydrazide proton. The second most acidic proton from luminol's structure should be an aniline one due to hydrogen bonding and higher charge separation. The acidity order for luminol's protons is in agreement with luminol's tautomer stability, *i.e.*, the driving forces for structure stabilization are practically the same with the same strength.

6 - Spectroscopic Studies

The next section of the work both present and discuss the electronic spectra (UV/Visible absorption and fluorescence) of luminol, isoluminol, its synthesized derivatives and the aminodiphthalate, light emissive species in luminol's chemiluminescent reaction. It also presents the collected chemiluminescence spectra of luminol and the other hydrazides.

The section is presented in a continuous fashion. First we present and analyse all luminol and isoluminol data, then the aminodiphthalate species and only then luminol's acyl derivatives. The following section deals with chemiluminescence decay analysis and kinetic studies, being ultimately presented the summary of conclusions.

Regarding the conditions, absorption and fluorescence for luminol and its derivatives were studied in aqueous media, DMSO and in DMF. Besides, luminol's solid state spectra and spectra in a 9:1 EtOH-MeOH mixture are also studied, the latter at both room temperature and 100 K. In respect to chemiluminescence, it was only quantified in aqueous media using conditions from Rauhut and co-workers[25] at high pH. Luminol's derivatives aqueous spectra were also collected in high pH media. In respect to the aminodiphthalate, only spectra in aqueous media at different pH values were collected and therefore presented. Additionally, theoretical calculations on luminol's and aminodiphthalate absorption were performed and are analysed in their respective sections.

All presented spectra are normalized to absolute maximum absorption or emission wavelengths. Therefore, tables that contain intensity information may and must be used for a more comparative analysis of the bands and the compounds.

In respect to atom labelling, Figure's 5.2 nomenclature was adopted.

6.1 - Luminol and Isoluminol

The first section of this discussion deals with luminol and its amino isomer, isoluminol.

6.1.1 - Luminol's Absorption and Fluorescence in Aqueous Media

Luminol's electronic absorption spectra in aqueous media at several pH values are presented in Figure 6.1. Figures 6.2 and 6.3 present its fluorescence dependence on pH at different excitation wavelengths (in Figure 6.2 the excitation is at 300 nm while in Figure 6.3 the excitation is at 350 nm).

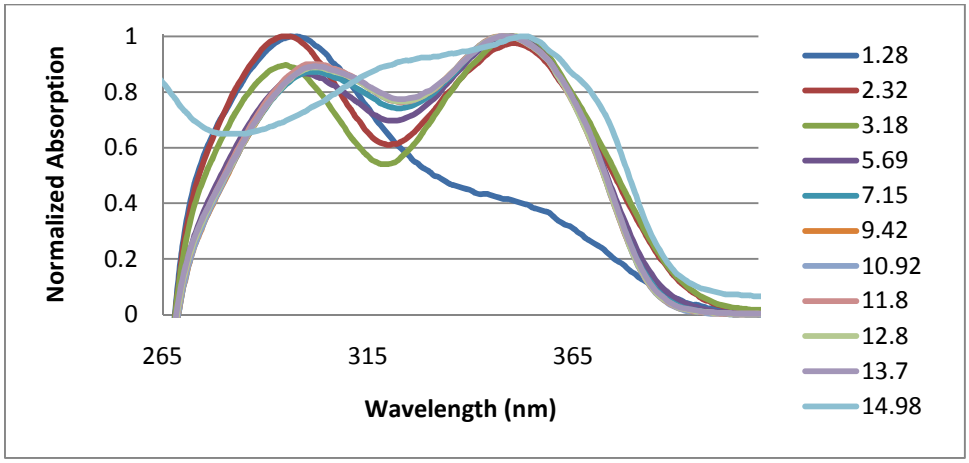

Figure 6.1: Absorption spectra for luminol in aqueous media from pH 1.28 to pH 14.98. Data on the absolute intensity of each band can be found in Table 6.1.

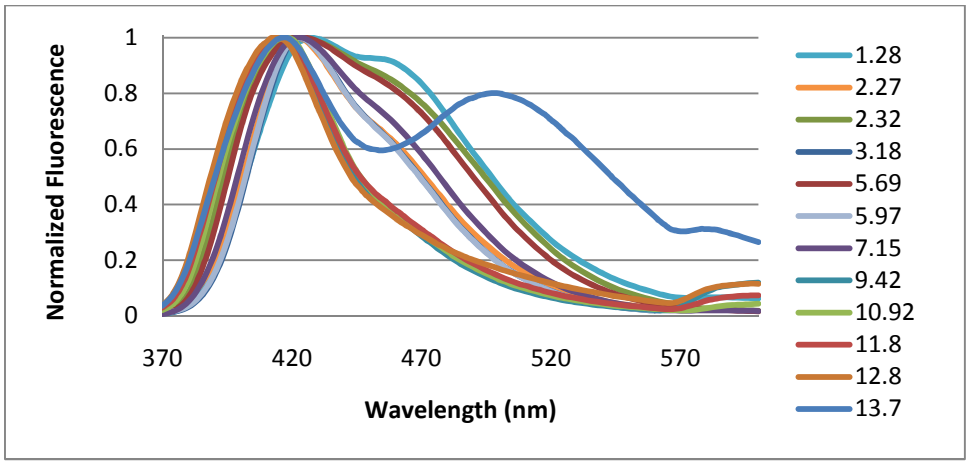

Figure 6.2: Luminol's fluorescence in aqueous media from pH 1.28-13.7. Lowest excitation wavelength used. Data on the absolute intensity of each band as well as excitation wavelengths can be found in Table 6.1.

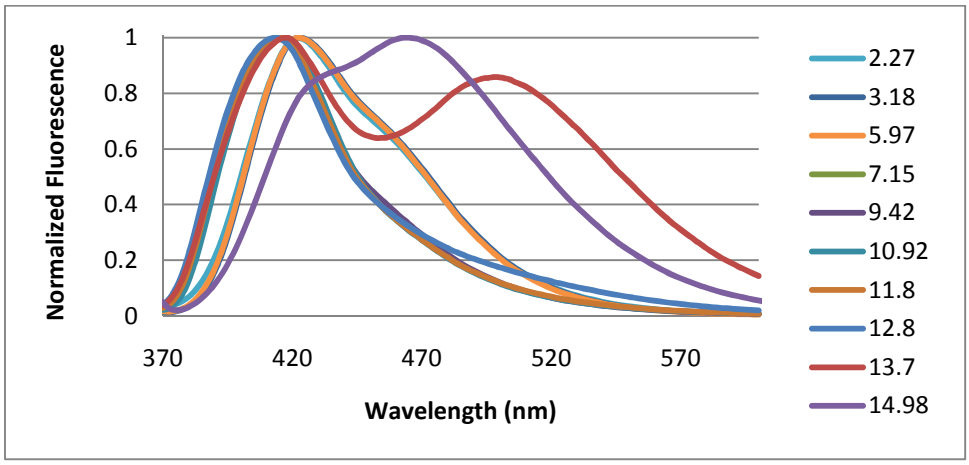

Figure 6.3: Luminol's fluorescence in aqueous media from pH 1.28-14.98. Highest excitation wavelength used. Data on the absolute intensity of each band as well as excitation wavelengths can be found in Table 6.1.

Table 6.1: Data concerning the absolute intensity for absorption spectra presented in Figure 6.1 and fluorescence spectra in Figures 6.2 and 6.3. All solutions had luminol in a concentration of 5.1×10^{-5} M except for the ones at pH 2.27, 3.18 and 5.97 that had it 100 times diluted (5.1×10^{-7} M). Relative fluorescence intensities presented come from data acquired with similar experimental conditions.

	Absorption				Fluorescence		
pH	$\lambda_{max\ 1}$ (nm)	$A[\lambda_{max\ 1}]$	$\lambda_{max\ 2}$ (nm)	$A[\lambda_{max\ 2}]$	λ_{exc} (nm)	λ_{max} (nm)	$I_{rel}[\lambda_{max}]$
1.28	297	0.226	---	---	300	428	0.179
2.27	---				305	422	0.091
					350	422	0.135
2.32	295	0.251	350	0.245	305	422	0.863
					350	---	
3.18	295	0.262	350	0.292	305	422	0.208
					350	422	0.269
5.69	300	0.286	350	0.33	300	420	0.816
					350	---	
5.97	---				300	422	0.206
					350	422	0.275
7.15	300	0.294	350	0.337	300	424	1.00
					350	420	0.850
9.42	304	0.309	350	0.346	300	414	0.116
					350	414	0.135
10.92	302	0.313	350	0.348	300	418	0.025
					350	418	0.029
11.8	300	0.315	348	0.35	300	416	0.060
					350	414	0.067
12.8	302	0.312	349	0.351	300	414	0.102
					350	414	0.120
13.7	302	0.325	348	0.364	300	416 500	0.088 0.071
					350	418 500	0.111 0.095
14.98	352	0.277	---	---	355	464	0.290

Analysing luminol's absorption spectra we find that at almost all pH values, two bands are present, one at 300 nm and another at 350 nm. The latter is significantly inhibited at low pH but it is also present throughout the whole range of pH values tested, even at 14.98. Regarding the other absorption band, it also present throughout the range of pH's tested, being its relative intensity towards the absorption band at 350 nm conserved (except for extremely low and high pH values, 1.28 and 14.98). To account for that course, due to luminol's structure and its acid-base behaviour,[14,22,24,34] we can assume that at low pH values the aniline functionality is protonated,[60] yielding therefore one species whose oscillator strength at 350 nm is much lower than the neutral conjugates (aniline has pK_a of 9.13)[54]. On the other hand, for pH's of at least 2.32 until pH 13.7, luminol's aqueous absorption spectrum remains unchanged. Because for sufficiently high pH luminol exhibits acidic

behaviour,[14,22,24,34] to account for the assigned behaviour we must assume that at least neutral and monoanionic luminol absorption is practically the same. Regarding the nature of the absorption bands, with the collected data nothing can be concluded: they can be both from excitation of two different species (for instance tautomers) or from at least two distinct singlet excited states.

Assuming now that luminol exists in all those media in only one form (no tautomerization or acid-base behaviour) we can estimate the molar extinction coefficients. This is merely an approximation because, as we have seen in section 5.3, luminol should exist in solution as a combination of at least two tautomers. On that approximation, we verify that, when undoubtedly identified, both transitions (300 nm and 350 nm) have molar extinction coefficients in the range of 4.45×10^3 – 7.2×10^3 $M^{-1}.cm^{-1}$ for all pH's studied (the second transition, 300 nm, shows a lower maximum, at 6.4×10^3 $M^{-1}.cm^{-1}$). These values are evidence for a predominant $\pi\pi^*$ character in both electronic transitions in luminol's aqueous absorption. Besides, we have also verified that the molar extinction coefficient increases from pH 1.28 (where it is in the absolute minimum) to pH 13.7 (where it has its absolute maximum) and then decreases once again at maximum pH achieved with luminol's solutions (or disappears in the case of the transition at 300 nm). Because the absorption spectra only depends on the absorbing species (in their ground state), we conclude that luminol's monoanionic base conjugates are more efficient in UV light absorption (in the range tested) than the correspondent neutral forms. Assuming that dianionic species could only be achieved at higher pH values, namely pH 14.98, we conclude that their absorption should be less efficient than the absorption by monoanionic luminol base conjugates. Also, because we have only observed changes in luminol's absorption spectrum at pH close to 15, we state that luminol's second pK_a value in water should be close to that value (*cf.* Luminol's theoretical absorption spectra discussion in section 6.1.4).

Regarding the emission spectra, as can be verified by Figures 6.2 and 6.3, it remains unchanged on both excitation wavelengths studied. This proves that the absorption bands observed in Figure 6.1 are at least partly due to two close-lying singlet states. Thus, exciting a luminol aqueous solution at 300 nm puts the chromophore in the second singlet excited state, S_2, while excitation at 350 nm would give the first singlet excited state, S_1. After excitation at higher energies, the excited state species will relax (by internal conversion) to S_1 and will further emit light (or relax to S_0 also by non-radiative internal conversion). Taking as reference the spectra in Figure 6.2, once again no vibrational resolution is distinguishable. In addition, at some pH values, the emission process appears not to come solely from one species, *i.e.*, several emission bands exist for one solution (shoulders on spectra). Of course that we can think about proposing that those bands are due to at least two low-lying singlet excited states but that would go against the expected behaviour from Fermi's golden rule. To explain those observations, acid-base reactions in the first singlet excited state (acid-base reactions are extremely fast and are able to achieve the equilibrium situation during the extremely small excited state lifetime obtained from a $\pi\pi^*$ transition) can be invoked. Of course that tautomerism can also play an important role but with the information presented so far, the only conclusion that can be made is that luminol's tautomers must have practically the same excitation energies. The equilibrium geometry (and energy) of the first singlet excited state should also be sufficiently close.

Applying Förster's cycle (*cf.* Figure 6.4) for excited state acid-base reactions and assuming that the variation of entropy associated with the acid-base reaction is independent of the electronic state occupied by the involved species, we get equation (2). Annex 8 presents the deduction of this expression. Figure 6.4 defines some of the system's variables and therefore should be taken into account.

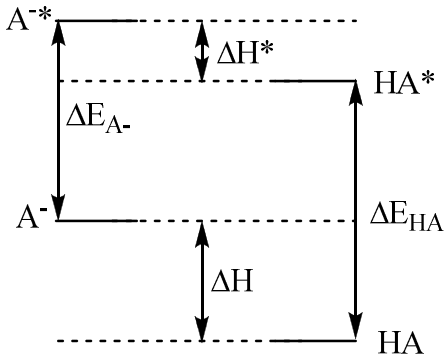

Figure 6.4: Förster's cycle for excited state acid-base reactions. ΔE_{A^-} is the excitation energy for the base species of the equilibrium, ΔE_{HA} the excitation energy for the acid species from the equilibrium, ΔH is the variation of enthalpy associated with the acid-base reaction in the ground state and ΔH^* is the same parameter for the reaction in the excited state.

$$pK_a^* = pK_a + \frac{hc\Delta\lambda}{\lambda_{HA}.\lambda_{A-}}\frac{1}{k_B T log(10)} \qquad (2)$$

In equation (2), h is Planck's constant, c the speed of light, λ_{HA} the wavelength associated with transition from ground to first excited state of the acid, λ_{A-} the wavelength associated with the transition from ground to first excited state of the base compound and $\Delta\lambda$ the difference of the gaps of the first excited state and ground state (for the base and the acid species) in wavelength $(\lambda_{A-} - \lambda_{HA})$. k_B is Boltzmann's constant, T the absolute temperature (kelvin) and $log(10)$ the natural logarithm.

Assuming that emission at 460 nm (in Figure 5.2) is due to luminol's neutral form and that emission at 420 nm is due to monoanionic species, if luminol's first pK_a is 6.3 as previously suggested[34] then we expect that in the first excited state, luminol has a pK_a of 3.6. Assuming now that luminol's neutral forms are as efficient in light emission as luminol's monoanionic species, at pH's of 1.28, 2.27 and 2.32, neutral luminols would be the main light emissive species. This is not the observed behaviour, *i.e.*, emission at 460 nm is a relative maximum but not the absolute one even at pH 1.28. To justify that, we invoke both the Franck-Condon geometry contamination and the time that the acid-base reaction needs to achieve equilibrium. While the former is related to the fact that the transitions occur from equilibrium geometry of the starting PES to the same structure but in another electronic level (Franck-Condon geometry), the latter is a usual drawback on Förster's cycle[55] and is related to the non-instantaneity of the reaction to reach the equilibrium situation. To justify the somewhat chaotic behaviour of luminol's fluorescence spectra (at pH's 2.27 and 5.96 the intensity of

the shoulder is closer to the one in fluorescence at pH 7.15 than in pH's 2.32 and 5.69), the concentration of the chromophore must be invoked: in pH 2.27 and 5.96, luminol's concentration is 100 times smaller than in the solutions for the other pH values.

Regarding the presented spectra, one last parameter should be discussed, that is Stokes shift. On the basis of the proposed hypothesis for the origin and nature of the absorption bands, the Stokes shift should be between 70 (monoanionic species) and 110 nm (neutral forms of luminol). Due to the complexity of the absorption spectrum of a luminol solution at pH 14.98 (at least 3 different absorption peaks in the range of 315-360 nm) any comment would be extremely speculative and will not be performed. Attending to luminol's chemical nature (three chemical functionalities that may interact with hydrogen bonding donors or acceptors), it is expected a change in the solvent cage from ground to excited state. On the other hand, all transitions are $\pi\pi^*$, meaning that molecular orbitals involved should be insensitive to hydrogen bonding (but not to solvent's dielectric constant). Besides, anti-bonding molecular orbitals in the π system are occupied upon excitation, being expected severe structural changes in that process. Because all factors are accompanied by changes in the solvent cage, we can therefore justify the observed Stokes shifts in neutral and anionic luminols by assuming that the excitation on charged and non-charged molecules yields practically the same geometrical distortions. Due to the $\pi\pi^*$ nature of the transition, the anionic charges remain localized in the same atoms in both ground and first electronic excited state. The solvent cage in luminol's charged species is then expected to be closer in S_1 and S_0 than in the neutral forms, being therefore the Stokes shift smaller.

6.1.2 - Luminol's Absorption and Fluorescence in Aprotic Media

Luminol's UV/Vis absorption and fluorescence spectra were also collected in aprotic media, namely DMF and DMSO. These spectra are presented in Figures 6.5 (DMSO) and 6.6 (DMF).

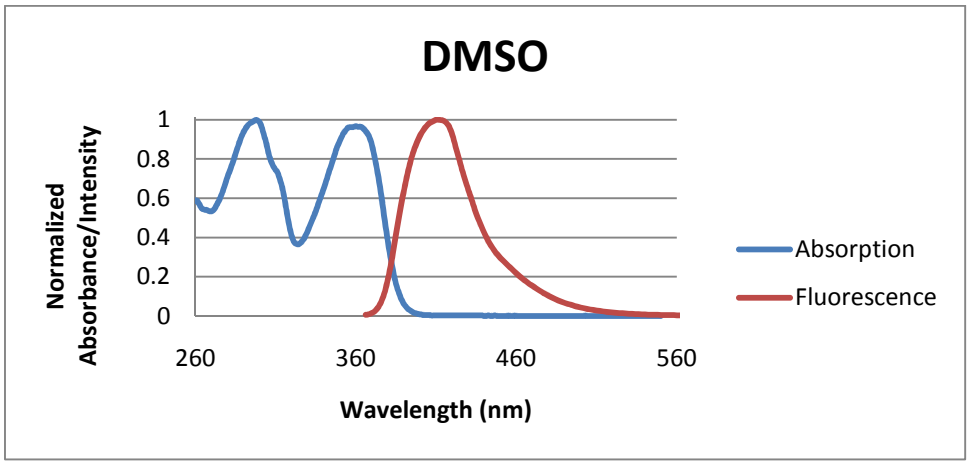

Figure 6.5: Luminol's absorption and fluorescence spectra in DMSO. Absorption spectrum normalized at 298 nm while fluorescence spectrum was normalized at 410 nm.

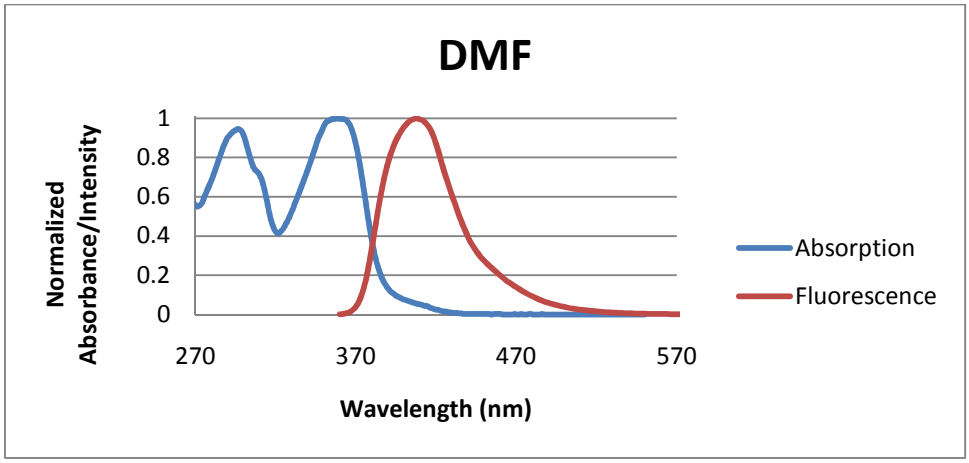

Figure 6.6: Luminol's absorption and fluorescence spectra in DMF. Absorption spectrum normalized at 359 nm while fluorescence spectrum normalized at 408 nm.

Table 6.2: Data concerning the absolute intensity of spectra in Figures 6.5 and 6.6. Luminol's concentration in all solutions was 5.4×10^{-5} M.

		DMSO	DMF
Dielectric Constant[56]		46.7	38
Absorption	$\lambda_{max\,1}$ (nm)	298	296
	$A[\lambda_{max\,1}]$	0.403	0.349
	$\lambda_{max\,2}$ (nm)	360	358
	$A[\lambda_{max\,2}]$	0.39	0.369
Fluorescence	λ_{exc} (nm)	306	358
	$\lambda_{max\,1}$ (nm)	410	408
	$I[\lambda_{max\,1}]$	3.13×10^{7}	3.24×10^{7}

As we can verify from Figures 6.1, 6.5 and 6.6, the general form of luminol's absorption spectrum is equal in both aprotic (DMF and DMSO) and protic (H_2O) media, *i.e.*, two main absorption bands are present, one at 300 nm and the other at 350 nm. Nevertheless, differences arise in a finer analysis of the spectra. In water (Figure 6.1), the first singlet excited state of luminol possesses higher oscillator strength than the second one, *i.e.*, the first electronic transition is more favourable than the second. While that order of relative intensity is retained in DMF, DMSO shows the opposite behaviour. Besides, in aprotic solvents, a shoulder is identifiable in the second absorption band (300 nm), being this shoulder more evident in DMF's absorption spectrum. The origin for this transition can either be vibrational or electronic, *i.e.*, the absorption band with maximum at 300 nm corresponds to the transition to two distinct singlet excited states of luminol, either to S_2 and to S_3 or from distinct tautomeric forms. On the basis of the first hypothesis (vibrational transition), the wavenumber of the vibrational mode associated with the transition would be of 1600 cm^{-1}. Because vibronic transitions within one electronic transition use typically vibrational modes of CH bonds (in this case aromatic), we would expect to observe an absorption peak around that wavelength in luminol's IR spectrum. According to the literature,[57] luminol's IR spectrum presents such band as one of the most intense

ones. Because no assignment is performed in the source, we can assume the usual IR spectra interpretation[58] and therefore that band would be due to aromatic CC double bond stretch (this result is also confirmed by the theoretical calculations performed). Because the error in the estimation of the wavenumber between those two transitions is extremely high, no concrete conclusions can be performed, being the three hypotheses still valid.

Regarding now the solvent's polarity effect on the maximum absorption wavelength, the transition towards S_1 is the most affected one, being the shift 8-10 nm (2-4 nm in 300 nm transition), higher in DMSO. To rationalize this slight red shifting when solvent's polarity is increased, we can simply rely on the $\pi\pi^*$ nature of the transition. Because the process in study is the transition from thermal equilibrium geometry to the Franck-Condon species (with the same molecular orbitals as the ground state), for the transition to be practically solvent insensible, the molecular orbitals (π in nature) involved in this process must be such that the charge distribution is weakly affected during the transition.

Assuming once again that luminol only exists in one tautomeric form, we verify that transitions in aprotic media have higher molar extinction coefficients than transitions in water, being the same parameter slightly higher in DMSO (than in DMF). To account for it, increase in $\pi\pi^*$ nature of the transitions is invoked (meaning also that these transitions have some $n\pi^*$ character). Therefore, we conclude that luminol's electronic transitions remain practically unchanged in their character in all media studied.

Regarding now luminol's fluorescence, we verified that only one band is present, even when different excitation energies were used. That is in agreement with the assigned electronic nature of the transitions (to S_1 and S_2). Because the emission is characterized in these media by only one band, we conclude that the nature of the two observed bands in water is acid-base equilibrium within the first excited state (when the polarity is decreased it is commonly observed an enhancement of vibrational resolution). As for the effect of the solvent in the maximum emission wavelength in luminol's fluorescence, the major difference is between the two sets studied, aprotic media and water (408 nm in DMF, 410 nm in DMSO and in water, at pH 7.15, 420-424 nm). Because the difference is of 10-16 nm, we can rely on the solvent's polarity to account for the shifts. The effect of hydrogen bonding is therefore extremely small, being that conclusion also in agreement with the $\pi\pi^*$ nature of the transitions. As for the relative emission intensity on the maximum emission wavelength, results are similar to the ones in the absorption, *i.e.*, the relative intensity is slightly higher in aprotic media.

The last parameter to be analysed is the Stokes shift. According to spectra in Figures 6.5 and 6.6, the Stokes shift for aprotic solvents studied is 50-60 nm (for further discussion the average value of 55 nm will be assumed). This is 15 nm below the Stokes shift in water meaning that besides variation of charge distribution in the two electronic states (fact that is also reflected in change of solvent cage), a great change in molecular geometry takes place with the electronic transition. The results from Stokes shift in aprotic media also agree with a small effect of hydrogen bonding in the first two electronic states of luminol.

6.1.3 - Luminol's Solid State Spectra

Luminol's excitation and emission spectra were also recorded in the solid state. These are both presented in Figure 6.7. The excitation wavelength for fluorescence spectrum was 350 nm.

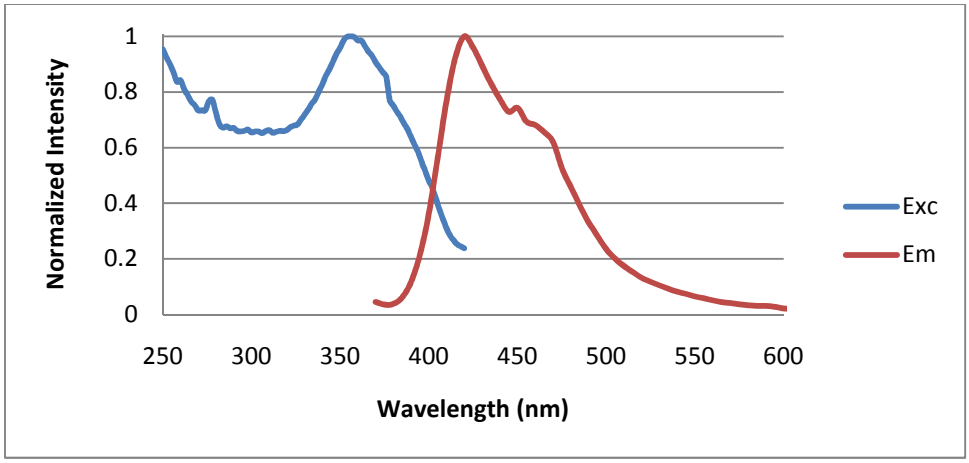

Figure 6.7: Luminol's excitation and fluorescence spectra in solid state. Exc stands for excitation and Em for emission. The excitation wavelength for fluorescence was 350 nm. Maximum excitation occurs at 342 nm with intensity 1.73×10^6 and maximum emission occurs at 420 nm with intensity 2.22×10^6.

As can be seen from the last Figure, the excitation pattern (analogous to absorption but measured by following the light emission intensity at a certain excitation wavelength) changes from solution to solid state. The main feature that distinguishes those spectra is the number of absorption bands. In solid state only one is perfectly identifiable, at 350 nm. This yields to the curious observation that the first maximum absorption (excitation) wavelength, the one we verified to be more sensitive to the surrounding media, is retained from solid state to solution. In respect to the second absorption band, it is not observed in solid state. That can be either a shifting effect (red shift that causes overlap to the first transition or blue shift that puts that absorption maximum below 250 nm) or intensity decrease.

Regarding peak width enlargement, we need to look to the molecular structure of luminol's powder. Being a powder, and knowing that luminol tends to form crystals in adequate conditions (totally different from the powder), we conclude that the sample used is an amorphous solid, *i.e.*, it contains luminol in several conformations and no pattern (unitary cell) can possibly be assigned. Therefore, deviations from solution's equilibrium geometries and molecular aggregations (due to molecular proximity) may contribute for the enlargement of absorption bands.

As for emission spectra, maximum emission also occurs at 420 nm. Besides, the emission band is thinner than the absorption, meaning that the emission spectrum is more selective than the excitation one (as expected). Because the maximum emission wavelength is retained from solution, we can propose that the conformational restriction is not too high and molecular accommodations are viable (that would make molecular aggregations responsible for background absorption in luminol's excitation spectrum). We can also assume that only some specific molecular geometries allow light emission in the first excited state. As for Stokes shift, in solid state, it is of 78 nm. This is the highest

value obtained for luminol so far, suggesting that in luminol's solid phase, interactions between luminol molecules (now the media) should not be null but rather stronger than any other intermolecular interaction previously observed. Using literature's crystallographic data for luminol,[35] hydrogen bonding should be the strongest interaction in these molecular aggregations. These not only would justify the higher band width but also could possibly justify the shoulder observed in luminol's emission (similarly observed in water and assigned to acid-base behaviour).

6.1.4 - Luminol's Theoretical Absorption Spectra

The next section deals with theoretical predictions for luminol's absorption spectra. Calculations were performed for the computationally most stable species regarding neutral, mono- and dianionic luminol (*cf.* sections 5.3 and 5.4). The species in study here are therefore tautomers A, B and C as well as conjugate bases α, δ, β, ε and ζ. The main information collected directly from theoretical calculations is presented in Table 6.3. This table only presents results for TD DFT calculations because these yielded the best results. Maximum absorption wavelengths were incorrectly (with higher error) predicted by TD HF calculations and therefore, those results are only presented in Annex 9 – TD HF and TD DFT in Gas Phase. Gas phase excitations are also in that annex because no direct interpretation can be performed to them. In Annex 10 - Molecular Orbitals involved in tautomer B transitions we present the molecular orbitals involved in tautomer B first three electronic excitations.

Table 6.3: Data collected for electronic transitions of luminol's tautomers A, B and C as well as its conjugate bases α, δ, β, ε and ζ. The table is separated in three different tables, each regarding each transition. TN stands for transition nature. In those columns, brackets may indicate the origin of excitation. Cont. stands for contamination and f is the oscillator strength.

		Transition 1			
		λ_{max} (nm)	F	TN	Orbitals
A	H_2O	339.65	0.15	ππ*	44 – 48; 46 – 47
	DMSO	340.7	0.16	ππ* (Ring1)	44 – 48; 46 – 47
B	H_2O	329.2	0.17	ππ* Cont. σπ*	43 – 48; 46 – 47
	DMSO	330.4	0.19	ππ* (Ring1) Cont. σπ*	43 – 48; 46 – 47
C	H_2O	328.9	0.17	ππ* Cont. σπ*	43 – 48; 46 – 47
	DMSO	330.1	0.19	ππ* Cont. σπ*	42 – 48; 46 – 47
Alpha (α)	H_2O	348.4	0.13	ππ* (Ring2)	46 – 47
	DMSO	350.7	0.14	ππ* (Ring2)	46 – 47
Delta (δ)	H_2O	351.0	0.14	ππ*	46 – 47
	DMSO	353.4	0.15	ππ*	46 – 47
Beta (β)	H_2O	403.7	0.16	ππ*	46 – 47
	DMSO	406.2	0.18	ππ*	46 – 47
Epsilon (ε)	H_2O	391.5	0.20	ππ*	46 – 47
	DMSO	391.5	0.20	ππ*	46 – 47
Zeta (ζ)	H_2O	422.3	0.135	ππ* (Ring1)	46 – 47
	DMSO	425.1	0.15	ππ* (Ring1)	46 – 47

		Transition 2			
		λ_{max} (nm)	F	TN	Orbitals
A	H_2O	286.3	0.02	ππ* Cont. σπ*	42,45 – 47; 46 - 48
	DMSO	286.8	0.02	ππ* (Ring1) Cont. σπ*	42,45 – 47; 46 - 48
B	H_2O	293.3	0.11	ππ* Cont. σπ*	43,45 – 47; 46 – 48
	DMSO	294.0	0.12	ππ* (Ring2) Cont. σπ*	43,45 – 47; 46 – 48
C	H_2O	295.4	0.18	ππ* Cont. σπ*	43,45 – 47; 46 – 47
	DMSO	294.6	0.16	ππ* Cont. σπ*	43,45 – 47; 46 – 48
Alpha (α)	H_2O	313.9	0.11	ππ* (Ring2) Cont. σπ*	42 – 47; 46 – 48
	DMSO	315.6	0.12	ππ* (Ring2)	46 – 48
Delta (δ)	H_2O	309.9	0.13	ππ* Cont. πσ*	42,45 – 47; 46 – 48
	DMSO	311.5	0.14	ππ* Cont. πσ*	42,45 – 47; 46 – 48
Beta (β)	H_2O	341.6	3.7×10^{-3}	ππ*	46 – 48
	DMSO	344.4	3.7×10^{-3}	ππ*	46 – 48
Epsilon (ε)	H_2O	344.1	4.9×10^{-3}	ππ* Cont. πσ*	46 - 48,49
	DMSO	344.1	4.9×10^{-3}	ππ* Cont. πσ*	46 - 48,49
Zeta (ζ)	H_2O	351.2	4.2×10^{-3}	ππ* (Ring1) Cont. πσ*	46 - 48,50
	DMSO	354.6	4.3×10^{-3}	ππ* (Ring1) Cont. πσ*	46 - 48,50

		Transition 3			
		λ_{max} (nm)	F	TN	Orbitals
A	H_2O	280.4	0.061	$\pi\pi^*$	44,45 – 47; 46 – 48
	DMSO	280.9	0.067	$\pi\pi^*$ (Ring1)	44,45 – 47; 46 – 48
B	H_2O	275.9	0.053	$\pi\pi^*$	45 – 47; 46 – 48
	DMSO	276.6	0.057	$\pi\pi^*$	45 – 47; 46 – 48
C	H_2O	274.2	0.046	$\pi\pi^*$	44 – 47
	DMSO	273.6	0.043	$\pi\pi^*$	45 – 47
Alpha (α)	H_2O	294.7	0.041	$\pi\pi^*$ (Ring1) Cont. $\sigma\pi^*$	42 – 48; 44,45 – 47
	DMSO	295.1	0.045	$\pi\pi^*$ (Ring2) Cont. $\sigma\pi^*$	42 – 48; 44,45 – 47
Delta (δ)	H_2O	298.0	0.018	$\pi\pi^*$ Cont. $\sigma\pi^*$	42,46 – 48; 45 – 47
	DMSO	298.6	0.021	$\pi\pi^*$ Cont. $\sigma\pi^*$	45 – 47; 42,46 – 48
Beta (β)	H_2O	320.8	0.13	$\pi\sigma^*$ Cont. $\pi\pi^*$(Ring1)	45 – 47; 46 – 49
	DMSO	322.4	0.16	$\pi\sigma^*$ Cont. $\pi\pi^*$	45 – 47; 46 – 49
Epsilon (ε)	H_2O	334.3	0.25	$\pi\sigma^*$ Cont. $\pi\pi^*$	46 - 48,49
	DMSO	334.3	0.25	$\pi\sigma^*$ Cont. $\pi\pi^*$	46 - 48,49
Zeta (ζ)	H_2O	330.2	0.13	½ $\pi\pi^*$ ½ $\pi\sigma^*$	43,45 – 47; 46 – 49
	DMSO	331.8	0.15	½ $\pi\pi^*$ ½ $\pi\sigma^*$	43,45 – 47; 46 – 49

According to this latter table, all luminol's electronic excitations correspond to transitions with (mainly) $\pi\pi^*$ character. As for contaminations in the first two transitions, B and C have some $\sigma\pi^*$ character and therefore distinct behaviour from the other neutral form of luminol. Their third transition is, according to theoretical calculations, a pure $\pi\pi^*$ one. These results are in good agreement with the analysis performed in the former sections. Also, from the similarity in oscillator strengths for the species that may be involved in the excitations (namely A, B, C, α and δ) we conclude that the one luminol form hypothesis for molar extinction coefficient estimation should be valid to evaluate the character of the transition that will yield the electronic excited states. Another curious fact is that the transitions have the exact same qualitative composition (slight changes in the relative weight were observed) independently of the solvent where the calculations were performed. It is therefore expected (and computationally verified) that the electronic transitions in those two solvents have similar excitation wavelengths, fact that is in good agreement with experimental results.

In a more detailed analysis we are also able to verify from Table 6.3 that the oscillator strengths in DMSO are always slightly higher than the ones for water, also experimentally observed (*cf.* Tables 6.1 and 6.2). An even more interesting fact regarding this parameter is that in water, if media's pH changes to higher values, the intensity of the absorption band should be slightly decreased, the exact opposite conclusion that we previously took from the molar extinction coefficients analysis.

As for the second electronic transition, the oscillator strengths for tautomer A and all dianionic luminol derivatives are decreased towards the first electronic transition. Unfortunately, the third electronic transition is extremely close and we cannot rule out the former species from the absorption

spectra. As for that third electronic transition, it is mainly significant for dianionic luminol derivatives, being here significant, as intense as the first excitation.

As for the dianionic species, some curious results arise. First, the whole spectrum is theoretically predicted to be red shifted, *i.e.*, the first transition is at 400 nm, being this transition as significant as the 350 nm one for neutral and monoanionic luminol forms. Besides, the transition at 350 nm is also silenced. Comparing to the spectrum obtained at pH 14.98, high discrepancies arise and therefore no comparison and assignment can be performed. What can be in fact taken is that the abstraction of a second proton induces (theoretically) changes in the absorption spectrum and differences were in fact observed at the highest pH tested. That is the basis for the performed estimation of luminol's second pK_a in water performed in section 6.1.1.

Regarding the ability for the applied theoretical model to predict excitation wavelengths, Figures 6.8 and 6.9 allow a better evaluation. They present the experimental normalized spectrum (in water – Figure 6.8 – and DMSO – Figure 6.9) superimposed with theoretical electronic.

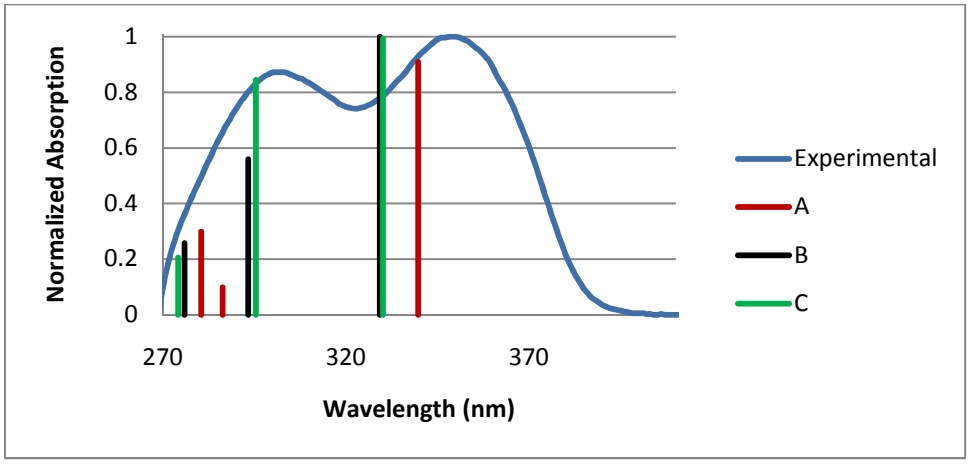

Figure 6.8: Luminol's absorption spectrum in water superimposed with excitation wavelengths for its three most stable tautomers.

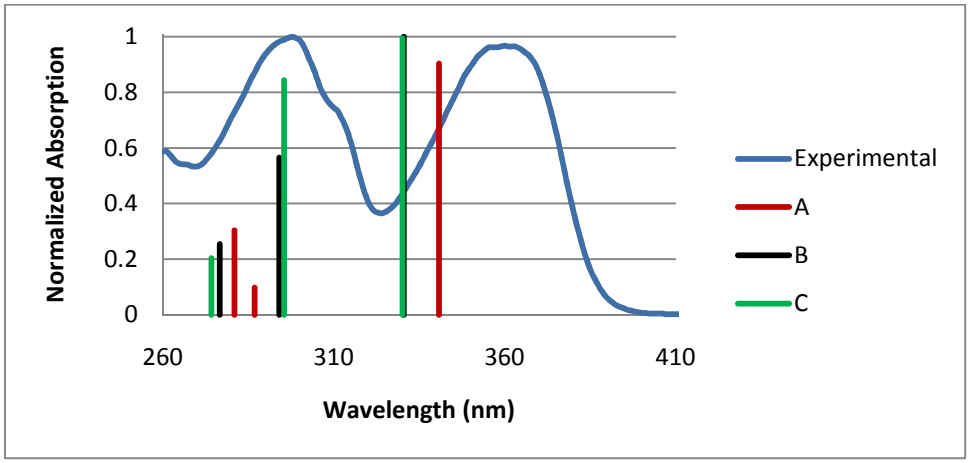

Figure 6.9: Luminol's absorption spectrum in DMSO superimposed with excitation wavelengths for its three most stable tautomers.

According to Figures 6.8 and 6.9, theoretical predictions are all blue shifted relative to experimental results. In the first electronic transition, it is perfectly clear that tautomers B and C excitations are superimposed, being these (in both solvents) the worst possible predictions for the method. It is also verifiable that this absorption band can be perfectly explained by absorption of both tautomers B and C and, for tautomer A to contribute to this electronic transition, it would be necessary practically perfect superposition with absorption of tautomers B and/or C to yield the experimentally observed peak configuration. As for the second transition band, once again it could be explained by the presence of tautomers B and C, at least in water. The experimental decrease in intensity would be explained by decrease in oscillator strength for both species, especially for tautomer B. As for the second transition in DMSO, the peak shape can be explained once again by tautomers B and C but this time sacrificing the accuracy of theoretical calculations on the excitation wavelength. Assuming that the transition towards S_2 for tautomer B is blue shifted, the maximum and the shoulder around 300 nm can be theoretically justified by luminol's tautomerism and not by vibrational resolution or even transitions towards two distinct electronic states within one same tautomer (or simultaneously in both species). As for the third electronic transition in DMSO, due to increase in solution absorbance near 260 nm, no conclusions can be made.

In respect to molecular orbital selectivity of the first transition, Table 6.3 shows that the less selective are for neutral forms of luminol. Tautomers B and C, chemically closer, show the same type of molecular orbital (MO) contamination in the same percentage. Because the $\sigma\pi^*$ contamination blue shifts the electronic transition, probably its contribution for the first transition is overestimated. When changing to anionic forms, the MO selectivity of the transition increases and the transition can be perfectly predicted by the energetic gap between the HOMO and the LUMO. As for the other two transitions, their selectivity is maintained or increased in neutral luminol but decreased for anionic species. Once again $\sigma\pi^*$ contamination is present in the less accurate prediction, where the error is of 14 nm. Therefore, from this analysis we can verify that the amount of $\sigma\pi^*$ contamination may significantly affect the accuracy of theoretical calculations. Still on this parameter, we can try to justify the lack of accuracy of TD DFT calculations with the relative contribution of N2 to molecular orbitals involved in the transition because the geometry optimization method and method used to calculate theoretical absorption spectra yield significantly distinct descriptions for that atom (*cf.* section 5.2). Therefore, plotting the error in theoretical calculations for the electronic transitions and the relative contribution of N2 to molecular orbitals involved in the transitions we obtain in Figure 6.10.

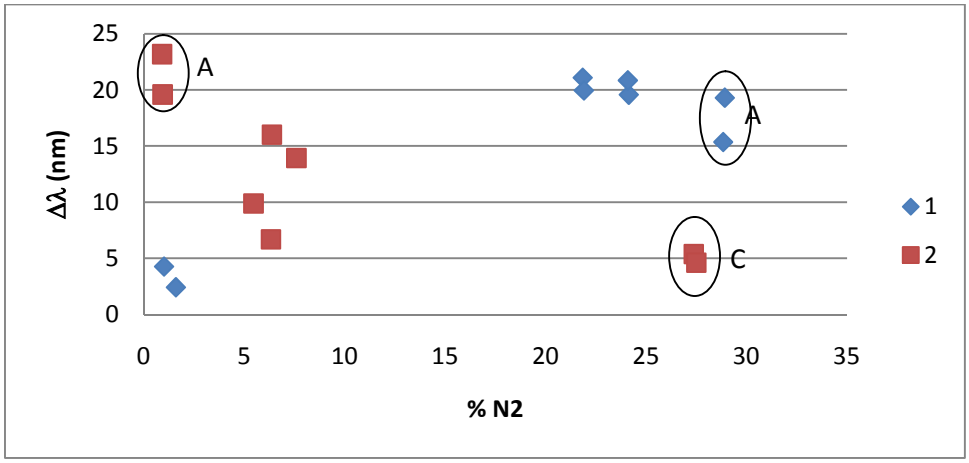

Figure 6.10: Error in estimation of excitation wavelengths Vs. The relative contribution of N2's atomic orbitals to molecular orbitals involved in transitions 1 and 2 in water and DMSO.

As we can verify, for the first transition (blue), a linear correlation appears to exist if we neglect luminol's tautomer A (determination coefficient of 0.97 is obtained by linear regression in those conditions). Even though the number of points is insufficient for precise conclusions, the contribution of N2 to MO's in electronic transition appears to have some influence in the error observed in the first transition estimation. As for the second electronic transition, no evident correlation exists and if to, an inverse relation (line with negative slope) would be obtained, going the error in that transition in opposite way of the expected. One factor that would go against this latter hypothesis is that pure DFT calculations (geometry optimization and TD DFT) using B3LYP functional[59] yielded similar errors in excitation energies estimation. Because not only the methods but also the basis sets used were completely different no direct comparison can be performed on both systems. Besides, it should be reminded that those DFT calculations yielded completely different conclusions regarding luminol's tautomerism.

As for other weak points in performed calculations, oscillator strengths for the second electronic transition in DMSO are to be also pointed out.

Besides the results discussed above, two other parameters can be estimated using these theoretical calculations. Those are radiative lifetimes of the excited states (only computed for the first singlet excited states because those are the only ones with physical meaning) and the anisotropy between excited states. In order to obtain the first parameter, information regarding the transition moments (the square of the norm) was used, being equation (3) applied to calculate this parameter.

$$\tau = \frac{3\varepsilon_0 h}{16\pi^3}\frac{\lambda^3}{\mu^2} \qquad (3)$$

Here, ε_0 is the vacuum permittivity, h the Planck constant, λ the (theoretical) excitation wavelength and μ^2 the square of the norm of transition moment vector.

Regarding anisotropies of the excited states (r), they can be computed theoretically by expression (4),[59]

$$r = \frac{3cos^2(\alpha) - 1}{5} \qquad (4)$$

where α is the angle between the associated transition moment vectors for the two excited states. Tables 6.4 and 6.5 present the results from those calculations. Regarding anisotropies, only results from calculations in water's dielectric are presented because they can be compared with experimental results in similar media (*cf.* section 6.1.5). For aprotic media, known glasses are inadequate due to luminol's low solubility in low polarity media.

Table 6.4: Luminol's tautomers (A, B and C) radiative lifetimes (in nanoseconds) in DMSO and water.

	A	B	C
DMSO	11.0	8.7	8.7
Water	11.0	9.4	9.6

Table 6.5: Computed anisotropies for S_1-S_2 and S_1-S_3 excited states in water. Angles between transition moments, in degrees, are inside brackets. $(S_1 \leftarrow S_0).(S_n \leftarrow S_0)$ stands for the scalar product between the transition moments for the transitions $S_1 \leftarrow S_0$ and $S_n \leftarrow S_0$, where n is the n^{th} excited state.

	A	B	C
$(S_1 \leftarrow S_0).(S_2 \leftarrow S_0)$	0.074 (132.5)	-0.19 (96.9)	-0.15 (73.2)
$(S_1 \leftarrow S_0).(S_3 \leftarrow S_0)$	-0.11 (66.7)	0.007 (126.0)	-0.18 (79.6)

In respect to radiative lifetimes of luminol's tautomers, they are a reflection of the nature of the transition towards the excited state involved and of course of the oscillator strengths associated. In order to prove theoretical calculations in radiative lifetimes, low temperature experiments should be performed (in order to freeze non-radiative processes in luminol's photophysics). If the fluorescence kinetic constant is weakly affected by the temperature then the radiative lifetime can also be calculated using the fluorescence quantum yield and the excited state lifetime.

Regarding anisotropies between excited states, as expected, tautomer A exhibits a behaviour completely different from the other two species. Complete orthogonality between transition moments (r = -0.2) should never be observed for $(S_1 \leftarrow S_0).(S_2 \leftarrow S_0)$ and $(S_1 \leftarrow S_0).(S_3 \leftarrow S_0)$. As for the other two tautomers, the second excited state's transition moment is practically orthogonal to S_1's transition moment and low anisotropies are expected at 300 nm. Also from theoretical calculations we verify that tautomer's B anisotropy is lower at 300 nm than tautomer's C. As for the transition moment for the third excited state, tautomers B and C exhibit quite different behaviour. While in B the two vectors are oriented in the same direction in one of x and y axes, in tautomer C the two transition moments are close to orthogonality. The last figure of this section, Figure 6.11, presents the direction of the

projection on xy plane of the transition moment vectors for luminol's tautomers, A, B and C, in order to give visual interpretation of previously discussed subjects.

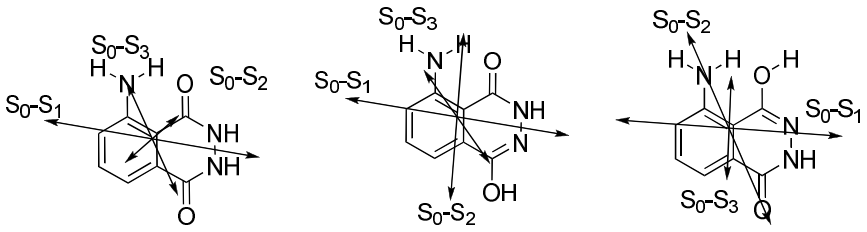

Figure 6.11: Projection on xy plane of transition moment vectors for the first three excitations in luminol's most stable three neutral forms. The axes were deliberately omitted in the representation above for the sake of simplicity.

6.1.5 - Luminol's Excitation and Emission in Ethanol-Methanol Mixture

Luminol's spectroscopic properties were also studied in a mixture of 9EtOH:1MeOH because this particular mixture allows studies in both liquid phase (room temperature) and in a glass (extremely low temperature, namely 100 K). The great interest in studying luminol's excitation and emission in glasses is that experiences with polarized light can be performed allowing experimental access to the excitation anisotropies.

The following figures present excitation and emission spectra for luminol in the so referred media both at room temperature (298 K) and low temperature (100 K). Due to the relative concentration of the chromophoric species and also to allow direct comparison between RT and low-temperature spectra, no absorption spectra are presented. Table 6.6 comprises main data regarding these spectra.

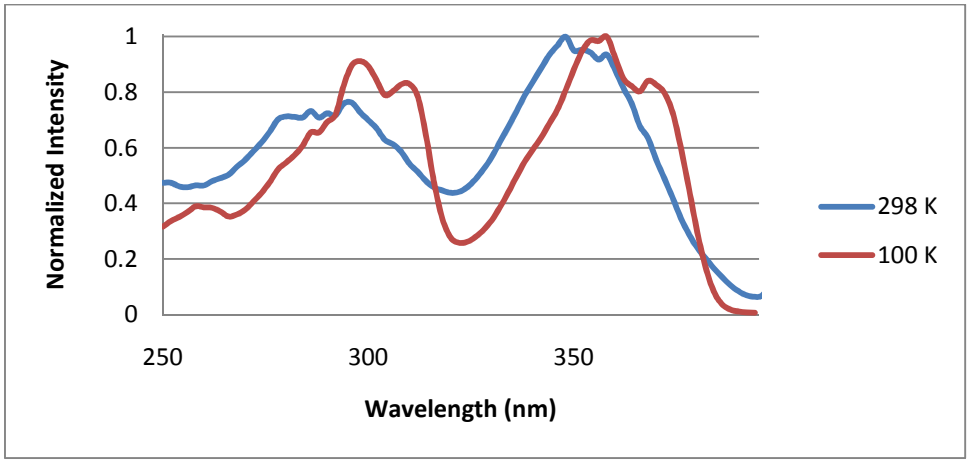

Figure 6.12: Normalized excitation spectra for luminol in 9:1 EtOH-MeOH in both RT (298 K) and 100 K. Data regarding these two spectra in Table 6.6.

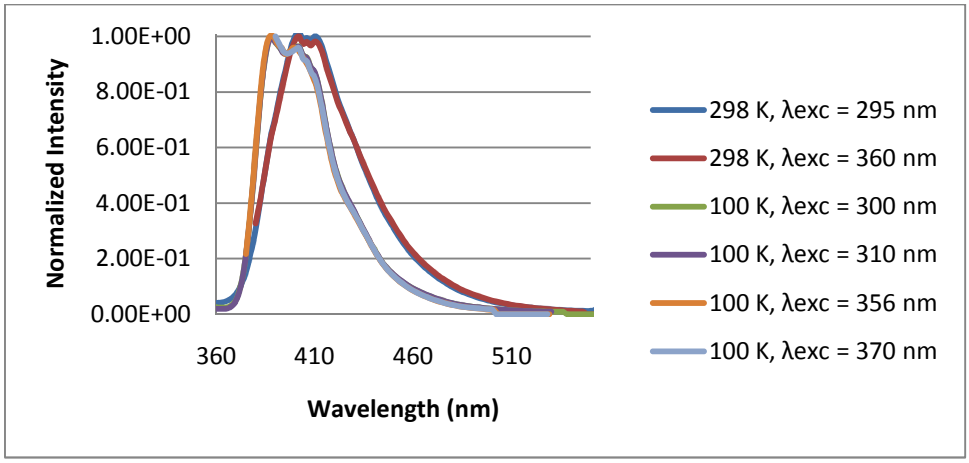

Figure 6.13: Normalized emission spectra for luminol in 9:1 EtOH-MeOH in both RT (298 K) and 100 K. Data related to these spectra in Table 6.6. Before normalization, emission intensities were corrected.

Table 6.6: Information regarding spectra presented in a) Figure 6.12 and b) Figure 6.13. In all solutions luminol's concentration was 5.0×10^{-7} M.

a)	Excitation	
T (K)	100	298
λ_{exc} (nm)	---	---
λ_{em} (nm)	414	414
$\lambda_{max\ 1}$ (nm)	258	296
$I[\lambda_{max\ 1}]$	5.27×10^{6}	5.20×10^{6}
$\lambda_{max\ 2}$ (nm)	298	348
$I[\lambda_{max\ 2}]$	1.24×10^{7}	6.82×10^{6}
$\lambda_{max\ 3}$ (nm)	310	---
$I[\lambda_{max\ 3}]$	1.12×10^{7}	---
$\lambda_{max\ 4}$ (nm)	356	---
$I[\lambda_{max\ 4}]$	1.33×10^{7}	---
$\lambda_{max\ 5}$ (nm)	370	---
$I[\lambda_{max\ 5}]$	1.12×10^{7}	---

b)	Emission					
T (K)	298	100	100	100	298	100
λ_{exc} (nm)	295	300	310	356	360	370
λ_{em} (nm)	---	---	---	---	---	---
$\lambda_{max\ 1}$ (nm)	400	388	388	389	402	390
$I[\lambda_{max\ 1}]$	3.97×10^{6}	1.27×10^{7}	1.15×10^{6}	1.38×10^{7}	5.13×10^{6}	1.40×10^{7}
$\lambda_{max\ 2}$ (nm)	410	402	402	399	---	402
$I[\lambda_{max\ 2}]$	3.97×10^{6}	1.22×10^{7}	1.11×10^{7}	1.32×10^{7}	---	1.34×10^{7}

From collected data, RT excitation spectrum of luminol in the alcoholic mixture is not much changed from previously presented absorption spectra. The two maxima, one in the gap of 296-301

nm and the other in the gap 348-360 nm are retained and once again we confirm the practically null effect of hydrogen bonding in those systems. As for main differences, the excitation spectrum of luminol in 9:1 EtOH-MeOH shows what appears to be lack of resolution, noise, but that must be a concentration effect. When cooling to 100 K, almost all vibrational motion is frozen and, as expected, the excited spectrum bands get thinner. Besides, resolution on the spectrum is increased and the two well defined maxima in each band as well as a shoulder at lower wavelengths appear. Besides, one extra maximum appears at lower wavelengths (258 nm). To account for the first effect, split of the absorption bands into two new absorption bands, the two previously proposed hypothesis are still valid, *i.e.*, tautomerism or vibrational resolution. The difference in wavenumber for those two maxima in each excitation band is of 1050 cm^{-1} (slightly higher for absorption band towards S_2) and, once again, luminol's IR spectrum[57] shows a peak at 1060 cm^{-1} that is not usually associated with CH aromatic bonds but to group vibrations.[58] Regarding the extra excitation band, theoretical calculations previously presented (*cf.* section 6.1.4) indicate that the transition towards S_3 excited state can justify the result. The high distance (30 nm) towards the transition at 300 nm also goes along the previous statement. Therefore, luminol's excitation in this alcoholic solvent appears to confirm some results from theoretical calculations.

Regarding the fluorescence spectra, a slight blue shift in this solvent at RT is observed towards neutral aqueous conditions. Because in aprotic media the maximum emission wavelength in luminol's fluorescence is also blue shifted, that effect is assignable to media's polarity. In respect to the shape of the emission band, it has retained from other solvents tested. Curiously, some "loss of resolution occurs in the maximum emission wavelength seeming to be the separation of two emission maxima. When cooled down, the emission band of luminol gets thinner (expected) and once again acquires two well defined maxima in the emission, being one 1.1 times stronger than the other (the same factor between excitation maxima in each band). As for the difference in wavenumber between those two maxima, the value obtained is 1000 cm^{-1}, being the same conclusions for excitation spectra valid for fluorescence. If not for the wideness of the slits used in excitation, the retention of the emission spectrum with different excitation wavelengths would be evidence for vibrational nature of the two emission bands observed.

In respect to the effect of temperature lowering in excitation and emission spectra, the excitation is red shifted and the emission is blue shifted. We therefore have to considerer that the interactions between solute and the media are slightly affected by lowering the temperature. Assuming that the energy of Franck-Condon structures is retained, upon temperature lowering luminol's ground state equilibrium structure is unstabilized while thermal equilibrated first singlet excited state is stabilized towards RT conditions. Because all van der Waals forces increase their strength when the temperature is lowered $\left(E \propto -\frac{1}{T}\right)$ [60], we conclude that when lowering the temperature, luminol's interactions with the solvent get stronger being the intramolecular hydrogen bonding stabilization sacrificed. Because fluorescence is (slightly) red shifted, the equilibrium electronic excited state must be stabilized and we conclude that intermolecular hydrogen bonding

stabilizes the structure. For that to occur, the significance of intramolecular hydrogen bonding in the first singlet excited state must be extremely small.

Regarding Stokes shift, at RT, it is of 60 nm and when media's temperature is decreased the parameter decreases to 20-50 nm. These values are in agreement with previous discussion. To account for the decrease in Stokes shift upon temperature lowering, we can rely on the proposed change in interactions with the solvent cage.

In respect to anisotropies on luminol's glass excitation, we can use relation (5).

$$r = \frac{(VV) - \frac{(VH)(HV)}{(HH)}}{(VV) + 2\frac{(VH)(HV)}{(HH)}} \qquad (5)$$

Here, (XY) are emission intensities at certain wavelength as a function on excitation wavelength where X identifies the polarization in excitation monochromator and Y the polarization in emission monochromator (V stands for vertical polarization and H for horizontal). With this, luminol's excitation anisotropies were calculated at emission wavelengths of 390 and 406 nm. The results are presented in Figure 6.14.

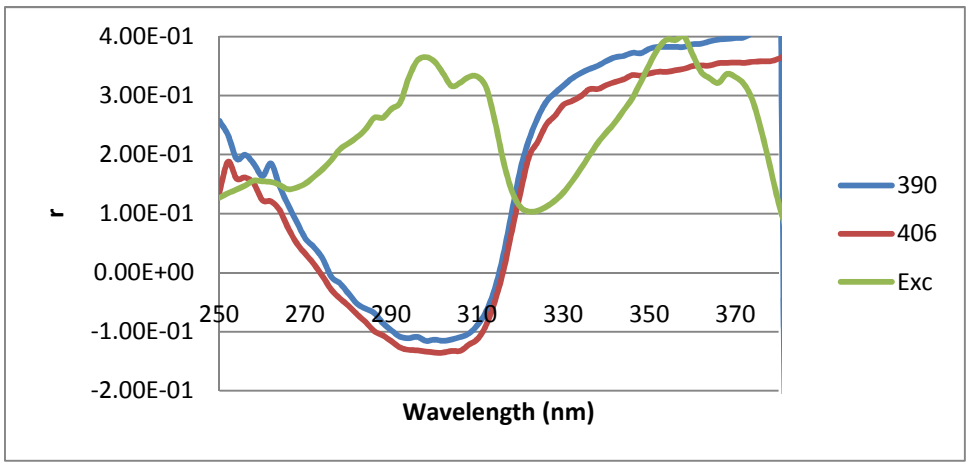

Figure 6.14: Anisotropies for luminol's glass in 9:1 EtOH-MeOH. Emission wavelengths were 390 nm and 406 nm. Excitation spectrum is also presented in green. This spectrum was normalized to 0.4.

The anisotropy plots presented in the last figure are extremely similar. As we can see, using emission at 390 nm we obtain practically the same curve as we obtain when following the emission 16 nm above. This is evidence that if two species are involved in luminol's absorption, they must have quite similar behaviour in solution and in the glass. Therefore, from this first analysis and from theoretical calculations results we can start to rule out luminol's tautomer A as a significant tautomeric contributor. Regarding the transitions *per se*, we observe that the only anisotropy that goes to the theoretical anisotropy for the first transition, 0.4, is with the excitation at 390 nm. When that happens ($r_{390\,nm} = 0.4$), the anisotropy at 406 nm is at 0.365. Even though not agreeing with the theoretically expected value, it means not that the data is incorrect. According to the literature,[59] if the experimental

anisotropy in the first transition goes not to the theoretically limiting value (0.4) it is said that the anisotropy has a limiting anisotropy. That can be accounted by several factors, namely molecular motion (vibrations, rotations) and a non-null Stokes shift, *i.e.*, change in molecular geometry and solvent cages between different electronic states.[59] As for the second electronic transition, we observe extremely similar anisotropies at 390 nm and 406 nm but both above -0.2 (specifically, between -0.115 and -0.135). To account for it, we may have also an effect of the molecular geometry in those transitions but here at least a slight increase is theoretically expected (*cf.* Table 6.5), especially for tautomer C. Besides, because the predicted oscillator strengths for the second transition in water (for both tautomers) are slightly underevaluated and because theoretical calculations are applied solely to the interaction of luminol with the dielectric constant of water we can perhaps account for the observed discrepancy between theory and experience. In respect to the third theoretically predicted transition, the anisotropy experience appears not to distinguish it (or perhaps it is close to 250 nm and there, absorption by the media starts to be significant).

Regarding the similarity between anisotropies at 390 nm and 406 nm in emission, it does not also mean that luminol only exists in one tautomeric form. The similarity between those two anisotropies can be used to rule out luminol's tautomer A because even with the inherent accuracy of the theoretically applied methods, its presence would not account for the observed behaviour. In respect to tautomers B and C, all theoretical calculations predict extremely similar properties, namely theoretical absorption spectrum in water (see in Figure 6.8 that predicted excitation energies are all superimposed). Therefore, because we had an experimental resolution of 9 nm (in both excitation and emission), if the theoretical calculations for the excitation energies of B and C are correct (in the proximity of the transitions), then we did not have resolution enough in the experiments to distinguish those species. In resume, we cannot state that our theoretical calculations results are in agreement with experimental results but we can say that those are so far the only calculations able to account for all collected spectra of luminol.

6.1.6 - Luminol's Chemiluminescence

Using conditions reported by Rauhut and co-workers,[25] luminol's chemiluminescence spectrum was recorded. These conditions were chosen due to their ability to decrease the reaction speed, allowing the acquisition of a more realistic chemiluminescence spectrum. Because those same authors refer that luminol's chemiluminescence reaction has its emission maximized at pH close to 11.5, [25] the spectra were only collected at pH values close to those. The oxidants that allowed those reaction conditions were hydrogen peroxide and potassium persulphate. Figure 6.15 presents luminol's normalized chemiluminescence spectrum at pH 11.8 superimposed with luminol's fluorescence at pH 11.8 (also presented in Figure 6.2) and aminodiphthalate's fluorescence at pH 11.9 (also presented in Figure 6.22).

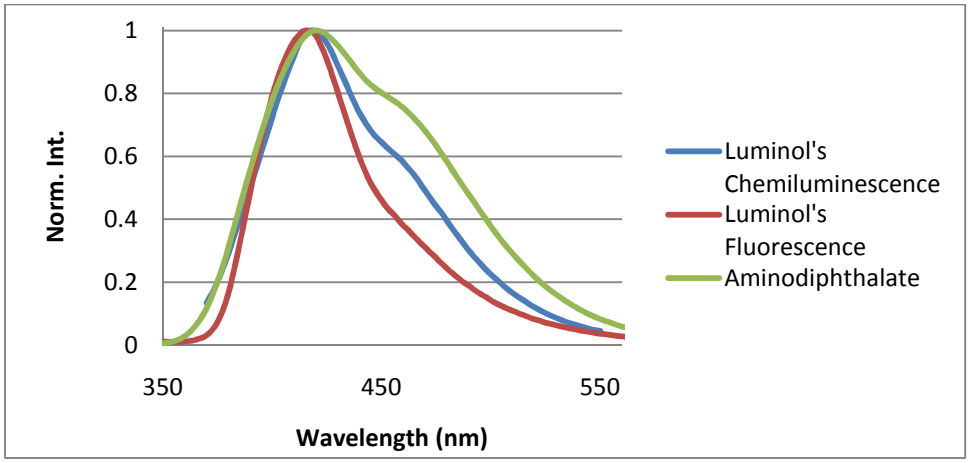

Figure 6.15: Luminol's normalized chemiluminescence spectrum at pH 11.8 superimposed with luminol's normalized fluorescence at pH 11.8 and aminodiphthalate's normalized fluorescence at pH 11.9 using in both excitation at 300 nm. Luminol's concentration was 5.2×10^{-5} M while hydrogen's peroxide concentration was 4.6×10^{-2} M and potassium persulphate's concentration was 6.0×10^{-2} M. Spectrum normalized at 418 nm whose emission intensity was 3.46×10^{5}.

Comparing all presented spectra we conclude that maximum emission wavelength is retained, *i.e.*, all observed transitions have the same energy. Because in aqueous solvents luminol's absorption spectrum has a maximum at 350 nm, if sufficiently concentrated and at low reaction times, energy transfer processes can occur. But because all species emit at the same wavelength, these processes may go unnoticed. Also because luminol's normalized chemiluminescence spectrum remained the same through large time intervals (where luminol's concentration was decreasing) and due to the relative concentration of the species in the media, we can state that in luminol's chemiluminescence, the emission came solely from the aminodiphthalate. Besides the retention of the maximum emission wavelength, both luminol's chemiluminescence and aminodiphthalate's fluorescence possess a shoulder. To account for it, the emission from two distinct species must be invoked, being these aminodiphthalate (420 nm) and its acid conjugate (around 450 nm) (*cf.* section 6.2),[27] the latter formed by acid-base reaction during excited state's lifetime. Curiously enough this is the first time that type of behaviour is observed in luminol's oxidation reaction. In the literature almost all studies on luminol's oxidation reaction use potassium ferricyanide as substituent of potassium persulphate yielding much faster reaction rates. Besides, the presence of the iron would also promote alternative ways for the return to ground state from the first electronic excited state of the aminodiphthalate (by charge transfer processes), reducing the time available for the acid-base reaction in the excited state to take place. To justify the fact that the authors from whom the reaction conditions were taken did not report the presence of such shoulder in luminol's chemiluminescence spectrum, only the resolution of the collected spectra can be so far pointed.

As a final remark, luminol's chemiluminescence is in great agreement with aminodiphthalate's fluorescence spectrum, being that result confirmed.

6.1.7 - Isoluminol

One commercial luminol derivative is isoluminol, with the amino group shifted to the position in the aromatic ring where it is in the *meta* and *para* positions in respect to carboxylic groups (instead of *ortho* and in the *para* position). Figure 6.16 presents isoluminol's structure.

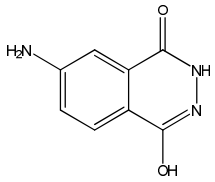

Figure 6.16: Structure of isoluminol, isomer of luminol with the aniline moiety shifted in the aromatic ring. The structure assigned was based on luminol's solid state structure.

The great interest in this species comes from the fact that the aniline functionality can no longer interact intramolecularly by hydrogen bonding with any of the carboxyl groups. Therefore, it is not odd if significant differences from luminol's behaviour are observed. Perhaps the most marked discrepancy is in chemiluminescence quantum yield that is 10-100 fold minor than luminol's.[13] Because in isoluminol the mesomeric effect should be similar to the one exhibited by luminol, this decrease in chemiluminescence quantum yield is accounted by the effect of intramolecular hydrogen bonding. For that great difference to be observed, the stabilization of excited state structure and molecular conformation induction in reaction's intermediates that maximize the yield for the formation of the aminodiphthalate in its electronic excited state must be negatively affected.

Like in luminol's case, isoluminol's absorption and fluorescence spectra were collected in DMF, DMSO and water, this time only at one pH. These are presented in Figure 6.17. Figure 6.18 presents isoluminol's fluorescence spectra in the same three solvents using an excitation wavelength of 300 nm. Isoluminol's chemiluminescence spectrum in aqueous media is presented in Figure 6.19. This last figure also presents luminol's chemiluminescence for comparison purposes. Table 6.7 resumes main information regarding the solutions and the respective spectra.

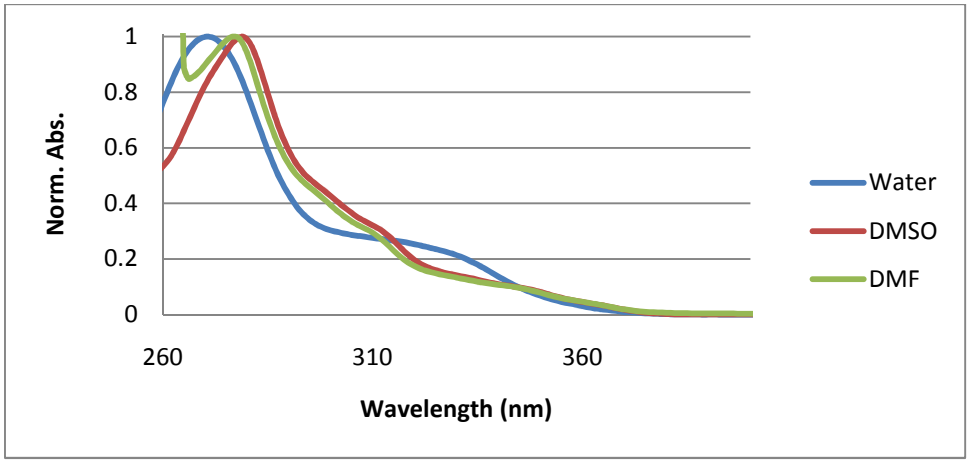

Figure 6.17: Isoluminol's absorption spectra in aqueous KOH, DMSO and DMF.

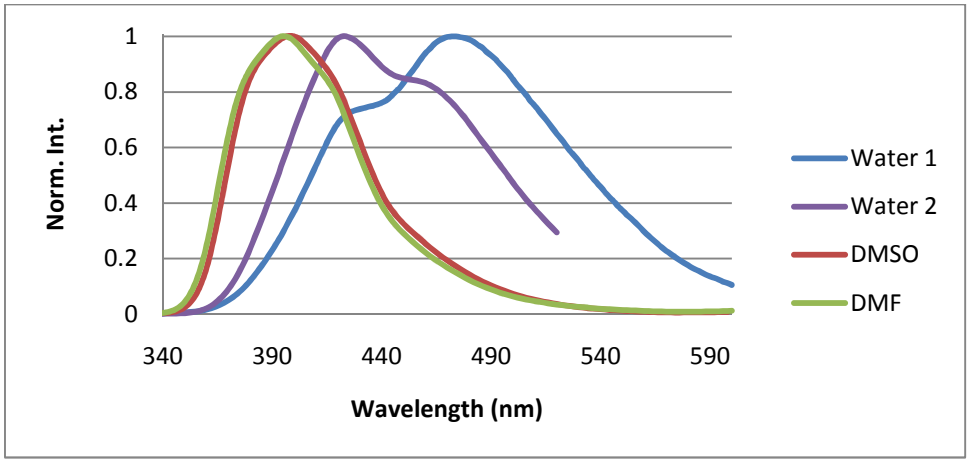

Figure 6.18: Isoluminol's fluorescence spectra in aqueous KOH, DMSO and DMF.

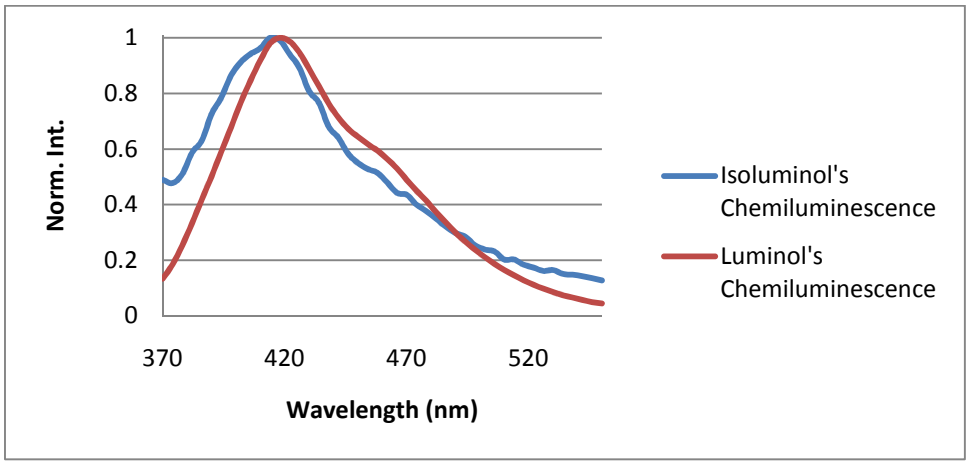

Figure 6.19: Isoluminol's chemiluminescence spectra in aqueous KOH.

Table 6.7: Data concerning the absolute intensity for absorption spectra presented in Figure 6.18, fluorescence spectra in Figure 6.18 and chemiluminescence in Figure 6.19.

	Absorption		
Solvent	DMSO	DMF	Water
C (M)	5.6×10^{-5}	5.6×10^{-5}	5.5×10^{-5}
pH	---	---	11.75
$\lambda_{max\ 1}$ (nm)	279	277	271
$A[\lambda_{max\ 1}]$	1.512	1.934	1.266

	Fluorescence			
Solvent	DMSO	DMF	Water 1	Water 2
C (M)	5.6×10^{-5}	5.6×10^{-5}	5.5×10^{-5}	5.0×10^{-7}
pH	---	---	11.75	7
λ_{exc} (nm)	300	300	310	270
$\lambda_{max\ 1}$ (nm)	400	396	474	422
$I[\lambda_{max\ 1}]$	2.8×10^{7}	2.6×10^{7}	5.1×10^{7}	2.58×10^{7}

	Chemiluminescence KOH (aq)
C (M)	5.5×10^{-5}
C_{H2O2} (M)	4.6×10^{-2}
C_{K2S2O8} (M)	6.0×10^{-2}
pH	11.75
$\lambda_{max\ 1}$ (nm)	414
$I[\lambda_{max\ 1}]$	1.16×10^{4}
C (M)	5.5×10^{-5}
C_{H2O2} (M)	4.6×10^{-2}

Comparing luminol's (*cf.* Figures 6.1, 6.5 and 6.6) and isoluminol's absorption spectra several differences arise immediately. The first is that isoluminol only possesses one main absorption band, being this centred at 280 nm in aprotic media and 270 nm in water. One to three shoulders are also present. Because the significant absorption starts at 360 nm, the origin for those shoulders may not be related to vibrational resolution (at least solely), having therefore electronic transitions in nature. Apart from that, the change from aprotic to protic media yields significant change in the maximum absorption wavelength. This hypsochromic shift is of 10 nm and due to its magnitude it can be perfectly assigned to the change of solvent's polarity. Therefore, the contribution from hydrogen bonding remains unknown (absorption spectra in alcoholic solutions would answer that question). One last hypothesis to account for that behaviour may also be the change in the absorbing species, from neutral isoluminol in DMF and DMSO to one of its base conjugates in water.

Regarding the maximum absorption wavelengths and comparing them to luminol's, if we establish a connection between isoluminol's absorptions at 315 nm and 270 nm and luminol's absorptions at 350 nm and 300 nm (respectively), the transition towards S_1 in isoluminol is much less allowed, being the other significantly favoured (5 times more intense).

Assuming now that isoluminol is just present in one form in all those solutions, we can once again estimate molar extinction coefficients at the maximum absorption wavelength, being these between 2.3×10^{4} $M^{-1}.cm^{-1}$ (aqueous KOH) and 3.4×10^{4} $M^{-1}.cm^{-1}$ (DMF). We can therefore conclude that, like luminol, $\pi\pi^*$ transitions are observed and the change in aniline's group position removes $n\pi^*$ character from that electronic transition (the molar extinction coefficients increase one magnitude order). To rationalize those effects, with the change in that group's position, the intramolecular interaction is destroyed and the electron giving ability of that nitrogen to the rings is therefore reduced.

Regarding the fluorescence spectra in aprotic media the emissions are almost perfectly superposable, being the emission in DMF slightly blue shifted (in agreement with $\pi\pi^*$ transition). Besides, emission in these solvents is merely composed by one band, fact that is not observed in water where two emission bands are perfectly distinguishable. The existence of two maxima can be assigned either to tautomeric forms or to acid-base conjugates due to the high value of the aqueous solution's pH. To clear that, we performed isoluminol's spectra at lower pH (Water 2, pH 7) and we verified that the relative intensity of the emission maximum and the shoulder are reverted. Due to this,

we have assigned the emission peak at 422 nm to neutral isoluminol, being the emission peak at 474 nm to its acid-base derivative. Regarding the origin of monoanionic isoluminol, it can be assigned to acid-base in the excited state because the absorption spectrum at neutral pH, even though not exhibited, was equal to absorption spectrum at higher pH.

As for solvatochromic effects observed, having the transitions $\pi\pi^*$ character, we expected batochromic shifts in the absorption, not hypsochromic. As it is stated in the previous paragraph, in aprotic media the expected shift is observed but, when passing from those two organic solvents to water, the odd hypsochromic shift appears. Because, the absorbing species in water is the same as in both DMF and DMSO, the observed solvent shift cannot be rationalized solely by change in media's polarity. Intermolecular hydrogen bonding should then provide the observed shift in those solvents. For fluorescence, the expected batochromic shift is verified being that in good agreement with the assigned character of the electronic excited state of isoluminol. We can also conclude from these results that the intermolecular hydrogen bonding that is so significant in isoluminol's ground state must be destroyed in the first excited electronic state. That favours the assignment of a second excited state to the transition at 270-280 nm.

In respect to Stokes shifts, in DMF it is of 119 nm. As for DMSO, 121 nm is the observed value. In water, the Stokes shift is 151 nm. Comparing now to luminol's (50-60 nm in aprotic media and 65 nm in water), we verify that by slightly changing the NH_2 functionality in ring 1 in one position, the Stokes shifts doubles. To account for that great increase, once again we invoke the intramolecular hydrogen bonding (the mesomeric effect is similar in both luminol and isoluminol). Because in isoluminol the aniline moiety is not bound to the carboxylic group, different interactions with the solvent are expected, being the ground state of isoluminol significantly stabilized. To understand the increase in Stokes shift in both DMSO and DMF with that same proposal, we must verify that if the intramolecular hydrogen bonding is inexistent, both two groups will be more available to interact with the solvent's dielectric constant and the solvent cage, accounting for the observed effect.

As for isoluminol's chemiluminescence spectrum, the first thing to point is the increase of noise in the emission due to decrease in the chemiluminescence quantum yield. Using the ratio of intensities at maximum emission wavelength (in chemiluminescence) we estimate isoluminol's chemiluminescence quantum yield to be 3 % of luminol's, being this in agreement with the previously proposed values.[13] The curious fact is that the chemiluminescence emission of those two isomers is superimposed, at least in maximum emission wavelength. That should mean that the electronic excited states responsible for the spectra are similar in those two compounds. Assuming now that isoluminol's chemiluminescence follows a similar pathway to luminol's, then the aniline's position does not affect the energetic gap between ground and first electronic excited singlet state. For that to be true, not only the excitation must be localized in the carboxyl functionalities of the aminodiphthalate, but also the hydrogen bonding effect in those two electronic states must be of little significance. To be in agreement with the proposed effect of intramolecular hydrogen bonding, we can assume that during the step that will form the electronic excited state, the hydrogen bonding strength is

significantly diminished due to the excited state PES. That would conciliate the retention of the maximum emission wavelength with the decrease in the intensity (assigned to decrease in quantum yield for excited state formation). The mesomeric effect of the aniline moiety to the carboxylic functionality should therefore be similar in both isomers.

As conclusion, in isoluminol, we verified here that the quantum yield for the electronic excited state formation is 10-100 times smaller than in luminol, being that an effect of the stereo constriction induced by the hydrogen bonding between NH_2 group and the *ortho* carboxyl group in luminol. Besides, during the reaction step where the excited state is supposedly formed, the hydrogen bonding effect is significantly and negatively affected. The aminodiphthalate species formed in the oxidation of luminol and isoluminol will therefore be geometrically and energetically similar in the chromophoric region, both the first singlet excited state and in the Franck-Condon structure of the ground state PES.

6.2 - Aminodipthalate

This next section of the work deals mainly with the aminodiphthalate species, luminol's derivative obtained upon oxidation. It is postulated in the literature that this is the light emissive species in luminol's oxidation reaction both in protic and aprotic media. Its structure is presented in Figure 6.20 and in Figure 2.1 (species B). Studies on this species were conducted to know the nature of the two emission bands in luminol's chemiluminescence spectrum and to gather a better insight on spectroscopic properties of the light emissive species in luminol's oxidation reaction.

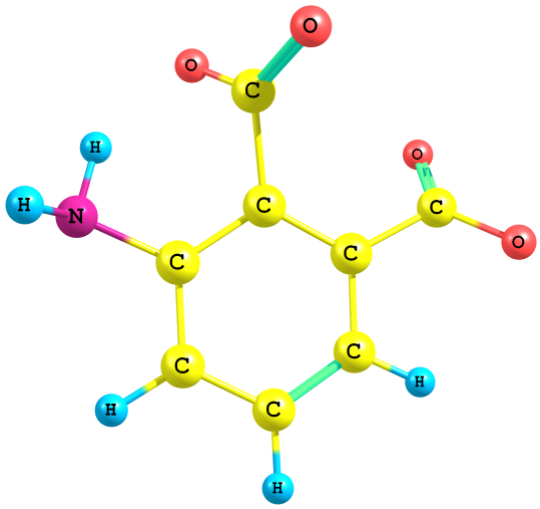

Figure 6.20: Aminodiphthalate's molecular geometry obtained with optimization with MP2/6-31G**.

6.2.1 - Aminodiphthalate's Absorption and Fluorescence

The next three Figures in the text present absorption and fluorescence spectra (with different excitation energies) in aqueous media at different pH of luminol's related diphthalate.

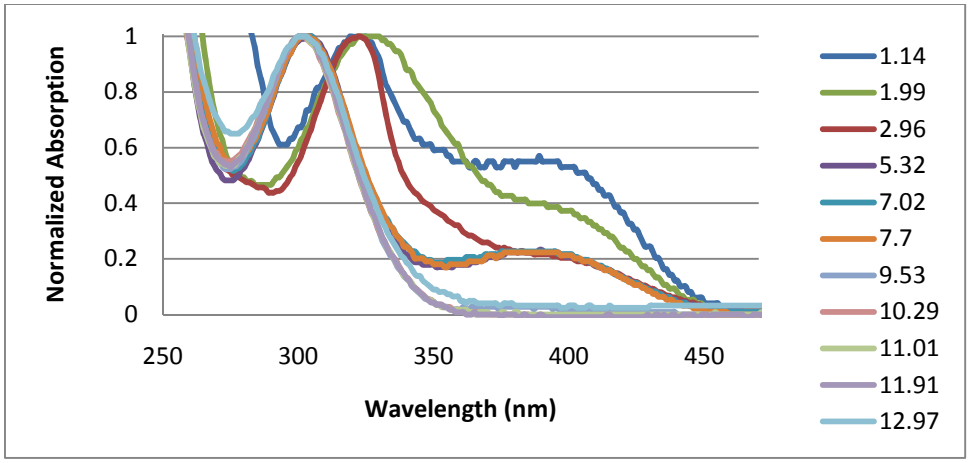

Figure 6.21: Absorption spectra for aminodiphthalate in aqueous media from pH 1.14 to pH 12.97.

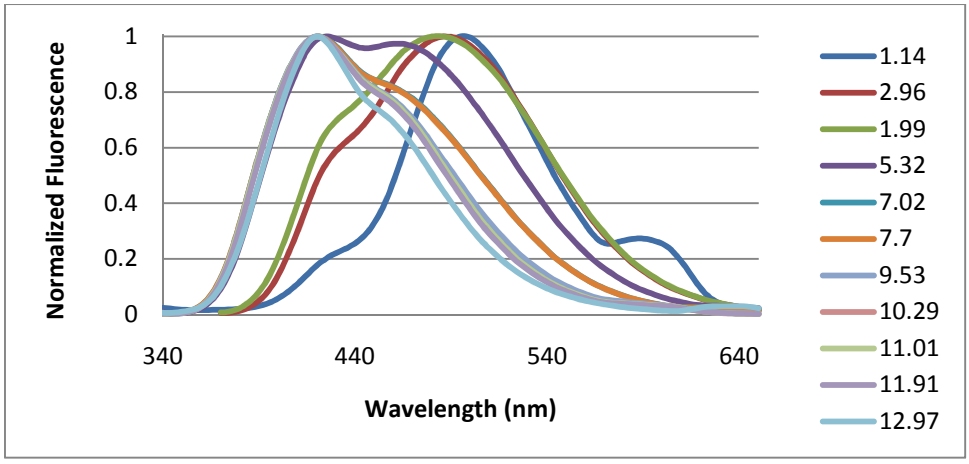

Figure 6.22: Fluorescence spectra for aminodiphthalate in aqueous media from pH 1.14 to pH 12.97 using lowest excitation wavelength for each solution.

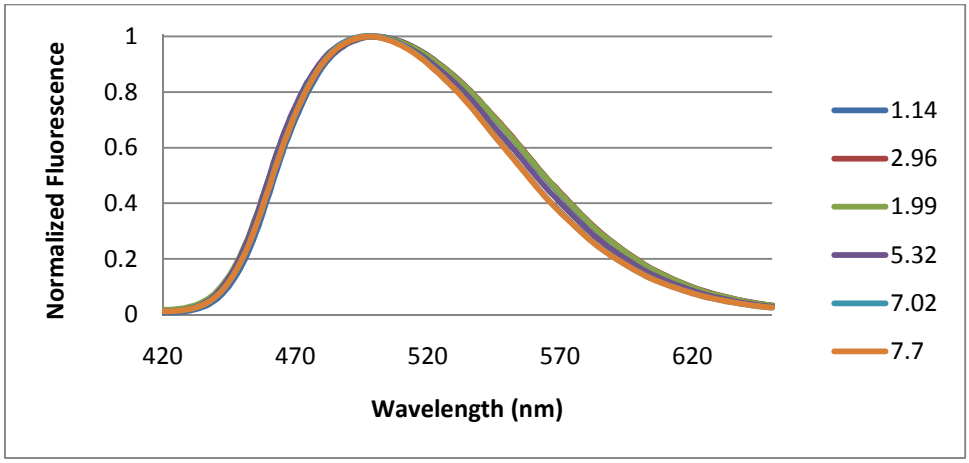

Figure 6.23: Fluorescence spectra for aminodiphthalate in aqueous media from pH 1.14 to pH 7.70 using highest excitation wavelength.

Table 6.8: Data concerning the absolute intensity for absorption spectra presented in Figure 6.21 and fluorescence spectra in Figures 6.22 and 6.23. Aminodiphthalate concentration was 6.2×10^{-5} M in all solutions.

	Absorption				Fluorescence		
pH	$\lambda_{max\ 1}$ (nm)	$A[\lambda_{max\ 1}]$	$\lambda_{max\ 2}$ (nm)	$A[\lambda_{max\ 2}]$	λ_{exc} (nm)	λ_{max} (nm)	$I[\lambda_{max}]$
1.14	320	0.049	389	0.028	320	498	4.96×10^{6}
					400	500	1.43×10^{7}
1.99	322	0.075	---	---	350	488	1.50×10^{7}
					400	500	1.49×10^{7}
2.96	322	0.162	---	---	350	480	1.76×10^{7}
					400	500	1.51×10^{7}
5.32	305	0.112	390	0.026	325	424	2.17×10^{7}
						460	2.11×10^{7}
					400	500	1.43×10^{7}
7.02	305	0.097	390	0.022	320	420	2.38×10^{7}
					400	500	1.29×10^{7}
7.7	303	0.094	390	0.021	320	420	2.38×10^{7}
					400	500	1.29×10^{7}
9.53	300	0.109	---		300	420	3.18×10^{7}
10.29	300	0.112	---		300	420	3.07×10^{7}
11.01	300	0.116	---		300	420	3.15×10^{7}
11.91	300	0.115	---		300	420	2.96×10^{7}
12.97	300	0.123	---		300	420	1.15×10^{7}

The first point to comment on the presented spectra is the high noise level at lower pH values. Using Table 6.8, we verify that the absorption is extremely small in those media, meaning that the oscillator strengths for those species are extremely low. At low pH values we also observe an absorption band around 390 nm that only disappears in the pH range of 7.70-9.53. To account for it, and due to relative acidity of carboxyl groups[61] and typical acidity for aniline[54], we propose that that

the absorption band is due to a zwitterionic (or cationic) aminodiphthalate derivative, being the aniline group protonated and with a formal unitary positive charge. Besides justifying aminodiphthalate's absorption spectra, this hypothesis accounts for the fluorescence observed with excitation at 400 nm. Of course those spectra could also be assigned to some impurity in those samples but the origin for those contaminations would remain a mystery because solutions with pH lower than 5 were prepared with hydrochloric acid addition, solutions with pH 7.02 and 7.70 were prepared by addition of an aqueous KOH solution, and all solutions were prepared from a mother aminodiphthalate solution, even the ones whose pH is higher than 9.53. Because both carboxylic acid moieties would not resist a pH change from 1.14 to at least 7.70,[61] and because slight changes in the maximum absorption wavelength appear to exist, acid-base derivatives of that proposed species (aminophthalic acid with aniline group protonated) would have similar absorption wavelengths, *i.e.*, the excitation affects a functionality in these species that is pH insensitive. Figure 6.24 presents the structure for the species that we assign to absorption bands at 400 nm and the fluorescence spectra at higher excitation wavelengths (named aminiumphthalic acids).

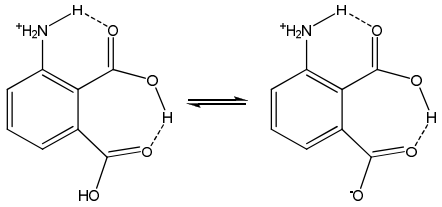

Figure 6.24: Aminophthalic acid-base derivatives (aminiumphthalic acids) assigned to be responsible for absorption band at 400 nm and for the fluorescence observed at higher excitation wavelengths.

The other two absorption bands presented in all absorption spectra would therefore have to be assigned to pure aminodiphthalate species, *i.e.*, without the extra proton in the aniline functionality. Due to the observed pH behaviour, we must propose that absorption bands at 300 nm are due to aminodiphthalate anions while absorption bands at 320 nm are mainly due to aminophthalic acid (APA). Regarding the aminomonophthalate (AMP), because absorption at 320 nm is extinguished at a pH below 5.32, it must have absorption maximum superimposed with the aminodiphthalate. Therefore, the chromophoric group in those species is related to the most acidic moiety of APA.

One other parameter regarding the pH effect on the absorption spectra is the relative magnitude of the absorbance of those solutions. At lowest pH, aminiumphthalic acids are favoured (but the equilibrium exists because the absorption band from aminophthalic acid is present). Therefore, adding the absorbance at maximum absorption wavelengths we may conclude that the molar absorptivities of aminiumphthalates are smaller than the ones for aminophthalic acid and its base conjugates. Thus, protonation of aminodiphthalate's nitrogen decreases the oscillator strength related to the transition to the first excited singlet state. Comparing now the sum of the absorbances at maximum absorption wavelengths on the pH ranges of 5.32-7.70 and 9.53-12.97, we verify that the value is practically conserved (0.12). Because in the first interval range aminiumphthalates still significantly affect the absorption, we can only say that the aminodiphthalate's oscillator strength in

the excitation towards the first singlet excited state must be smaller than the ones for aminomonophthalate and no precise conclusion can be taken for the relative value for the oscillator strength for the transition $S_1 \rightarrow S_0$ in AMP and APA. It should be also noted that the absorption bands in aminodiphthalate's absorption spectra are thinner than the ones for luminol. Because the degrees of freedom in luminol are expected to be lower, that may have to do with tautomerization effect.

As for the molecular orbital nature of these transitions, the molar extinction coefficients can provide an answer. Because the total concentration of aminiumphthalates is unknown, we only have accuracy for pH higher than 9.53. Therefore, dividing the absorbance at maximum absorption wavelength in those solutions by the total concentration of the absorbing species (the length of the quartz cell was 1 cm) we verify that the molar absorptivity of ADP is 1.85×10^3 $M^{-1}.cm^{-1}$. This is consistent with a $\pi\pi^*$ transition but with high $n\pi^*$ contamination (much higher than in luminol's case). Hydrogen bonding intramolecularly and with the solvent will therefore play a central role in the maximum absorption (and emission) wavelength as well as solvatochromic effects. Data presented in State of the Art (section 2) confirms those effects at least in ADP's fluorescence (*cf.* Table 2.1).

As for the fluorescence spectra (at lower wavelengths), once again a complex behaviour is observed, *i.e.*, several maxima are observed. Due to the collected absorption spectra, the presence of those maxima (even at pH higher than 9.53) can be justified by excited state acid-base behaviour of aminodiphthalate. Therefore, the strongest emission at lower pH values would have to be justified by the formation of aminiumphthalate's whose previously assigned emission perfectly superposes. Because this emission band appears to be present even at the highest pH tested (perhaps slightly shifted due to acid-base behaviour), we must therefore assume that AMP also emits at that wavelength, being that in good agreement with previous assignments.[27] In respect to the aminodiphthalate, its emission band would be at 416 nm, being this analysis consistent with luminol's chemiluminescence. Because between pH 11.01 and 11.91 two emission bands are observed in luminol's chemiluminescence, we have now gathered evidence that supports their acid-base nature (both ADP's absorption and emission) and the mechanistic scheme in Figure 6.25 can be proposed for luminol's oxidation reaction in aqueous media.

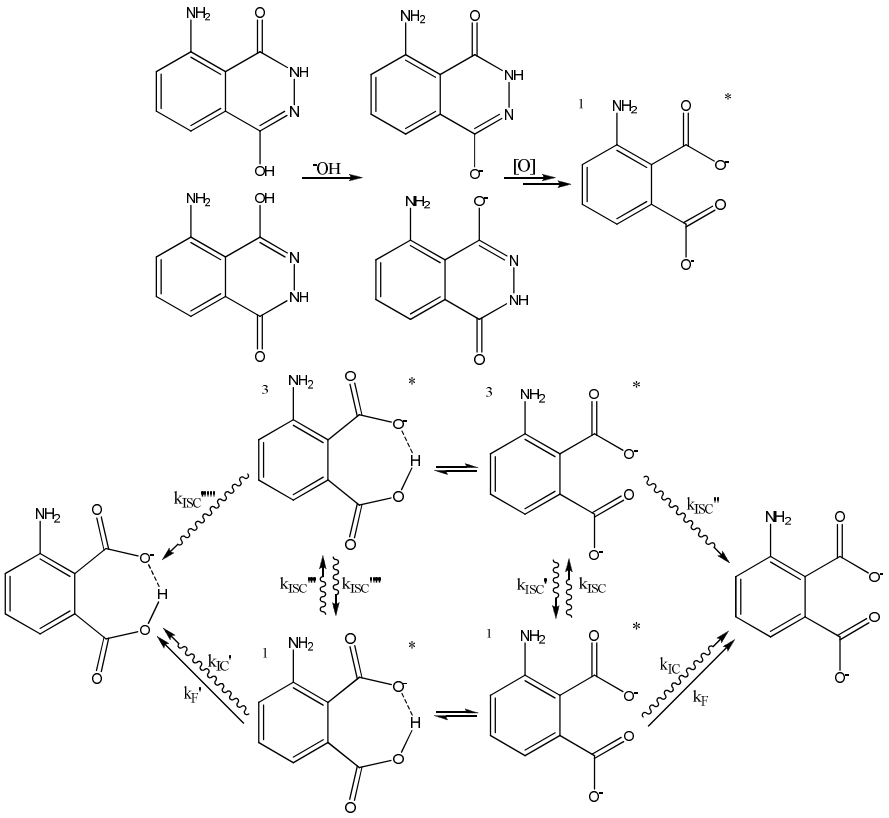

Figure 6.25: Mechanistic proposal for luminol's oxidation reaction according to aminodiphthalate's absorption and fluorescence spectra. While the first part of the proposed mechanism deals with the formation of the excited state species, the second part deals with photophysical and photochemical processes that may then occur.

It should be denoted that we propose in that mechanism that aminodiphthalate's protonation occurs in such a fashion that an intramolecular hydrogen bond is formed. That arises from the fact that the reaction conditions used were extremely slow, giving time for the system to achieve the minimum energy configuration (*cf.* State of the Art)[27]. In this mechanism it is also proposed that ADP is the excited state species formed within luminol's oxidation.

Regarding the excited state pK_a, equation (2) and literature values for APA pK_a's (3.0 and 5.7)[27] can be used, allowing us to estimate the value of 4.6 (using once again the average between the maximum absorption wavelength and the maximum emission wavelength).[55] AMP's excited state pK_a is estimated to be 10.2. Therefore, as expected for carboxylic acids, upon excitation, aminophthalic acid and base conjugates get less acidic.[55] Perhaps it should be underlined that these results neglect the aniline's acid-base behaviour because there are still no experimental or theoretical results that allow its pK_b estimation. These results for excited aminophthalic acids relative acidity decrease is in perfect agreement with fluorescence spectra for these species as well as luminol's chemiluminescence spectrum. Regarding tabled pK_a's for the ground state species and the collected absorption spectra, we confirm at least the first acidity constant (we cannot distinguish absorption from AMP and ADP).

Regarding the presented spectra, one last parameter is to be commented: Stokes shift. From Table 6.8, it increases upon protonation of aminodiphthalate (ADP) to aminophthalic acid (APA), from 116 nm to 136 and then 160 nm. Assuming that molecular orbital composition of the excitations is somewhat conserved in all compounds, the main cause for that trend must be the charge distribution (higher asymmetry), being this translated in higher discrepancies in solvent cages of each compound. The considered high $n\pi^*$ character of the transition (and therefore interaction with solvent cage) is in agreement with that, justifying the great discrepancy towards luminol. Besides, the increase in the degrees of freedom can also account for the increase in Stokes shift compared to luminol. Still regarding the observed trend, upon protonation of the aminodiphthalate, the strength of the intramolecular hydrogen bonding should be decreased, meaning that that interaction with water molecules would be favoured. The fact that all compounds exhibit high Stokes shift is evidence for some wide changes in molecular geometry and their interactions from the ground singlet state and the first singlet excited state.

6.2.2 - Aminodiphthalate's Theoretical Absorption Spectra

Applying the method previously used to predict luminol's absorption spectrum to the aminodiphthalate we gathered the results presented in Table 6.9.

Table 6.9: Theoretical previsions for aminodiphthalate's absorption spectra in both water and DMSO. While f is the oscillator strength, TN stands for transition nature and Cont. is contamination. Inside brackets is the functional group source of electrons for the excitation.

	Phase	λ_{max} (nm)	f	TN	Orbitals
S_1	H_2O	270.6	0.058	$\pi\pi^*$ Cont. $\pi\sigma^*$	46 - 49,50; 47 - 48
	DMSO	270.6	0.064	$\pi\pi^*$ Cont. $\pi\sigma^*$	46 - 49,50; 47 - 48
S_2	H_2O	258.8	0.043	$\pi\pi^*$ Cont. $\sigma\pi^*$	40,44,46 – 48; 47 - 49
	DMSO	259.9	0.047	$\pi\pi^*$ Cont. $\sigma\pi^*$	40,44,46 – 48; 47 - 49
S_3	H_2O	254.2	0.0051	$\pi\pi^*$ (Carboxyl)	45 - 48
	DMSO	254.9	0.0065	$\pi\pi^*$ (Carboxyl)	45 - 48

As we can observe from this last table, the electronic transitions in aminodiphthalate are, compared to luminol, much less selective. Besides, the theoretical method employed gives an error of 30 nm (in water) for the only excited state experimentally observed (300 nm) and, once again, high contamination in the first two electronic transitions. Due to all that, we believe that perhaps the method overestimated those contaminations, yielding the observed blue shift and also the slight underestimation in oscillator strengths of ADP (compared to luminol). In spite all that, the theoretical calculations are in fact able to justify the decrease in molar extinction coefficients from luminol to the aminodiphthalate. That experimental result is an effect on the change of carboxylic group character (from softer hydrazide to harder carboxylate) that will give more expression to σ character molecular

orbitals in the transition (for instance, two localized π molecular orbitals are combined to form a σ interaction). Nevertheless, theoretical calculations give predominance of ππ* character in all transitions, which is in agreement with the experimental data. In respect to the relative shape of the spectra, theoretical models state that, even though shifted, the main shape of luminol's absorption spectrum is retained in aminodiphthalate: Of the three transitions, one is "isolated" from the other two; of the two closer transitions, the highest energy one is also the less allowed.

Regarding the source of error, because aprotic media's absorption spectrum for ADP was not performed, nothing but the inherent accuracy of TD DFT and the different way both theoretical models describe the species in question can be pointed. Besides, an increase in the transitions contaminations (lose of selectivity) may also account for the observed errors.

From these results, we conclude that to perform structure-(maximum emission wavelength) theoretical studies in virtual compounds, it is best to use compounds with an hydrazide functionality instead of the dicarboxylate groups if no correction factor is to be considered. Due to the relative hardness of the chemical functionalities, carboxylates tend to interact more with the solvent by hydrogen bonding than hydrazides and thus the error in estimations are expected to be higher. This may also give lack of significance to calculations even with correction factors.

6.3 - Luminol's Derivatives

This section of the work deals with UV/Vis absorption and fluorescence spectra of luminol's derivatives obtained upon reaction with carboxylic electrophiles. The species studied in this section were previously presented in sections 3 (synthesis) and 4 (experimental work to isolate them). In the following discussion are therefore presented the spectroscopic (absorption and fluorescence) and chemiluminescence properties of TFALum (trifluoroacetyl luminol derivative), ECLum (ethoxy carbonyl derivative), BnLum (benzoyl derivative) and DMU1Lum, whose structure is still unknown. As previously stated, DMU2Lum was never isolated in a pure enough form, being contaminated with luminol. Therefore, the chemiluminescence properties could not be conveniently characterized and no studies were performed.

6.3.1 - Luminol's Derivatives Absorption, Fluorescence and Aqueous Chemiluminescence

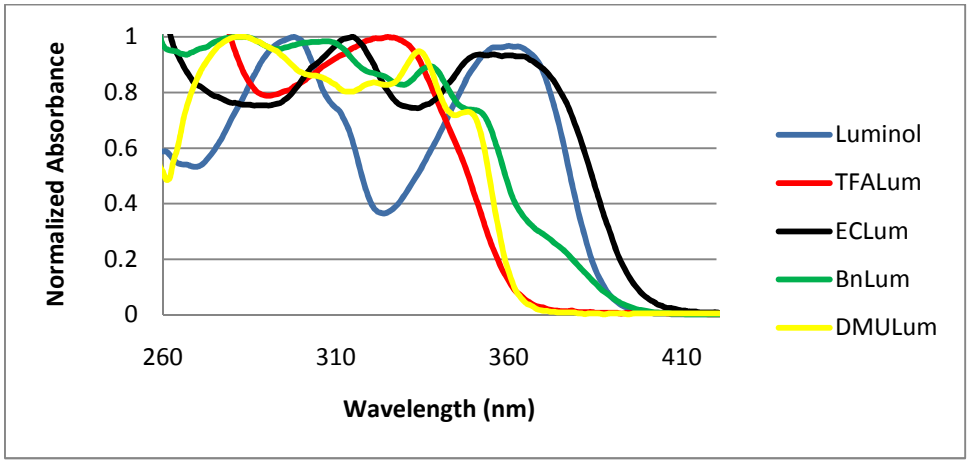

Figure 6.26: Normalized absorption spectra of luminol and its derivatives in DMSO. Data concerning these spectra is presented in Table 6.10.

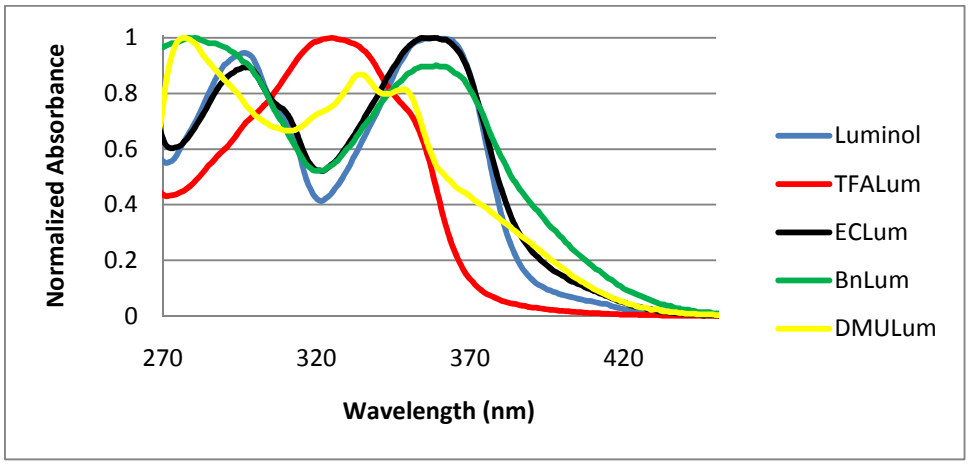

Figure 6.27: Normalized absorption spectra of luminol and its derivatives in DMF. Data concerning these spectra is presented in Table 6.10.

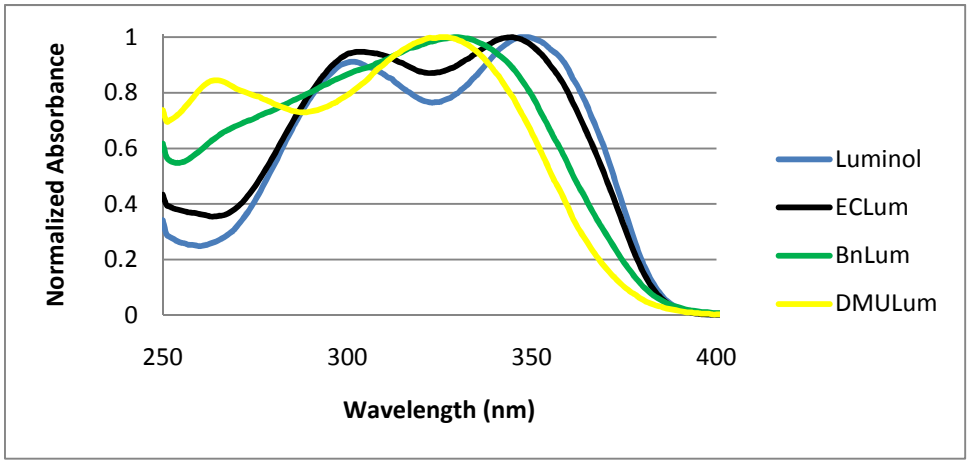

Figure 6.28: Normalized absorption spectra of luminol and its derivatives (except TFALum) in water at pH 11.7-11.8. Data concerning these spectra is presented in Table 6.10.

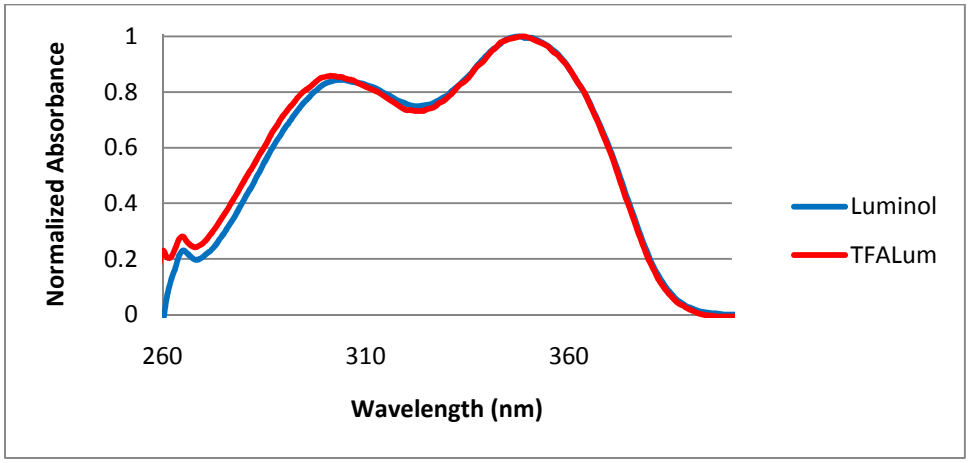

Figure 6.29: Normalized absorption spectra of luminol and TFALum in water at pH 11.4. Data concerning these spectra is presented in Table 6.10.

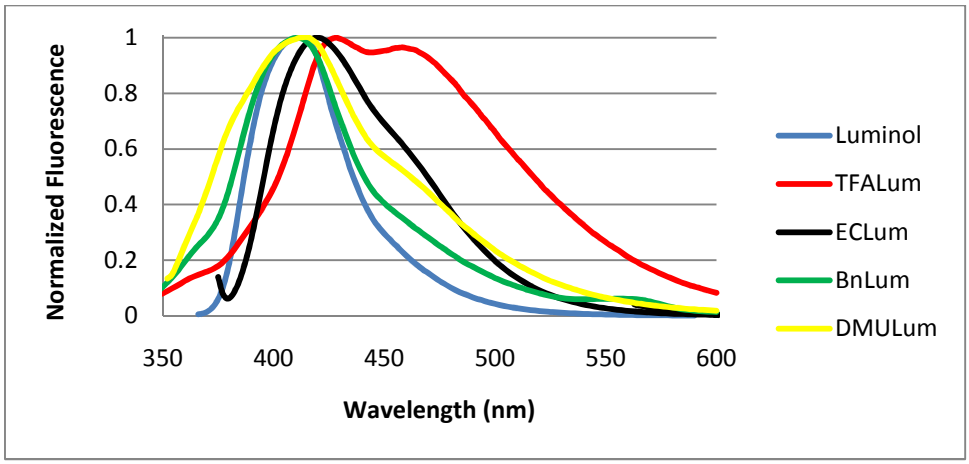

Figure 6.30: Fluorescence spectra for luminol and its derivatives in DMSO. Data on these spectra can be found in Table 6.10.

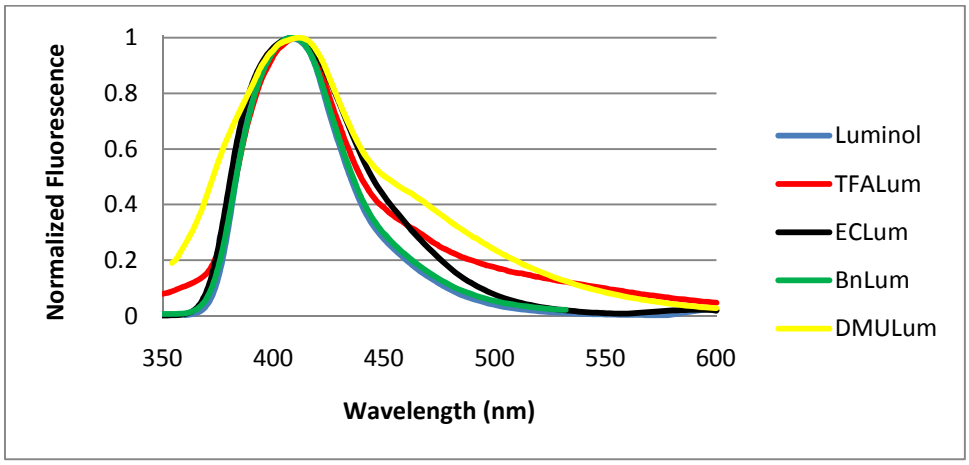

Figure 6.31: Fluorescence spectra for luminol and its derivatives in DMF. Data on these spectra can be found in Table 6.10.

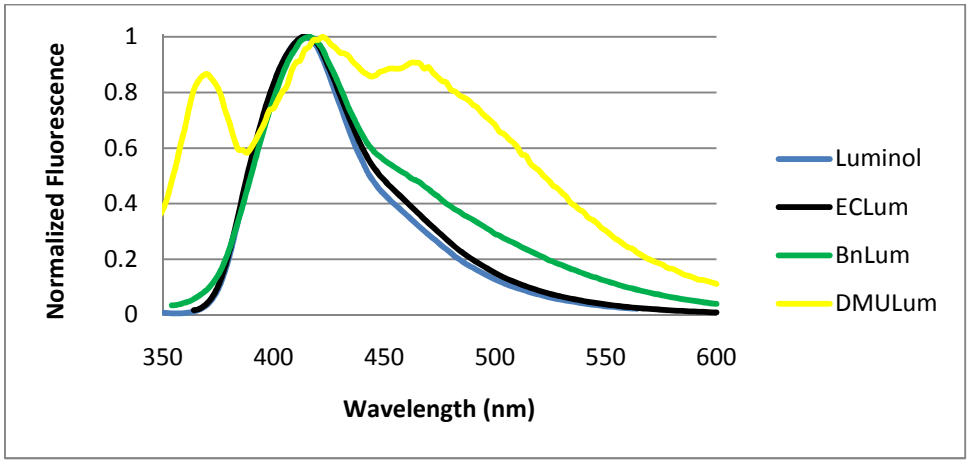

Figure 6.32: Fluorescence spectra for luminol and its derivatives (except TFALum) in aqueous media at pH 11.7-11.8. Data regarding these spectra can be found in Table 6.10.

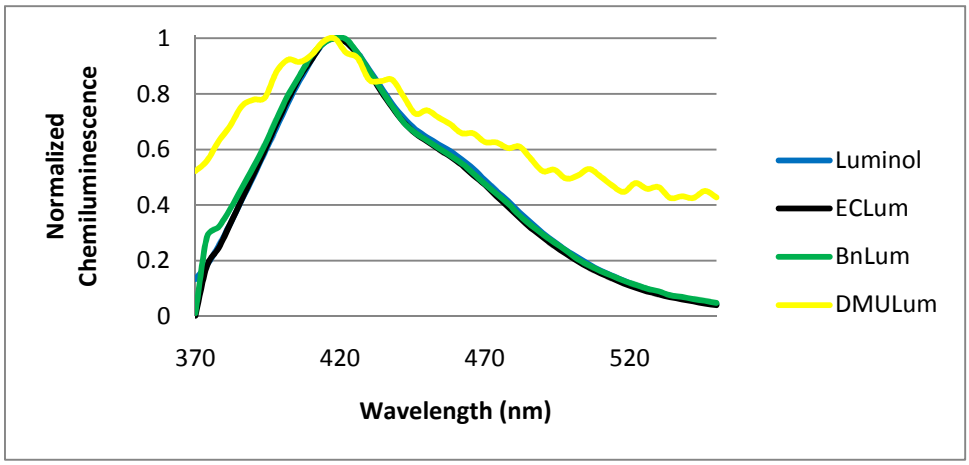

Figure 6.33: Chemiluminescence spectra luminol and its derivatives in aqueous media at pH 11.7-11.8. Data regarding these spectra can be found in Table 6.10.

Table 6.10: Data concerning the absolute intensity for absorption spectra presented in Figures 6.26 to 6.33. In all solutions luminol's concentration was 5.1×10^{-5} M. To identify the set of spectra one letter is used in a column in the left of the table. In these letters, A stands for absorption, F for fluorescence and C for chemiluminescence. Due to the fact that the structure is unknown, DMU1Lum's concentration appears in $g.mL^{-1}$.

	Solvent		Luminol	TFALum	ECLum	BnLum	DMU1Lum
A	DMSO	C (M)	5.4×10^{-5}	4.8×10^{-5}	5.6×10^{-5}	5.7×10^{-5}	1.4×10^{-5}
		$\lambda_{max\ 1}$ (nm)	298	258	315	280	282
		$A[\lambda_{max\ 1}]$	0.403	0.58	0.328	0.438	0.323
		$\lambda_{max\ 2}$ (nm)	360	325	355	306	321
		$A[\lambda_{max\ 2}]$	0.39	0.378	0.307	0.431	0.269
		$\lambda_{max\ 3}$ (nm)	---	---	---	337	334
		$A[\lambda_{max\ 3}]$	---	---	---	0.392	0.306
		$\lambda_{max\ 4}$ (nm)	---	---	---	---	348
		$A[\lambda_{max\ 4}]$	---	---	---	---	0.234
	DMF	C (M)	5.4×10^{-5}	5.0×10^{-5}	4.4×10^{-5}	4.3×10^{-5}	1.8×10^{-5}
		$\lambda_{max\ 1}$ (nm)	296	325	298	280	277
		$A[\lambda_{max\ 1}]$	0.349	0.59	0.295	0.214	0.377
		$\lambda_{max\ 2}$ (nm)	358	---	355	359	335
		$A[\lambda_{max\ 2}]$	0.369	---	0.33	0.193	0.327
		$\lambda_{max\ 3}$ (nm)	---	---	---	---	348
		$A[\lambda_{max\ 3}]$	---	---	---	---	0.307
	KOH (aq)	C (M)	5.2×10^{-5}	---	5.2×10^{-5}	5.0×10^{-5}	1.6×10^{-5}
		pH	11.76	---	11.72	11.75	11.76
		$\lambda_{max\ 1}$ (nm)	301	---	303	330	265
		$A[\lambda_{max\ 1}]$	0.36	---	0.566	0.515	0.332
		$\lambda_{max\ 2}$ (nm)	348	---	345	---	325
		$A[\lambda_{max\ 2}]$	0.395	---	0.597	---	0.393

	Solvent		Luminol	TFALum	ECLum	BnLum	DMU1Lum
F	DMSO	C (M)	5.4×10^{-5}	4.8×10^{-5}	5.6×10^{-7}	5.7×10^{-5}	1.4×10^{-5}
		λ_{exc} (nm)	306	325	362	280	334
		$\lambda_{max\,1}$ (nm)	410	428	421	410	416
		$I[\lambda_{max\,1}]$	3.13×10^{7}	1.43×10^{6}	1.43×10^{7}	7.44×10^{6}	3.38×10^{6}
		$\lambda_{max\,2}$ (nm)	---	458	---	---	---
		$I[\lambda_{max\,2}]$	---	1.38×10^{6}	---	---	---
	DMF	C (M)	5.4×10^{-5}	5.0×10^{-5}	4.4×10^{-5}	4.3×10^{-5}	1.8×10^{-5}
		λ_{exc} (nm)	358	325	295	360	335
		$\lambda_{max\,1}$ (nm)	408	410	410	410	412
		$I[\lambda_{max\,1}]$	3.24×10^{7}	5.79×10^{5}	3.50×10^{7}	1.55×10^{7}	1.68×10^{6}
	KOH (aq)	C (M)	5.2×10^{-5}	---	5.2×10^{-5}	5.0×10^{-5}	1.6×10^{-5}
		pH	11.76	---	11.72	11.75	11.76
		λ_{exc} (nm)	350	---	345	330	325
		$\lambda_{max\,1}$ (nm)	414	---	416	416	370
		$I[\lambda_{max\,1}]$	2.77×10^{6}	---	3.16×10^{6}	6.64×10^{5}	5.31×10^{4}
		$\lambda_{max\,2}$ (nm)	---	---	---	---	422
		$I[\lambda_{max\,2}]$	---	---	---	---	6.13×10^{4}
		$\lambda_{max\,3}$ (nm)	---	---	---	---	464
		$I[\lambda_{max\,3}]$	---	---	---	---	5.56×10^{4}

	Solvent		Luminol	ECLum	BnLum	DMU1Lum
C	KOH (aq)	C (M)	5.2×10^{-5}	5.2×10^{-5}	5.0×10^{-5}	1.6×10^{-5}
		C_{H2O2} (M)	4.6×10^{-2}	4.6×10^{-2}	4.6×10^{-2}	4.6×10^{-2}
		C_{K2S2O8} (M)	6.0×10^{-2}	6.0×10^{-2}	6.0×10^{-2}	6.0×10^{-2}
		pH	11.76	11.72	11.75	11.76
		$\lambda_{max\,1}$ (nm)	418	418	418	418
		$I[\lambda_{max\,1}]$	3.46×10^{5}	2.91×10^{5}	1.01×10^{5}	2.98×10^{3}

Before proceeding to analysis of the spectra of these luminol derivatives, it should be stated that for each solvent only one fluorescence spectrum is exhibited (only the spectra from one excitation wavelengths is presented). That is due to the fact that the only identifiable differences obtained in those spectra were the relative intensities, being the normalized spectra perfectly superposable.

Analysing the absorption spectra of these luminol derivatives in DMSO (Figure 6.26) we verify that upon derivatization, at least one of the absorption bands of luminol is shifted. Of all derivatives, the one with closest absorption to luminol (in DMSO) is ECLum. Two absorption bands are also observed, one at 355 nm (practically unshifted) and another at 315 nm. To account for this red shift, a substitution effect must be evoked, namely extension in π conjugation in the departure and arrival molecular orbitals. That extension would therefore be due to the carboxyl group introduced and the oxygen atom from the ethoxy moiety. It is therefore verified (even though in a different extent) the previously proposed batochromic shift upon extending aromaticity in luminol.[9,10] As for the other three

derivatives, only one band appears (TFA) or a more complex absorption takes place (Bn and DMU1 luminol's). For the more complex behaviour, mixture of tautomeric forms, change in electronic states energetic relation and vibrational resolution (not observed before) may all account for that effect. Regarding BnLum, these two latter hypotheses are the most attractive due to introduction of the phenyl ring in resonance to the whole structure (aromatic CH bonds). In respect to TFALum, the only absorption band that it exhibits in DMSO can be understood either with the hypsochromic shift of the whole spectrum or with the decrease in energetic discrepancies between the two low-lying singlet states (assuming that TFALum's electronic spectra is similar to luminol's, *i.e.*, that the chromophoric group for the first electronic transitions is the same). Because a blue shift towards luminol's spectrum must always be observed, we can understand the substituent effect as a reduction of the aromaticity extent (decrease in electronic density of closest atoms).

For molar absortivities of all these species in DMSO, on the basis of the previous assumptions regarding speciation, values higher than 10^3 $M^{-1}.cm^{-1}$ are always obtained, meaning that the $\pi\pi^*$ character of the transitions are retained from luminol. The contamination of other natures may change with the type of substitution introduced in luminol. For ECLum, the molar absorptivity is the lowest, possibly from contribution of the ethoxy group oxygen lone pair to increase the $n\pi^*$ character. Regarding BnLum, it has practically the same molar absorptivity of luminol probably because by allowing aromaticity extent, the benzoyl substituent does not remove electronic density from molecular orbitals involved in the electronic transitions (or greatly affect their composition). Curiously enough, TFALum shows a maximum molar extinction coefficient higher than luminol's. To account for it, either the electron withdrawing ability of the substituent reduces the energetic difference between electronic excited singlet states (and therefore the observed effect is cumulative) or, due to stereo constriction induced by the trifluoromethyl group, the electronic transition turns to be favoured. This latter hypothesis is based on perfluoroalkanes typical immiscibility with practically all organic compounds.[62]

As for fluorescence spectra in DMSO, BnLum have the closest to luminol. For other species, a shoulder is present and in the extreme case of TFALum a second maximum is present. Due to inexistence of acid-base behaviour in those conditions and because fluorescence from two extremely close singlet states is impossible, then the presence of the two maxima (and shoulders) can only be accounted by tautomerism. We therefore propose that luminol's derivatives possess several tautomeric forms like the ones predicted for luminol, but this time, due to substituent effect, with distinct energy (and quite probably equilibrium geometry) in each electronic state. Regarding maximum emission wavelength, all luminol derivatives exhibit red shifts in their fluorescence spectra (in the case of BnLum the red shift is null), meaning that the energetic difference between the first electronic excited singlet state and ground state's Franck-Condon structure is diminished upon derivatization. Curiously enough, that is opposite from the absorption spectra behaviour. To account for that observation, change in PES slopes around the absolute minimum may be at stake or, has proposed in luminol's low temperature spectra, a change in the nature of the interactions with the

solvent. Besides, light emission intensity at maximum emission wavelength decreases from luminol to its luminol derivatives, probably by favouring vibrational relaxation and internal conversion processes.

Regarding now Stokes shift in DMSO, it is increased upon derivatization of luminol. The closer derivative is ECLum with 66 nm. The other species have Stokes shifts of 68 nm (DMU1Lum), 73 nm (BnLum) and 103-133 nm (TFALum), showing that geometrical and charge density differences from ground to first singlet excited state are higher in luminol's derivatives. That may be a direct effect of the introduced substitutents because all should be able to strongly interact with the solvent.

As for absorption spectra in DMF of luminol's derivatives, towards absorption spectra in DMSO, ECLum changed the relative intensity of the absorption bands (the higher energy absorption is now the stronger). Besides, the second electronic transition also gets blue shifted and exhibits in DMF a shoulder, being that in agreement with previous discussions (respectively $\pi\pi^*$ character of the transition and tautomerism). For TFALum, the only absorption band that the compound exhibits retains the maximum absorption wavelength but gets wider and with a slight shoulder at 350 nm. That is evidence for both tautomeric manifestation or to decrease in energetic gap of the first two singlet excited states. For DMU1Lum and BnLum, greater discrepancies appear because in DMF two perfectly distinguishable absorption bands are present. Comparing to luminol's absorption, the two bands may be explained by at least two perfectly distinct singlet excited states, being the shoulders presented by these spectra in DMF a result either from tautomerism or vibrational resolution (more probable at least in BnLum). Also from these spectra we can observe that usually, when changing solvent, the highest energy absorption bands is just slightly shifted. Contrary to luminol's behaviour, the lower energy absorption band observed is typically blue shifted. That may be due to increase in $\pi\pi^*$ character (and thus decrease in $n\pi^*$ character) in the correspondent transitions.

Comparing now the molar extinction coefficients (the same basis of hypothesis) in DMF with DMSO's, except for TFA and ECLum, the derivatives show smaller molar absorptivities than luminol. Of the two exceptions, the most interesting result is for TFA whose molar extinction coefficient is now higher than 1.0×10^4 $M^{-1}.cm^{-1}$ (ECLum has a value closer to luminol's). The variation of this parameter with the solvents studied can only have to do with the effect of medium's polarity on the transition moment for the absorption.

Regarding fluorescence spectra in DMF, all transitions are now superposable (except for the region of higher wavelength's tail). The maximum emission wavelength is practically the same for all species (cf. Table 6.10) and therefore we verify that the relative position of maximum emission wavelength for the first singlet excited state is in agreement with the assigned $\pi\pi^*$ character for these transitions. As for Stokes shift, from DMSO, it is decreased in DMF. The most affected species are benzoyl luminol and TFALum (especially the species responsible for the second emission band in DMSO) with Stokes shifts in DMF of 51 nm and 85 nm (respectively). ECLum has in DMF a Stokes shift of 55 nm and DMU1Lum 64 nm. Because luminol exhibited the same Stokes shift in both those solvents, it is immediate that upon substitution, geometrical and charge distribution discrepancies from the first two singlet electronic states increase.

In respect to the last solvent tested, alkaline water solution, higher differences from DMSO and DMF arise in DMU1Lum and BnLum's absorption. Comparing to spectra in DMF (because they appear to have better resolution), besides getting wider, both substrates show the absorption band (in water) precisely in the absolute minimum of the interval 290-360 nm, *i.e.*, in the middle of the absorption bands in DMF. To account for it, both change in the composition of tautomeric forms (or acid-base derivatives) and strong interactions with the solvent (loss of resolution) may be invoked, meaning that once again the question regarding the nature of the several maxima and shoulders in DMU1Lum and BnLum spectra remains unanswered. As for ECLum, the absorption spectrum was also subject to some changes. The first is that the transitions got closer in water, *i.e.*, the energetic discrepancy between the first two singlet excited states slightly decreased. That is also accompanied by an increase of the absolute value of the minimum in the spectral region between 300-350 nm, also observed in luminol. It is also to report the disappearance of the small shoulder present in DMF, being that, in principle, an effect of hydrogen bonding and the high dielectric constant of the solvent. As for TFALum, from completely different to luminol's absorption spectrum (aprotic media) its absorption spectrum got, in water, exactly equal to luminol's. Comparing these results with the ones previously discussed both in this section and in the literature for acyl luminols,[8] we started to wonder about the hydrolysis of this compound in the aqueous conditions tested. To prove it, we collected the absorption spectrum for TFALum at neutral pH and even though we do not presented it, we report that in those conditions the absorption spectrum had a large absorption band at 330 nm, completely different to the absorption presented in Figure 6.29. We have therefore concluded that this luminol derivative hydrolysed at pH 11.5 and the collected spectra were solely from luminol. Therefore, TFALum's fluorescence in water at pH 11.5 and its chemiluminescence spectrum are not presented.

Regarding the molar extinction coefficients, we verified that for ECLum and BnLum, the oscillator strength for the absorptions is increased towards luminol (like in previously discussed solvents). The molar extinction coefficient of these luminol derivatives is in water 10.3×10^3 $M^{-1}.cm^{-1}$ for BnLum and 11.0×10^3 $M^{-1}.cm^{-1}$ and 11.5×10^3 $M^{-1}.cm^{-1}$ for ECLum. Due to the assigned character of the transition (obviously $\pi\pi^*$), to account for the increase of transition moment in water we have to rely in the solvent cage and the geometrical constriction induced by it.

As for the fluorescence spectra, from DMSO and DMF to water the spectra of luminol's derivatives ECLum and BnLum are red-shifted (in agreement with $\pi\pi^*$ character). The shift of maximum emission wavelength upon luminol's functionalization is once again neglectful. As for DMU1Lum, three emission bands appear, being this evidence for a quite complex composition of the media (no more concrete conclusions can be performed with collected data). Therefore, no Stokes shift was calculated for that luminol derivative. Regarding other species, the Stokes shifts increase from DMF to DMSO and then finally in water. Stokes shift for ECLum in water is 71 nm and for BnLum is 86 nm, being the results here presented justified by means of exactly the same arguments previously discussed for DMF and DMSO. Regarding the nature of the increase of Stokes shift, both solvent polarity and hydrogen bonding may account for it, but, due to the observed molar extinction coefficients, it is more probable that the solvent polarity is the main factor.

The last set of spectra to comment is the chemiluminescence ones. Like previously with isoluminol, the maximum emission wavelength is conserved, independently from the type of substituent introduced. This clearly indicates that the excited state formed, that is responsible for luminol's chemiluminescent blue emission, is independent of the substituent in the amino group, being therefore reasonable to conclude that the chemiluminescence maximum emission wavelength is independent of the relative position of the amino functionality and in some extent to its electron giving properties. From the presented spectra of luminol's derivatives we verify that the influence of the aniline functionality is in the relative intensity of chemiluminescence at maximum emission wavelength. Because that relative intensity is dependent on the yield for excited state formation and on the yield for the oxidation reaction, assuming that the latter is similar for all structures we conclude that the relative position and electronic character of the amino functionality in luminol's derivatives will mainly influence the yield for the excited state formation, reinforcing the idea that the hydrogen bond established by the group in question with the closer carboxyl functionality will geometrically affect the reaction intermediates. Therefore, the amino group will determine the amount of molecules that populate electronic excited states during the course of the reaction. With that hypothesis, we could propose that upon acylation, the N2's proton becomes more available to interact with the oxygen atom from the closest carboxyl group. That is of course true but to perhaps avoid mistakes on the real effect of that substitution, the sentence should be rephrased to "upon acylation, N2's proton acidity is increased" and therefore, at pH 11.7-11.8, that nitrogen atom must have acquired a negative charge from deprotonation. Also from the relative intensities of chemiluminescence emissions at maximum emission wavelength we can estimate the chemiluminescence quantum yield, using the small correction of the concentration ratio.

Table 6.11: Chemiluminescence quantum yield of luminol's derivatives relatively to luminol's chemiluminescence quantum yield weighted by the relative concentration of luminol derivatives initial concentration. Isoluminol's chemiluminescence quantum yield is also presented for comparison purposes.

ECLum	BnLum	DMU1Lum	*i*Luminol
84%	30%	1%	3%

These results for chemiluminescence quantum yield are the reflection of the discussion above.

6.3.2 - Luminol's Derivatives Aprotic Chemiluminescence

Besides the essays presented in the previous section, qualitative chemiluminescence studies of luminol's derivatives in DMSO and DMF were performed. To solutions with luminol or one of its derivatives with 5.0×10^{-4} M in the aprotic solvents, an excess of potassium *tert*-butoxide was added (qualitatively the same amount). In those conditions, all derivatives that exhibited light emission showed (qualitatively speaking) the same emission colour of luminol. As for intensities, ECLum

yielded the same light emission intensity as luminol, being the other chemiluminescent derivative, BnLum, significantly less chemiluminescent (20-30 %). The other species (DMU1Lum and TFALum) were non-chemiluminescent or at least did not emit photons in such intensity that naked human eye would detect. It should also be stated here that the reactions were all performed in a dark room and that in the end of the reaction the samples showed a dark powder in the bottom of the flask. The reaction development was also extremely fast. Due to inherent difficulty to add a dangerous powder to the quartz cell, the last two previous observations and to the fact that these reaction conditions are not so attractive for applications, no spectra recording was ever performed.

6.4 - Chemiluminescence Decay Analysis

Besides previously described experiments, chemiluminescence light emission intensity decay (at one emission wavelength) experiments were also conducted using Rauhut and co-workers reaction media.[25]

In Figure 6.34 is presented the chemiluminescence light emission intensity decay followed at 420 nm for luminol, ECLum, BnLum, iLum and DMU1Lum. Lines representing logarithmic linear fitting were included in black to all decay curves. The lines presented were built in order to connect the extreme points from each “linear” region of the decay. Table 6.12 presents data concerning the conditions in these experiments and Table 6.13 data related to mono and diexponential fittings performed. Representative residual plots regarding these fittings are presented in Figure 6.35. The model applied was the one presented in equation (6) where $I(t)$ is the chemiluminescence emission intensity at 420 nm observed at time t. a, b, c and d are fitting parameters. It should be denoted that monoexponential fitting is a diexponential fitting where c is null and d is undefined. The last referred table also presents a coefficient of multiple determination (R^2) that, like the determination coefficient, is a measure of the fitting adequacy.

$$I(t) = ae^{bt} + ce^{dt} \qquad (6)$$

All fits performed to Figure’s 6.34 chemiluminescence decays presented in Table 6.13 started at sufficiently high times (600 s) due to the non-linearity of the natural (and 10 base) logarithm of chemiluminescence light emission intensity in short times.

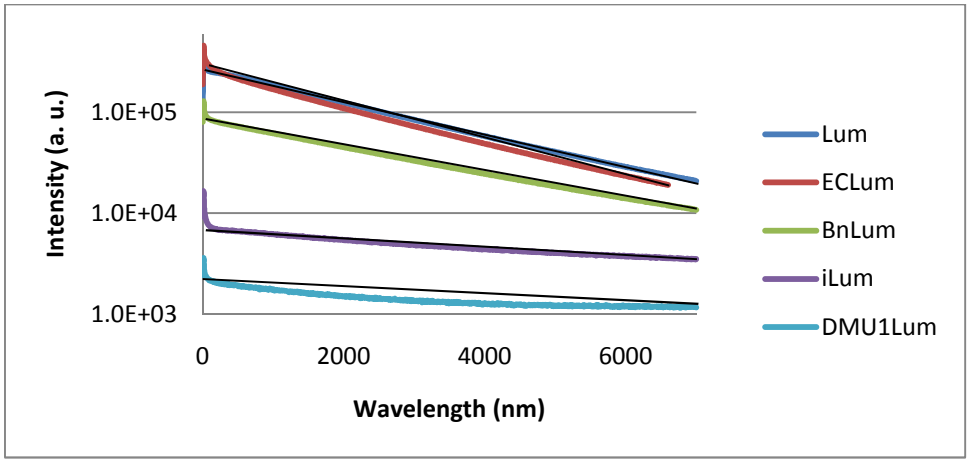

Figure 6.34: Chemiluminescence light intensity decay with time for luminol and its derivatives presented in a logarithmic scale.

Table 6.12: Data concerning experimental conditions for chemiluminescence light intensity decay presented in Figure 6.34.

	Luminol	ECLum	BnLum	*i*Lum	DMU1Lum
C (M)	5.2×10^{-5}	5.2×10^{-5}	5.0×10^{-5}	5.5×10^{-5}	1.6×10^{-3}
C_{H2O2} (M)	4.6×10^{-2}	4.6×10^{-2}	4.6×10^{-2}	4.6×10^{-2}	4.6×10^{-2}
C_{K2S2O8} (M)	6.0×10^{-2}	6.0×10^{-2}	6.0×10^{-2}	6.0×10^{-2}	6.0×10^{-2}
pH	11.5	11.5	11.5	11.5	11.5
λ_{em} (nm)	420	420	420	420	420

Table 6.13: Data concerning exponential fitting of chemiluminescence light emission intensity decay for luminol and its acyl derivatives. In this table M stands for monoexponential fitting, D for diexponential fitting, a, b, c and d are fitting coefficients identified in equation (7) and S_i standard deviations for each parameter.

		Luminol	ECLum	BnLum	iLum	DMU1Lum
M	a	2.693×10^{5}	2.524×10^{5}	8.310×10^{4}	6.70×10^{3}	1.777×10^{3}
	S_a	0.003×10^{5}	0.003×10^{5}	0.007×10^{4}	0.01×10^{3}	0.007×10^{3}
	b	-3.833×10^{-4}	-4.119×10^{-4}	-3.017×10^{-4}	-9.98×10^{-5}	-7.3×10^{-5}
	S_b	0.005×10^{-4}	0.006×10^{-4}	0.003×10^{-4}	0.05×10^{-5}	0.1×10^{-5}
	R^2	0.999375	0.99902	0.99943	0.98608	0.88497
D	a	2.61×10^{5}	1.01×10^{5}	2.8×10^{3}	2.4×10^{3}	1.13×10^{3}
	S_a	0.02×10^{5}	0.03×10^{5}	0.3×10^{3}	0.1×10^{3}	0.02×10^{3}
	b	-4.29×10^{-4}	-7.1×10^{-4}	0.07×10^{-5}	-4.0×10^{-4}	-4.3×10^{-4}
	S_b	0.02×10^{-4}	0.1×10^{-4}	1.24×10^{-5}	0.2×10^{-4}	0.1×10^{-4}
	c	1.7×10^{4}	1.66×10^{5}	8.22×10^{4}	4.8×10^{3}	9.9×10^{2}
	S_c	0.2×10^{4}	0.03×10^{5}	0.03×10^{4}	0.1×10^{3}	0.3×10^{2}
	d	-1.0×10^{-4}	-3.38×10^{-4}	-3.32×10^{-4}	-5.2×10^{-5}	1.9×10^{-5}
	S_d	0.1×10^{-4}	0.02×10^{-4}	0.01×10^{-4}	0.2×10^{-5}	0.3×10^{-5}
	R^2	0.99998	0.99998	0.99998	0.99922	0.99534

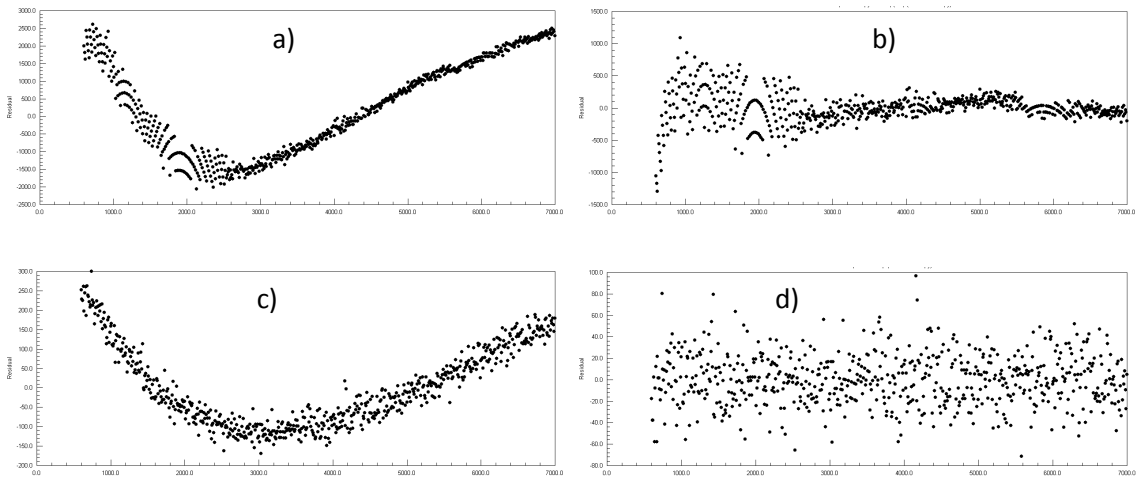

Figure 6.35: Representative residual plots for a) monoexponential fit to luminol's chemiluminescence decay, b) diexponential fit to luminol's chemiluminescence decay, c) monoexponential fit to isoluminol's chemiluminescence decay and d) diexponential fit to isoluminol's chemiluminescence decay.

Analysis of chemiluminescence decays from Figure 6.34 shows that chemiluminescence light emission decays are composed by two regions with different slopes: a region dominated by an extremely fast exponential decay at short times (extinguished in about 60 seconds after the absolute maximum emission is achieved) while the other region is controlled by a softer but also exponential decay (majorly valid 100 seconds after the absolute maximum emission is achieved). From that, the main conclusion is that luminol's chemiluminescence reaction can be rationalized as a two step mechanism, one for the formation of a key intermediary and the correspondent decomposition. Of course that mechanistically the reaction should be much more complex but kinetically only these two steps are discernible. Due resolution of the presented data, no information regarding the process at short times can be retrieved. To gain some insight in that step, higher resolution is needed and those experiments were performed only for luminol. Therefore, Figure 6.36 not only shows those points but also the applied fitting function. For these, only a monoexponential fitting was possible (in diexponential fittings the program split the monoexponential solution into two equal exponentials).

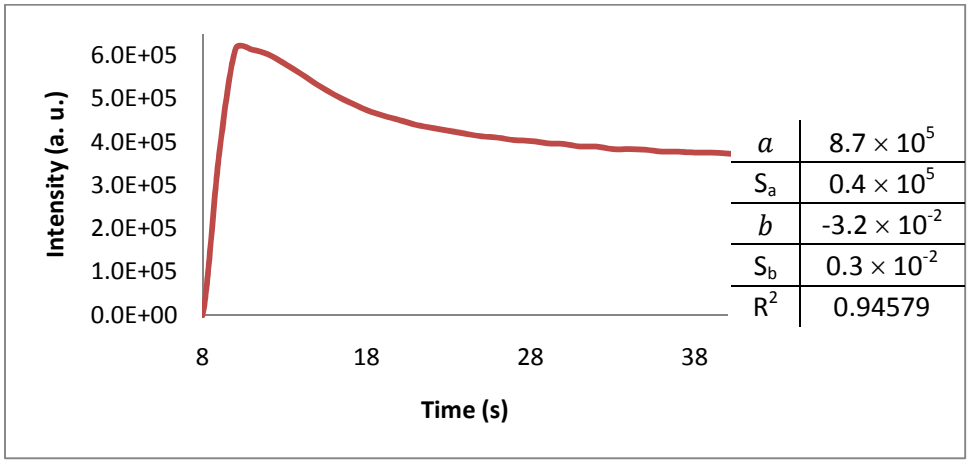

Figure 6.36: Chemiluminescence decay for luminol at low times with fitting function.

From visual trend lines and data from Table 6.13 analysis, both mono and diexponential fittings apply usually well for luminol and its derivatives chemiluminescence decay. The fit, either mono or diexponential is always best for the most chemiluminescent compounds, *i.e.*, luminol, ECLum and BnLum. Regarding isoluminol and DMU1Lum, the fitting functions are less adequate and higher deviations from models applied are observed. That can quite possibly be accounted by the decrease in light emission efficiency that introduces higher error in some regions of the decay or to secondary reactions. In respect to the models applied, the coefficients of multiple determination clearly show that the diexponential fitting is always best. But that does not mean that the second exponential function has any physical meaning. To determine its significance, we plotted the experimental chemiluminescence decay for luminol and each term of the diexponential fitting. The mono and the diexponential fittings are also plotted in Figure 6.37.

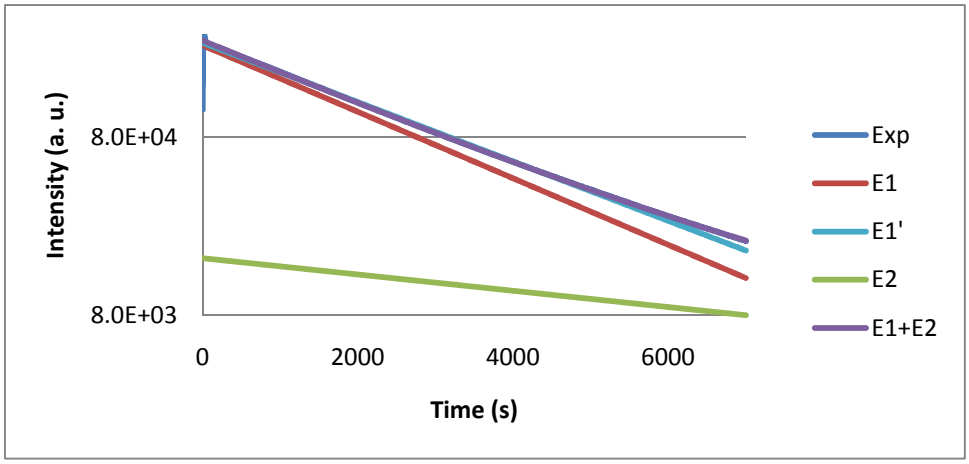

Figure 6.37: Experimental chemiluminescence decay for luminol (Exp), first exponential term (E1) and second exponential terms (E2) for diexponential model and total diexponential model (E1+E2). E1' is the monoexponential fitting. Exp and E1+E2 functions are completely superimposed in this representation.

As we can verify from Figure 6.37, the first term of the diexponential fitting is perfectly adequate for short times (E1). Besides, for the time gap considered, the second exponential term is not able to account for any region of the experimental decay, not even at extremely long times. Regarding the mono exponential model, its accuracy is only low at sufficiently long times, when the light emission intensity is extremely small (compared to the initial ones). Considering all this, the second exponential term obtained in diexponential fitting appears to be just a mathematical artifice to enhance the fitting accuracy, being therefore justified the fact that sometimes the exponential coefficients (constants b or d) associated to the lower pre-exponential coefficient are positive (the case of BnLum and DMU1Lum species). Therefore, we conclude that at sufficiently long times the non-linearity of the natural logarithm of the light emission intensity is due to the experimental conditions (lack of intensity that induces errors in the photodetector, secondary reactions,...).

In respect to residues plots, monoexponential decays have more biased ones, mainly due to the observed deviations from pure monoexponential fitting at long times.

As for short time analysis, it is observed that a slightly smaller kinetic constant is predominant at lower times. Even though the accuracy of that kinetic constant is not high (few experimental points, bad data collection due to inadequate experimental set up), that result is somewhat unexpected because the slowest step should always control the reaction rate. To justify this observation, mechanistic considerations must be performed. To begin with, is the presence of hydrogen peroxide. According to Rauhut and co-workers, the role of hydrogen peroxide (and hydroxyl anions too) is somewhat odd. The reaction is zero order in this species but it was also verified that chemiluminescence quantum yield increases when hydrogen peroxide concentration increases. To observe that type of behaviour, it was postulated that the two slow steps experimentally observed are bimolecular (being unimolecular not all requisites would be fulfilled).[25] Because it was also observed unitary order on persulphate anion, the overall rate limiting step would have to include this species. Because at extremely short times luminol's concentration is maximized, then we expect the reaction steps with that reagent to be at their maximum speed. Because the reaction also exhibits first order for luminol, then the first reaction step consists on the oxidation of luminol by persulphate anion. As for the second step, it can only be the bimolecular decomposition of a reaction intermediate whose initial concentration is so low that at sufficiently short times the step is the rate limiting one (the light emission from aminodiphthalate could also be proposed but the observed kinetic constant would be in disagreement with the expected magnitude of the excited state lifetime). When this intermediate's concentration increase, due to its high instability,[25,27,31] the slowest step in this reaction would become the first one, being it the rate limiting step during practically all the reaction (and therefore justifying the assignment of persulphate as luminol's oxidant). Because the kinetics in these reaction conditions have zero order in hydrogen peroxide but still the chemiluminescence quantum yield is affected by this species, the second step could be the reaction of the reactive intermediate with that oxidant, being that in agreement with the reaction with metal ions (assuming that the generic mechanism for light emissive pathway is somewhat conserved in both reaction conditions). Regarding now the intermediate species, based in the literature and in the assumptions referred, we propose that it is the diazaquinone (*cf.* Figure 2.5).[10,37] Of course that other intermediates are possible, for instance the ones from Figure 2.4 but that would not account for the hydrogen peroxide first order in other conditions and the proposed bimolecularity of the second step. Besides, we could also consider the reverse order of interactions, *i.e.*, luminol reacts first with hydrogen peroxide and then that intermediate species would react with persulphate in the rate limiting step but that would cause hydrogen peroxide to have first order in the kinetics while persulphate anion would have zero order. Therefore, to account for the need of hydrogen peroxide (persulphate could also react with the diazaquinone intermediate to yield the aminodiphthalate), we use the relative nucleophilicity those of species in the media (the most favourable mechanism consists on the nucleophilic attack to the diazaquinone). Therefore, the nature of the peroxide may determine the kinetics of the whole reaction being that in agreement with the intermediate assignment (diazaquinone).

Finally, integrating the chemiluminescence decay curves for each species (for instance, by means of the trapeze rule) and diving that area with the correspondent area for luminol's chemiluminescence decay curve, if we correct those ratios with the concentrations of luminol or its

derivatives, a better approximation to the chemiluminescence quantum yields can be obtained. Table 6.14 presents those results.

Table 6.14: Chemiluminescence Quantum Yields (Φ_{CL}) predicted by ratio of the integrals of chemiluminescence decay curves for luminol's derivatives and luminol. Concentration corrections considered.

	ECLum	BnLum	*i*Lum	DMU1Lum
Φ_{CL}	9.1×10^{-2}	3.9×10^{-2}	4.9×10^{-3}	1.5×10^{-3}

Even though higher, results from this method are similar to the previously obtained ones. Because the chemiluminescence intensity decay consists of extremely slow experiences (for the light emission to be neglected towards initial light emission intensity we had to wait at least 7000 seconds) it is much more convenient to directly use data from chemiluminescence spectrum. Besides, the latter methodology also took into account the long times where we assigned lower accuracy of the data. Regarding the reasoning for the obtained values, it was previously discussed.

6.5 - Conclusions

When in aqueous media, luminol presents two main absorption bands. Those are practically pH insensitive, being significant changes only observed in extreme pH's. At pH 1.28, the excitation towards the first singlet excited state is significantly less allowed than the transitions towards S_2 (40 %) while at pH 14.98 the absorption at 350 nm acquires some shoulders and the absorption at 300 nm is much less allowed (unquantifiable). In respect to fluorescence, several bands are observed, also pH dependent and we have proposed an acid-base equilibria in the excited state as origin. Besides, fluorescence spectra using different excitation energies yielded the same spectra, meaning that the two bands are electronic in nature. When changed to DMF or DMSO, luminol's absorption retains the generic form (two bands at 350 nm and 300 nm) but this time some shoulders appear in the 300 nm absorption band. According to theoretical calculations also performed, these shoulders can be justified by luminol's tautomerism. As for fluorescence, only one emission band is present being this in agreement with the proposed acid-base behaviour of luminol in water. In solid state, the emission is similar to aprotic media but a shoulder also appears. As for excitation, only one band is present.

Regarding luminol's theoretical absorption spectra in DMSO and water, we verified that the generic form of the spectrum can be theoretically predicted. As for the accuracy of the calculated parameters, oscillator's strength appears to be in good agreement with experimental results (except for the second transition in DMSO) but the excitation energies, at least in the transitions we had experimental access, are always blue shifted. We verified that this shift can be due to $\sigma\pi^*$ or $\pi\sigma^*$ contamination in some transitions or also to the contribution of N2 to the molecular orbitals involved in the transition (PBE1PBE and MP2 describe that atom in a significantly different fashion).

Nevertheless, theoretical calculations predicted the same transition character experimentally observed and accounted for the decrease in oscillator strength from DMSO to water. Besides, we estimated radiative lifetimes for luminol in DMSO and water and predicted the anisotropies between transition moments in water to compare.

One last system where we studied luminol's excitation and fluorescence was in 9:1 EtOH-MeOH mixture. That study came due to the formation of a glass at low temperatures (100 K). Therefore, we collected absorption and emission at RT and 100 K with and without polarizers. From studies without them, we have concluded that upon temperature lowering, luminol's two absorption bands split into two maxima being also both bands red-shifted. Fluorescence also shows the splitting behaviour but instead it is blue-shifted. We rationalized that behaviour by means of the nature of the interactions of luminol's ground and excited states with the solvent cage. From studies with polarizers we gained access to luminol's excitation anisotropies. Following the excitation at different emission wavelengths, we verified that the obtained curves are extremely similar but shifted in the anisotropy axis. Also, the experimental results obtained were not in perfect agreement with our theoretical calculations (results from different media are compared, inherent accuracy of the methods, resolution of the experimental data) but we have verified that our theoretical methodologies were so far the only ones able to account for luminol's anisotropies and excitation and absorption spectra.

Regarding its chemiluminescence, we have successfully applied Rauhut and co-workers reaction conditions[25] to collect the spectrum. We have verified that luminol's chemiluminescence is in agreement with the aminodiphthalate's fluorescence but we have also verified a shoulder in the former emission that we proposed to be the aminomonophthalate emission. That species would therefore be formed by acid-base equilibrium in the excited state. That induced us to propose that upon oxidation, in both aqueous and aprotic conditions, luminol forms the aminodiphthalate that will afterwards emit light.

In respect to the influence of the NH_2 group in luminol's structure, we have studied isoluminol's spectra. Besides absorption (blue shifted), emission is also affected (red shifted). Curiously enough, the chemiluminescence of isolumninol is only less intense than luminol's. All those results were accounted by the (in)existence of an intramolecular hydrogen bonding between the NH_2 group and the closest carboxyl functionality.

For luminol's derivatives, we observed that the absorption spectrum is always different from luminol's meaning that successful derivatization was achieved. The observed shifts can be accounted by π system extension or by electronic effect of the introduced moiety. Still, independently of the type of acylating agent used, the nature of the transitions of the derivatives is retained towards luminol, being sometimes the oscillator strength for some transitions higher. In fluorescence, typically the one band emission is retained and slight shifts are observed in the media. Exceptions are TFALum and DMU1Lum. While the former shows two bands in aprotic media that can be perfectly accounted as a tautomerism effect, the latter shows in water a quite complex behaviour (three emission bands)

whose nature can be either tautomeric or acid-base. Besides, we have also verified that at pH 11.5 TFALum hydrolysed to yield luminol and trifluoroacetic acid.

The last study presented here was the chemiluminescence light emission decay by application of Rauhut and co-workers conditions.[25] We have verified that all emissions followed a monoexponential decay at sufficiently long times and that at short times a second step is observed. The kinetic data suggests therefore a two step mechanism that should not be (in principle) elementary. As for the key intermediate, we propose that it is with higher probability White's diazaquinone.[10] From this data, we have estimated chemiluminescence quantum yield of our derivatives towards luminol's that allowed us to conclude that the introduced substituents all lowered the chemiluminescence quantum yield. Because we have also verified that the emission wavelength was retained, no improvement to the already existent systems was introduced.

7 - Conclusions

In this work we have analysed several key features on luminol and its derivatives physics and chemistry. To start with, we have verified that according to the literature, [8,16,40] two similar methodologies may be applied to synthesize related structures. The first is when an amine base (softer) is used to deprotonate luminol (it must be that way otherwise the observed selectivity would not be verified) yielding usually N2 substitution. On the other hand, when harder bases (MOH and MH) are used, the selectivity of the substitution is changed to yield O-luminol derivatives. In any case, to isolate a derivative, not only luminol must be completely dissolved but also the electrophiles (and the media) must fulfil certain requisites. From one of the last studies we presented (2-sulfo-benzoic cyclic anhydride), it is extremely hard to make luminol react weak electrophiles. On the other hand, if we use extremely strong electrophiles, not always a luminol derivative is isolated. It is fundamental that after the first chemical attacks (or hydrolysis), the secondary product is not able to compete with luminol. When that condition is not fulfilled (phenyl isocyanate example), luminol proves its inability to act as a nucleophile and no product is isolatable. Cases like trifluoroacetyl luminol derivative clearly show that when the secondary product, trifluoroacetate, is much less nucleophilic than luminol no problems exist. We therefore verified a motive that can be applied to other types of derivatization different from acylation of luminol.

Regarding other studies on this subject, results from benzoyl and acetyl luminol derivatives seem contradictory. Because benzoyl chloride is much less electrophilic than acetyl chloride, the non-isolation of acetyl luminol along with isolation of BnLum is improbable and, to account for it, we rely on the inadequacy of the analytical methods applied. That is also supported by TFALum. During its synthesis, we verified that no TLC analysis was able to distinguish the product from luminol, not only due to similarity in Rf but also due to the same tonality presented during TLC plaque revelation. Therefore, these examples underline that for luminol derivatives similar enough to the parent compound, different analysis methodologies must be applied, either by solvent change in TLC or, being more radical, by changing the technique, which is not so attractive due to the simplicity of that chromatography essay.

In cases where luminol needs to be activated to enhance its nucleophilicity, TMSCl (in DMF) seemed to be an efficient process. This act of desperation may sometimes be changed by the opposite approach, using silver nitrate to activate chlorine electrophiles at the cost of releasing silver (that is hard to remove from solids) and oxidizing luminol.

We have also verified that both pyridine and TEA were equally efficient bases to promote the derivatization reaction. Due to the observed advantage of product precipitation in TEA systems, this should be the first synthetic approach to explore. Regarding the amount of base, the higher the excess, the higher is the observed reaction yield, being that accounted by usual mechanistic interpretation of the reaction in question. When the amount of base is insufficient, the yield decreases possibly from the formation of the Vilsmeyer reagent yielding species that “were not desired” or due to

luminol's protonation. Therefore, we propose the use of an excess of base to increase the reaction yield. It should be pointed that a great excess is also not advantageous because in DMF it promotes luminol's oxidation by O_2. Still regarding bases and activators for the reaction, we have not observed advantages in the use of DMAP as acyl activator.

Besides derivatization conditions, from examples like benzoyl luminol, we believe to have given a good contribution in purification procedures of luminol derivatives. Of all derivatives obtained, this is the one where the most apolar moiety was introduced, being therefore the closest system we got to literature's reported aromaticity extent. We verified that crystals might be obtained in acetone, ethanol and in ethanol-water systems. These procedures may therefore be applied for purification purposes avoiding the time expensiveness and unsatisfactory purification for luminescence studies of chromatographic methods.

Regarding future work on this subject, we believe that it would be advantageous to test our methodologies (in reaction conditions but especially in purification) in other types of substitution, namely in imino isoluminol derivatives that attach well known chromophores to finely tune up the emission.[18,19]

As for computational studies, we concluded that, of all tested, the best method available to study luminol's system appears to be MP2, because it provides the best description of the whole structure. In DFT studies, PBE1PBE hybrid functional yield complementary results of B3LYP: while the latter gave slightly better aniline dihedral angles description, the former proved to be better in bond distance prevision.

As for single point energy calculations, because higher levels of theory (MP4, CC,...) were not possible to apply using our current computers (lack of physical and processor memory), MP2/aug-cc-pVTZ was selected.

Regarding luminol's tautomers, six were studied in several conditions. Like in other theoretical calculations, luminol's tautomer B was the most stable tautomer in both gas and solvent dielectric. On the contrary, we have predicted that luminol's tautomer C to be the second most stable one (where the enolized carboxyl group is the closest to the aniline group). Besides, we have assigned a set of parameters that influence and determine the relative stability of luminol's tautomeric forms. Those were, (i) aromaticity in ring 2 and (ii) electronic delocalization, (iii) hydrogen bonding and (iv) charge density distribution. The fact that aromaticity in the second ring is the less relevant stabilization parameter can be rationalized by a decrease in the mesomeric effect of aniline functionality to ring 2.

In respect to luminol's behaviour in alkaline media, when one equivalent of a strong base is added, both species α and δ should be formed, *i.e.*, a hydrazide proton is removed. The computationally second most acidic proton was determined to be an anilinic one. This is in disagreement with some literature statements but give some meaning to other syllogisms. The

relative stability of the studied luminol's base conjugates is in agreement with luminol's tautomer stability, *i.e.*, the driving forces for structure stabilization appear to be acid-base independent.

To complement these studies, because so far more refined *ab initio* methods are both time and computationally too expensive to be applied in geometry optimizations, we propose that a refinement in the single point energy calculations should be performed. That is merely because only one method was applied, MP2. Therefore, calculations using Couple Cluster theory should prove useful to verify the accuracy of MP2 calculations. Besides, after these basic tautomerization and acid-base studies, several reaction mechanisms studies should be undertaken. Regarding these, the most interesting case would of course be in water but due to the proposed charge transfer nature of the first reaction steps, it would be harder to study it computationally. Therefore, the first step would be to study and define a mechanism for luminol's oxidation in aprotic media. Both singlet and triplet molecular oxygen species should be considered. In respect to that, we must say that we are already performing those studies according to our proposed the methodologies.

In respect to the last set of studies presented, spectroscopic ones, we observed that luminol's absorption is mainly composed by two bands, electronic in nature. The first one is at 350 nm and the other at 300 nm. That main spectra composition appears to be both pH (some slight variations were observed in extreme cases) and media independent. Regarding a finer analysis, some differences appear in the relative intensity of the absorption bands and in the appearance of shoulder in aprotic media. In fluorescence two types of behaviour were observed: while in aprotic media only one emission band is present, in water, by means of acid-base reactions in the excited state, we observed typically 1-2 bands, except for higher pH's. As for luminol's theoretical absorption spectra in DMSO and water, we were able to predict the generic form of the spectrum and also to explain by tautomerism some results, like the origin of the shoulders in aprotic media's bands. As for the accuracy of the calculated parameters, despite being unsatisfactory in the second transition in DMSO, the oscillator strength appears to agree with experimental results. In the case for excitation energies, the transitions we had experimental access, were all theoretically blue shifted. We proposed that this shift comes from $\sigma\pi^*$ or $\pi\sigma^*$ contaminations as well as a possible contribution of N2 to the molecular orbitals involved (PBE1PBE and MP2 differently describe that atom). Regarding the nature of the transition, theoretical calculations state, like experimental results, that the transition has $\pi\pi^*$ character.

Besides these basic studies, we studied luminol's excitation and fluorescence in an alcoholic mixture that allowed access to low temperature spectra. When cooled down to a glass, luminol's absorption retained the main form but got red-shifted. Besides, we have also verified maxima splitting, *i.e.*, each maximum at RT was at 100 K split into two distinct maxima that may be accounted either as tautomerism manifestation or to vibrational resolution of the spectrum. Fluorescence also showed the splitting behaviour but instead it was blue-shifted. That shifting behaviour was justified by means of the nature of the interactions of luminol's ground and excited states with the solvent cage. From studies with polarized light we gained access to luminol's anisotropies in excitations. We verified that if two tautomeric forms of luminol exist, they are chemically and physically extremely similar.

Therefore, the experimental results obtained were not consistent with the presence of luminol's tautomer A, structure usually assigned to the compound and predicted by other theoretical calculations to be the second most stable luminol tautomer.

All these results consisted in a first set of data regarding luminol's photophysical and chemical properties. Even though concise conclusions were not provided in all cases, these studies should be performed to completely describe luminol's ground and excited states systems. Only then, a better insight on its oxidation reaction mechanism may be provided because driving forces for the process may be better understood. Also, these studies are extremely relevant because they provide us access to the chemical composition of luminol's ground state solutions, namely tautomerism. In respect to further studies, the solvent library should be increased to verify theory predictability. Besides, a set of (spectroscopic) experiments should be idealized (and performed) to provide an answer to the nature of the observed splitting in some bands (namely low temperature band splitting and the appearance of the shoulder in the second transition in aprotic media). Finally, the system's description will only be completed when excited state lifetimes and radiative lifetimes in at least one media are described. Those experiments would also be essential to define the accuracy of the theoretical methods. Besides, mechanistic studies must be performed to help clear out luminol's chemiluminescent reaction. Perhaps the most relevant ones would define the role of oxygen species and of course the role of the metal.

Regarding luminol's chemiluminescence, besides verifying that it is in agreement with the aminodiphthalate's fluorescence, we have observed a shoulder in the former emission that we proposed to be the aminomonophthalate (formed by acid-base equilibrium in the excited state). That induced us to propose that upon oxidation, the light emissive species is the aminodiphthalate.

To study the influence of the NH_2 group position in luminol, we decided to study isoluminol's spectra. Both absorption and emission are affected (blue and red shifted respectively) but curiously, the chemiluminescence of isoluminol is only less intense than luminol's. We therefore propose that the intramolecular hydrogen bonding and the associated conformational restrictions are the main differences in those systems.

Regarding luminol's acyl derivatives, we observed that the absorption spectrum is changed at least in the relative intensity of the bands but also that the transitions retain their main $\pi\pi^*$ character. The observed shifts in the spectra were justified either by π system extension or by electronic effect of the introduced chemical function. In fluorescence, the one band emission is usually retained being slight shifts observed. TFALum and DMU1Lum showed the most complex behaviour. While the former exhibited two fluorescence bands in DMSO (accounted either as manifestation of tautomerism or as vibrational resolution), the former showed in water three emission bands whose nature can be either tautomeric or acid-base. Besides, we have also verified that at pH 11.5 TFALum hydrolysed to yield luminol and trifluoroacetate. Because luminol's dissolution in water is extremely slow and because trifluoroacetyl luminol showed high dissolution rates at higher pH's, this type of substitution can be used not only to facilitate the dissolution of luminol but it also can be the precursor of some

sort of derivative with the same type of behaviour that could possibly act as a luminol transporter. Due to trifluoroacetyl luminol's chemiluminescence behaviour in aprotic media, we expect that only after hydrolysis chemiluminescence may be observed and therefore, selective identification of some specific conditions may be achieved.

Regarding the last studies of this work, we have verified that both luminol and its derivatives chemiluminescence emissions followed a monoexponential decay at sufficiently long times. At sufficiently short times, the kinetic data suggests a two step mechanism. The key intermediate was proposed to be White and co-workers diazaquinone.[10] From this data, we have estimated chemiluminescence quantum yield of our derivatives towards luminol's and concluded that no improvement was introduced to the state of the art (only more knowledge on the system was gathered). Therefore, no more chemiluminescent compound was synthesized and no shift in the maximum emission wavelength was observed. Even though not extensive, the derivatives library was wide enough to discourage further studies with this type of substitution. One hypothesis to apply the work performed with previously described systems is to use these functionalities (acyl) to act as spacers that bring together luminol and a known chromophore with the desired properties (with several chromophoric regions).[18] Even if they are not used, we believe to have provided useful knowledge regarding synthetic procedures and some particularities that luminol derivatives must not have.

References

1 - Albrecht H.O., *Z. Phys. Chem.*, **1928**, Vol. 10, 70.

2 - Luo Y., Li Y., Lv B., Zhou Z., Xiao D., Choi M. M. F., *Microchim. Acta*, **2009**, Vol. 164, 411.

3 - Ferreira E. C., Rossi A. V., *Quim. Nova*, **2002**, Vol. 25 (6), 1003.

4 - Yang C., Zhang Z., Wang J., *Microchim. Acta*, **2009**, Vol. 167 (91), 96.

5 - IUPAC Commission on Nomenclature of Organic Chemistry A Guide to IUPAC Nomenclature of Organic Compounds (Recommendations 1993); Blackwell Scientific publications, 1993.

6 - Voicescu M., Vasilescu M., Constantinescu T., Meghea A., *J. Lum.*, **2002**, Vol. 97, 60.

7 – http://www.usm.maine.edu/~newton/Chy251_253/Lectures/Solvents/Solvents.html, solvent dielectric constants, last checked January 31th 2010.

8 - Omote Y., Miyake T., Ohmori S., Sugiyama N., *Bull. Chem. Soc. Japan*, **1966**, Vol.39, 932.

9 - Dodeigne C., Thunus L., Lejeune R., *Talanta*, **2000**, Vol. 51, 415.

10 - White E. H., Roswell D. F., *Acc. Chem. Res.*, **1970**, Vol. 3, 54.

11 - Du J., Li Y., Lu J., *Analytica Chimica Acta*, **2001**, Vol. 448, 79.

12 - Brundrett R. B., White E. H., *J. Am. Chem. Soc.*, **1974**, Vol. 96 (24), 7497.

13 - Burdo T., Seltz W. R., *Anal. Chem.*, **1975**, Vol. 47 (9), 1639.

14 - Schiller J., Arnhold J., Schwinn J., Sprinz H., Brede O., Arnold K., *Free Rad. Res.*, **1999**, Vol. 30, 45.

15 - White E. H., Bursey M. M., *J. Org. Chem.*, **1966**, Vol. 31 (6), 1912.

16 – Chen G. N., Lin R. E., Zhuang H. S., Zhao Z. F., Xu X. Q., Zhang F., Anal. Chim. Acta, **1998**, Vol. 375, 269.

17 - White E. H., Bursey M. M., Roswell D. F., Hill J. M., *J. Org. Chem.*, **1967**, Vol. 32 (4), 1198.

18 - Yoshida H., Nakao R., Nohta H., Yamaguchi M., *Dyes and Pigments*, **2000**, Vol. 47, 239.

19 - Yamaguchi M., Yoshida H., Nohta H., *J. Chrom. A*, **2002**, Vol. 950, 1.

20 - White E. H., Matsuo K., *J. Org. Chem.*, **1967**, Vol. 32 (6), 1921.

21 - Ojima H., *Die Naturwissenchaften*, **1961**, 600.

22 - White E. H., Zafiriou O., Kägi H. H., Hill J. H. M., *Chem. Comm.*, **1963**, Vol. 86, 940.

23 - Rose A. L., Waite T. D., *Anal. Chem.*, **2001**, Vol. 73, 5909.

24 - Shevlin P. B., Neufeld H. A., *J. Org. Chem.*, **1970**, Vol. 35 (7), 2178.

25 - Rauhut M. M., Semsel A. M., Roberts B. G., *J. Org. Chem.*, **1966**, Vol. 31 (8), 2431.

26 - Vasilescu M., Constantinescu T., Voicescu M., Lemmetyinen H., Vuorimaa E., *J. Fluorescence*, **2003**, Vol. 13 (4), 315.

27 - Lind J., Merényi G., Eriksen T. E., *J. Am. Chem. Soc.*, **1983**, Vol. 105, 7655.

28 - White E. H., Bursey M. M., Chemiluminescence of Luminol and Related Hydrazides: The Light Emission Step, *Chem. Comm.*, **1963**, Vol. 86, 941.

29 - Yasuta N., Takahashi S., Takenaka N., Takemura T., *Bull. Chem. Soc. Jpn.*, **1999**, Vol. 72, 1997.

30 - Baj S., Krawczyk T., Staszewska K., *Lum.*, **2009**, Vol. 24, 348.

31 - Merényi G., Lind J., Eriksen T. E, *J. Biolum. Chemilum.*, **1990**, Vol. 5, 53.

32 - Albertin R., Arribas M. A. G., Bastos E. L., Röpke S., Sakai P. N., Sanches A. M. M., Stevani C. V., Umezu I. S., Yu J., Baader W. J., *Química Nova*, **1998**, Vol. 21 (6), 772.

33 - Hodgson E. K., Fridovich I., *Photochem. Photobiol.*, **1973**, Vol. 18, 451.

34 - McMurray H. N., Wilson B. P., *J. Phys. Chem. A*, **1999**, Vol. 103 (20), 3955.

35 – Paradies H. H., *Ber. Bunsenges. Phys. Chem.*, **1992**, Vol. 96, 1027.

36 - Merényi G., Lind J. S., *J. Am. Chem. Soc.*, **1980**, Vol. 102, 5830.

37 - Baldwin J. E., Thomas R. C., Kruse L. I., Silberman L., *J. Org. Chem.*, **1977**, Vol. 42 (24), 3846.

37 - White E. H., Nash E. G., Roberts D. R., Zafiriou O. C., *J. Am. Chem. Soc.*, **1968**, Vol. 90 (21), 5932.

38 - White E. H., Roswell D. F., Zafiriou O. C., *J. Org. Chem.*, **1969**, Vol. 34 (8), 2462.

39 - Armarego W. L. F., Perrin D. D., *Purification of laboratory chemicals*, 4th ed., Butterworth Heinemann: Oxford ; Boston, 1996.

40 - Nakazono M., Hino T., Zaitsu K., *Journal of Photochemistry and Photobiology A: Chemistry*, **2007**, Vol. 186, 99.

41 - http://riodb01.ibase.aist.go.jp/sdbs/cgi-bin/direct_frame_top.cgi, benzamide's proton NMR spectrum, last checked May 15th 2010.

42 - http://riodb01.ibase.aist.go.jp/sdbs/cgi-bin/direct_frame_top.cgi, benzoic acid's proton NMR spectrum, last checked May 15th 2010.

43 – Succinic anhydride properties, last checked February 19th 2010, http://www.sigmaaldrich.com/catalog/ProductDetail.do?N4=239690|Aldrich&N5=Product%20No.|BRAND_KEY&F=SPEC.

44 - Gaussian 03, Revision C.02, M. J. Frisch, G. W. Trucks, H. B. Schlegel, G. E. Scuseria, M. A. Robb, J. R. Cheeseman, J. A. Montgomery, Jr., T. Vreven, K. N. Kudin, J. C. Burant, J. M. Millam, S. S. Iyengar, J. Tomasi, V. Barone, B. Mennucci, M. Cossi, G. Scalmani, N. Rega, G. A. Petersson, H. Nakatsuji, M. Hada, M. Ehara, K. Toyota, R. Fukuda, J. Hasegawa, M. Ishida, T. Nakajima, Y. Honda, O. Kitao, H. Nakai, M. Klene, X. Li, J. E. Knox, H. P. Hratchian, J. B. Cross, C. Adamo, J. Jaramillo, R. Gomperts, R. E. Stratmann, O. Yazyev, A. J. Austin, R. Cammi, C. Pomelli, J. W. Ochterski, P. Y. Ayala, K. Morokuma, G. A. Voth, P. Salvador, J. J. Dannenberg, V. G. Zakrzewski, S. Dapprich, A. D. Daniels, M. C. Strain, O. Farkas, D. K. Malick, A. D. Rabuck, K. Raghavachari, J. B. Foresman, J. V. Ortiz, Q. Cui, A. G. Baboul, S. Clifford, J. Cioslowski, B. B. Stefanov, G. Liu, A. Liashenko, P. Piskorz, I. Komaromi, R. L. Martin, D. J. Fox, T. Keith, M. A. Al-Laham, C. Y. Peng, A. Nanayakkara, M. Challacombe, P. M. W. Gill, B. Johnson, W. Chen, M. W. Wong, C. Gonzalez, and J. A. Pople, Gaussian, Inc., Wallingford CT, 2004.

45 – a) Perdew J. P., Burke K., Ernzerhof M., *Phys. Rev. Lett.*, **1996**, Vol. 77, 3865; b) Perdew J. P., Burke K., Ernzerhof M., *Phys. Rev. Lett*., **1997**, Vol. 78, 1396.

46 - (a) Becke A. D., *J. Chem. Phys.*, **1993**, Vol. 98, 5648; (b) Stephens P. J., Devlin F. J., Ashvar C. S., Chabalowski C. F., Frisch M. J., *Faraday Discuss.*, **1994**, Vol. 99, 103; (c) Stephens P. J., Devlin F. J., Chabalowski C. F., Frisch M. J. J., *Phys. Chem.*, **1994**, Vol. 98, 11623; (d) Lee C., Yang W., Parr R. G., *Phys. Rev.*, **1988**, Vol. 37, 785.

47 - http://wanglab.bu.edu/g03guide/G03Guide/www.gaussian.com/g_ur/k_dft.htm, DFT methods used, last checked February 4th 2010.

48 - Jensen F., Introduction to Computational Chemistry, Wiley, 2nd Edition, England, 2006.

49 – Tomasi J., Persico M., *Chem. Rev.*, **1997**, Vol. 94, 2027.

50 – Barone V., Cossi M., *J. Phys. Chem.*, **1998**, Vol. 102, 1995.

51 – http://en.wikipedia.org/wiki/Carbon-nitrogen_bond, CN bond distances (average values), last checked February 6th, 2010.

52 – Moyon N. S., Chandra A. K., Mitra S., *J. Phys. Chem. A*, **2010**, Vol. 114, 60.

53 - Pérez-Ruiz R., Fichtler R., Miara Y. D., Nicoul M., Schaniel D., Neumann H., Beller M., Blunk D., *J. Fluoresc.*, **2010**, Published Online.

54 - http://en.wikipedia.org/wiki/Aniline, aniline's pK_a, last checked April 25th 2010.

55 – Costa S. M. B., Introdução à Fotoquímica Molecular, Instituto Superior Técnico, 1972.

56 - http://en.wikipedia.org/wiki/Solvent, solvent dielectric constants, last checked April 24th, 2010.

57 - http://riodb01.ibase.aist.go.jp/sdbs/cgi-bin/direct_frame_top.cgi, luminol's IR spectrum, last checked April 24th 2010.

58 – a) http://www.chem.ucla.edu/~webspectra/irtable.html, IR spectra peak assignment 1; b) http://wwwchem.csustan.edu/Tutorials/infrared.htm IR spectra peak assignment 2; http://orgchem.colorado.edu/hndbksupport/specttutor/irchart.html, IR spectra peak assignment 3, all checked April 24th 2010.

59 – Valeur B., Molecular Fluorescence, **2002**, Wiley-VCH.

60 – Romão Dias A. R., da Silva J. J. R. F., Calhorda M. J., Veiros L. F., Salema M. M., *Ligação Química*, **2006**, ISTPress.

61 - http://en.wikipedia.org/wiki/Carboxylic_acid, carboxylic groups typical acidity, last checked May 18th 2010.

62 - http://en.wikipedia.org/wiki/Perfluoroalkane, perfluoroalkanes properties, last checked May 18th 2010.

Annex

Annex 1 - NMR Spectra of BnLum

The collected NMR spectra for BnLum are presented below.

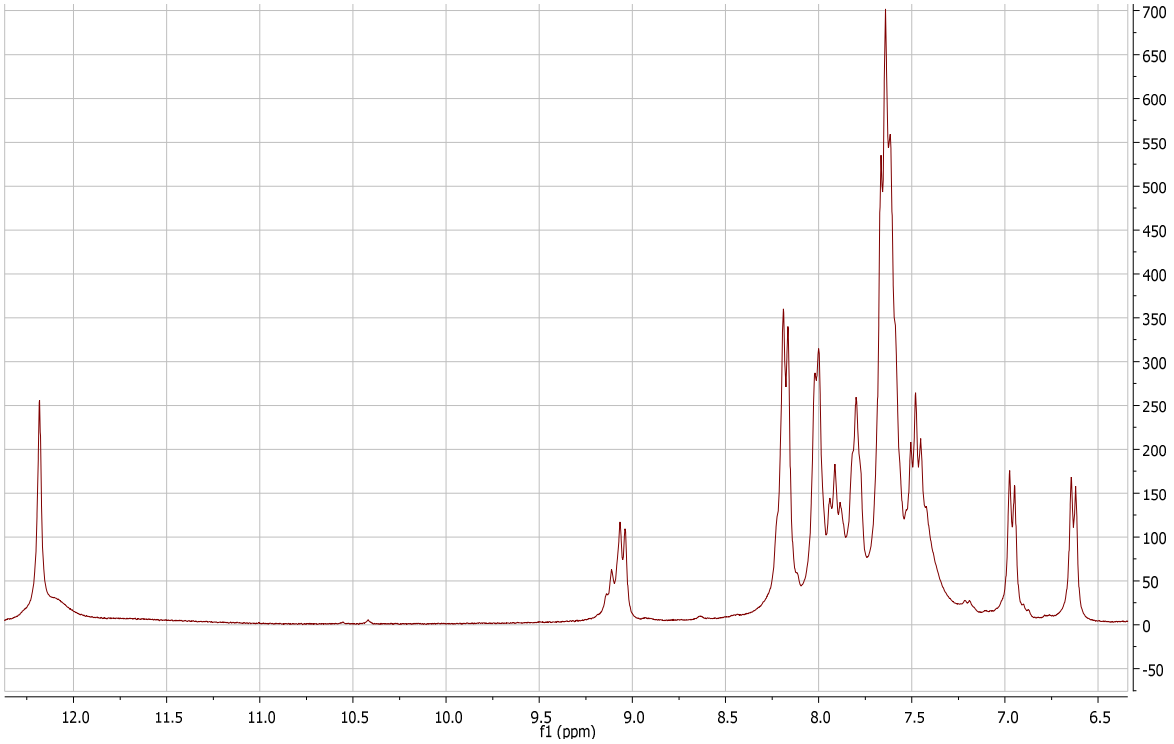

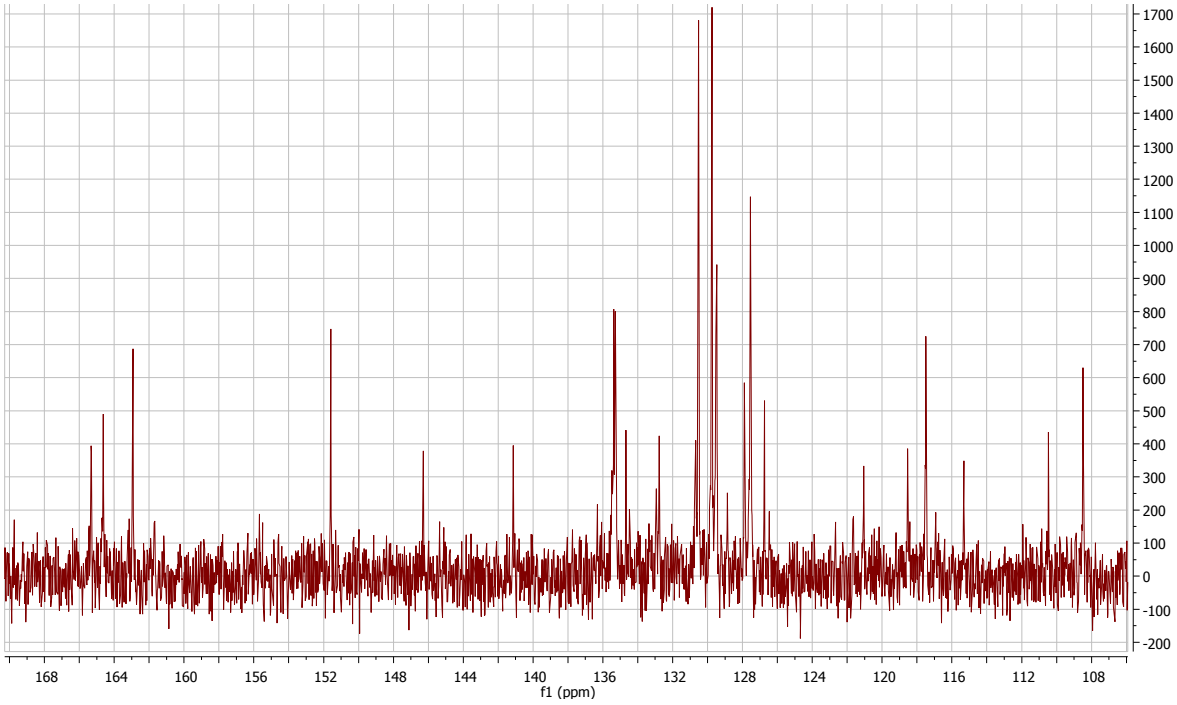

Annex 2 - NMR Spectra of ECLum

The collected NMR spectra for ECLum are presented below.

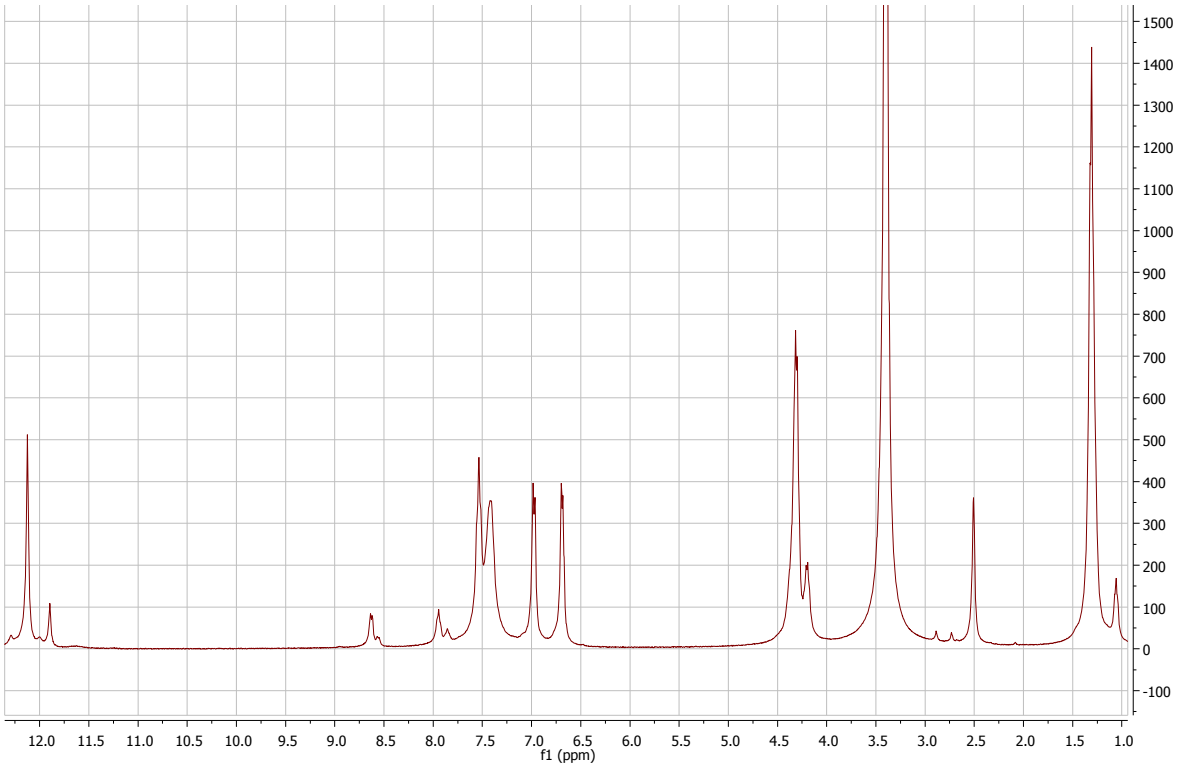

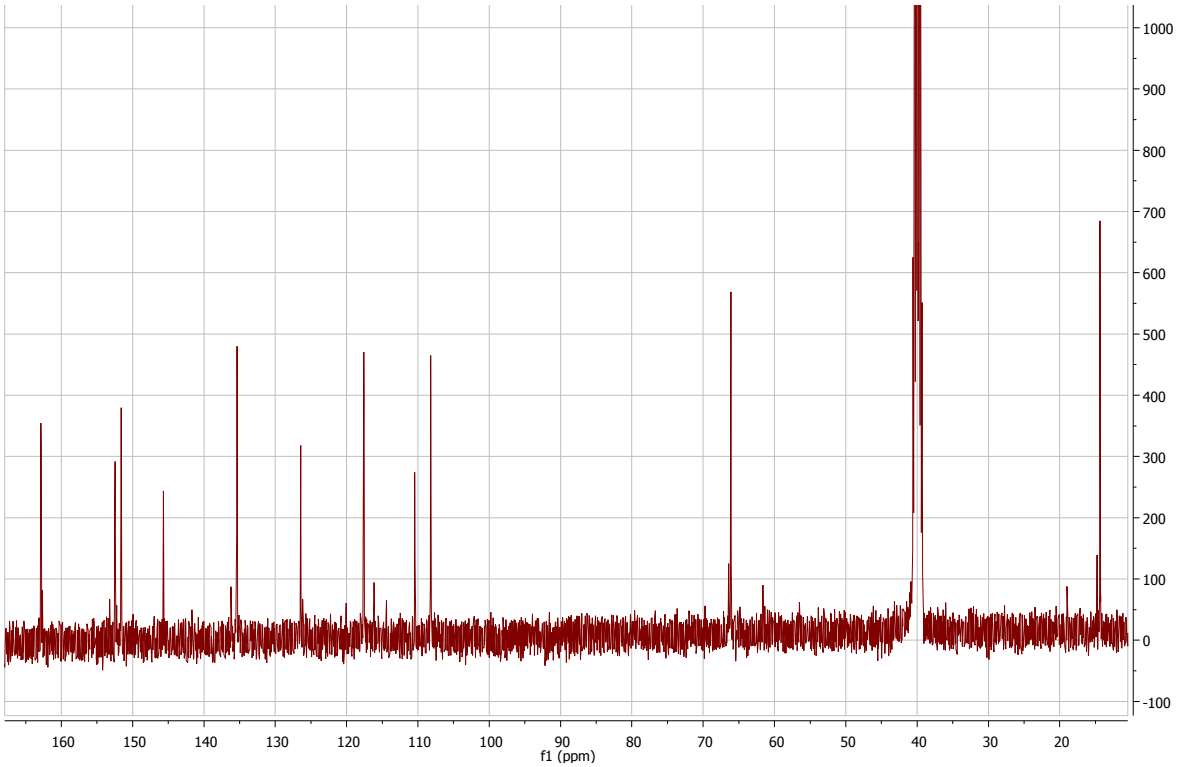

Annex 3 - NMR Spectra of TFALum

The collected proton and carbon NMR spectra for TFALum are presented below.

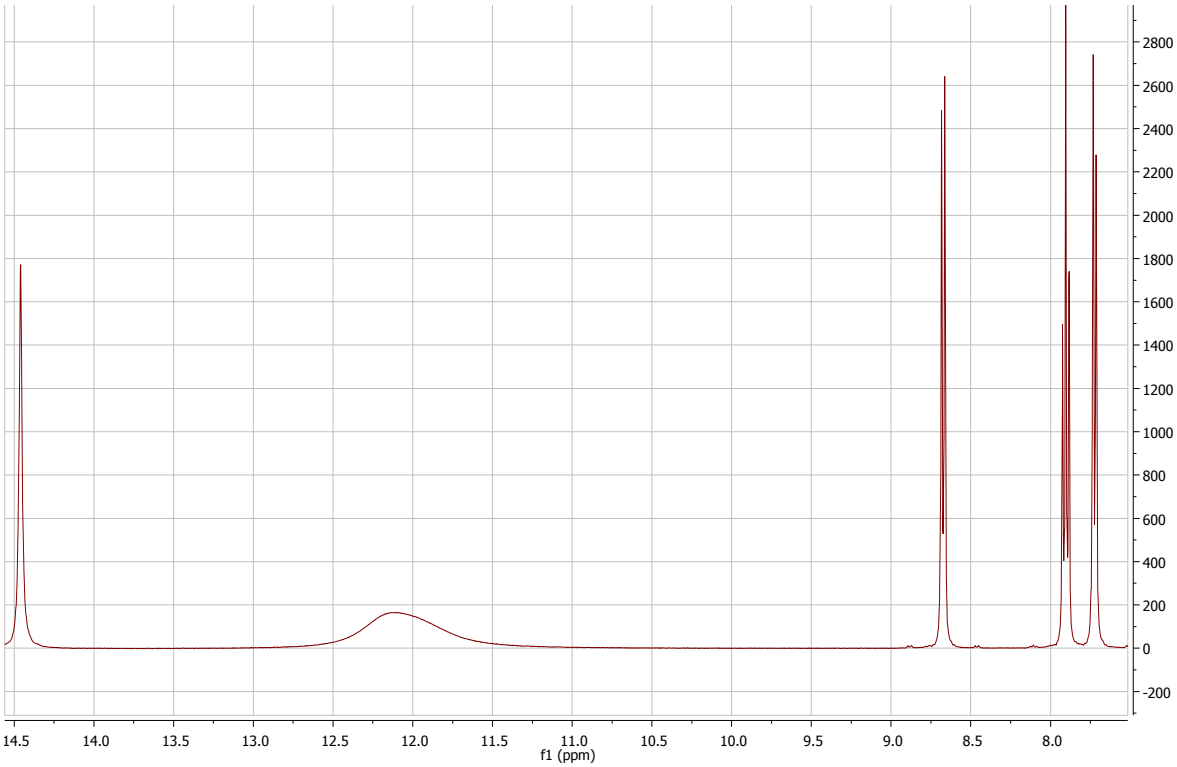

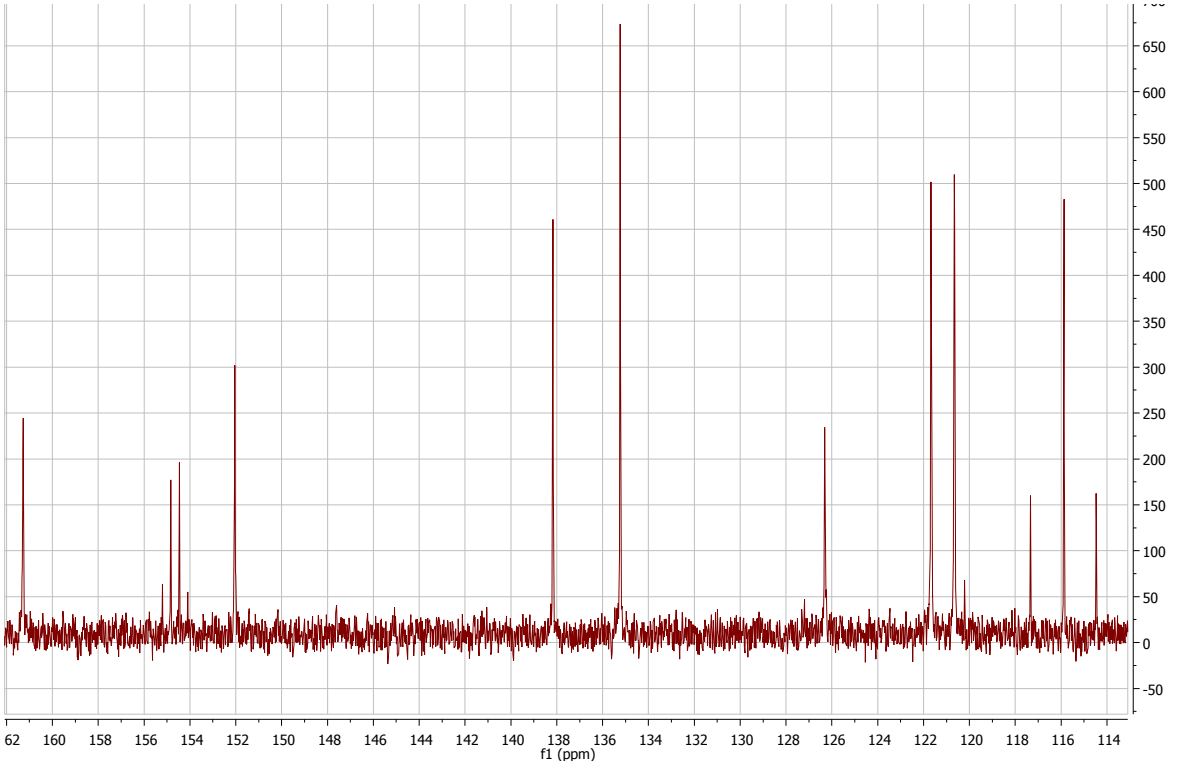

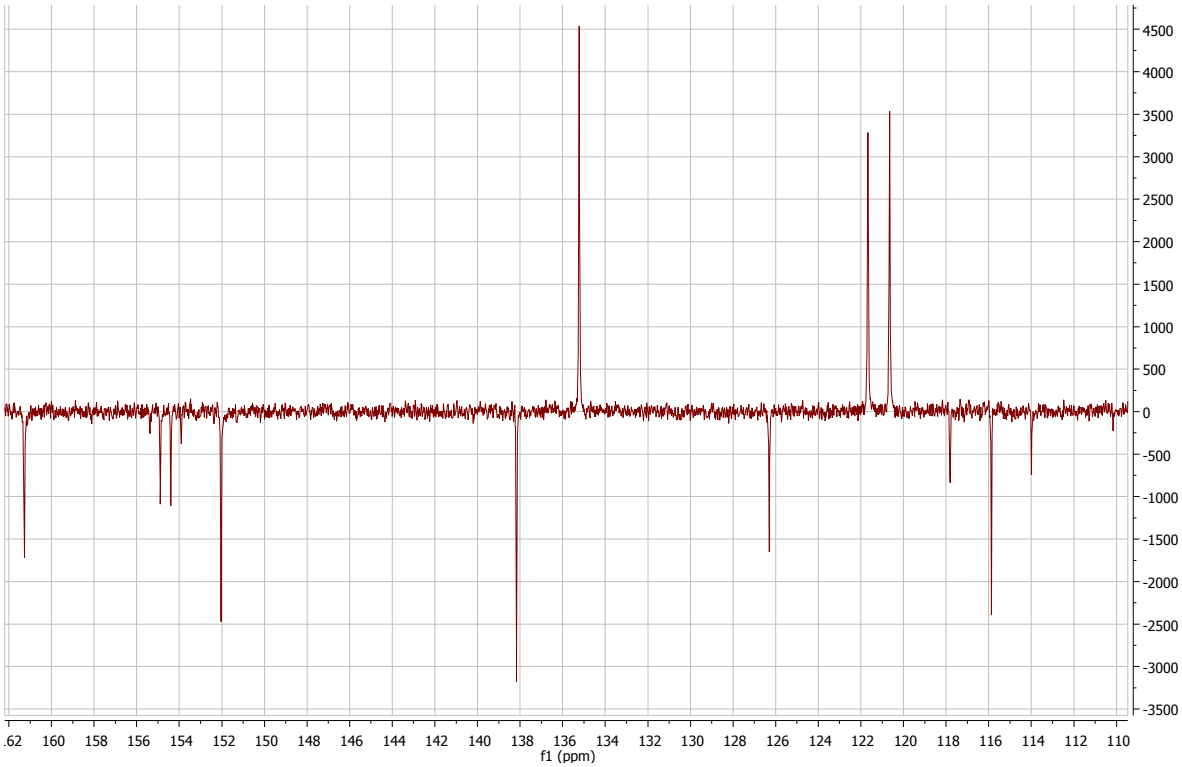

Annex 4 - NMR Spectra of DMULum's

The collected proton and carbon NMR spectra for DMU1Lum are presented below.

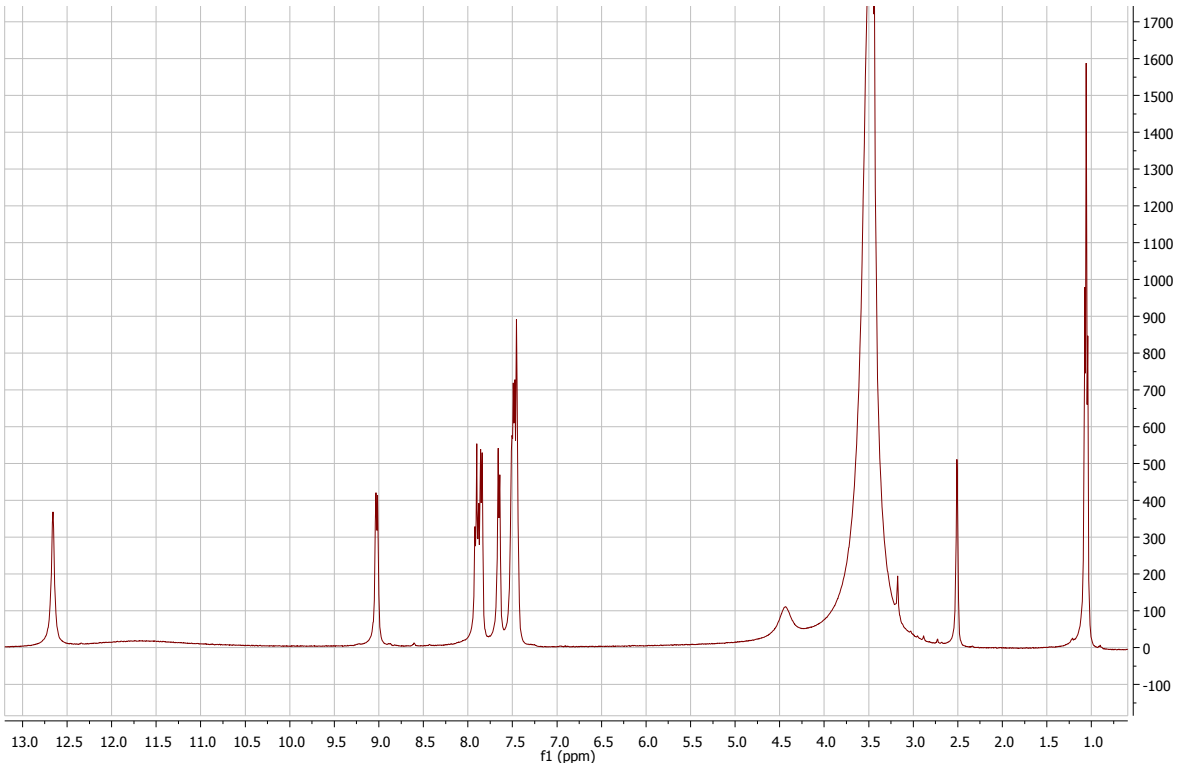

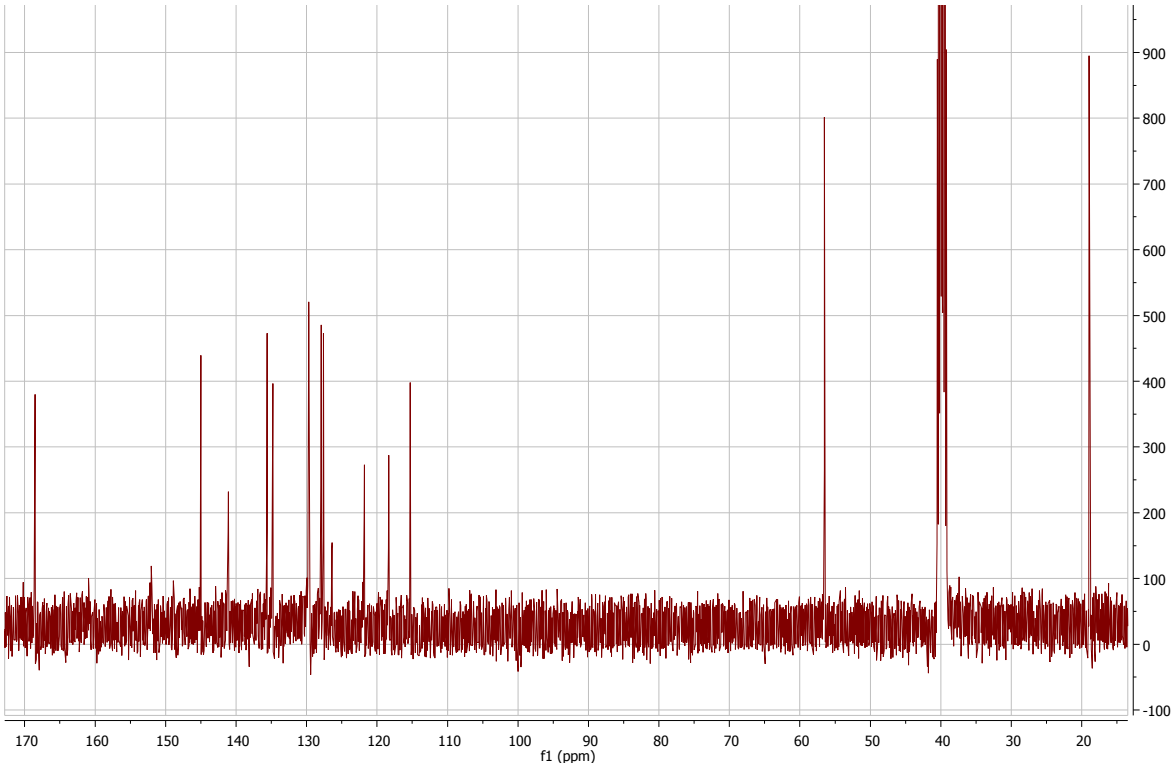

The collected proton and carbon NMR spectra for DMU2Lum are presented below.

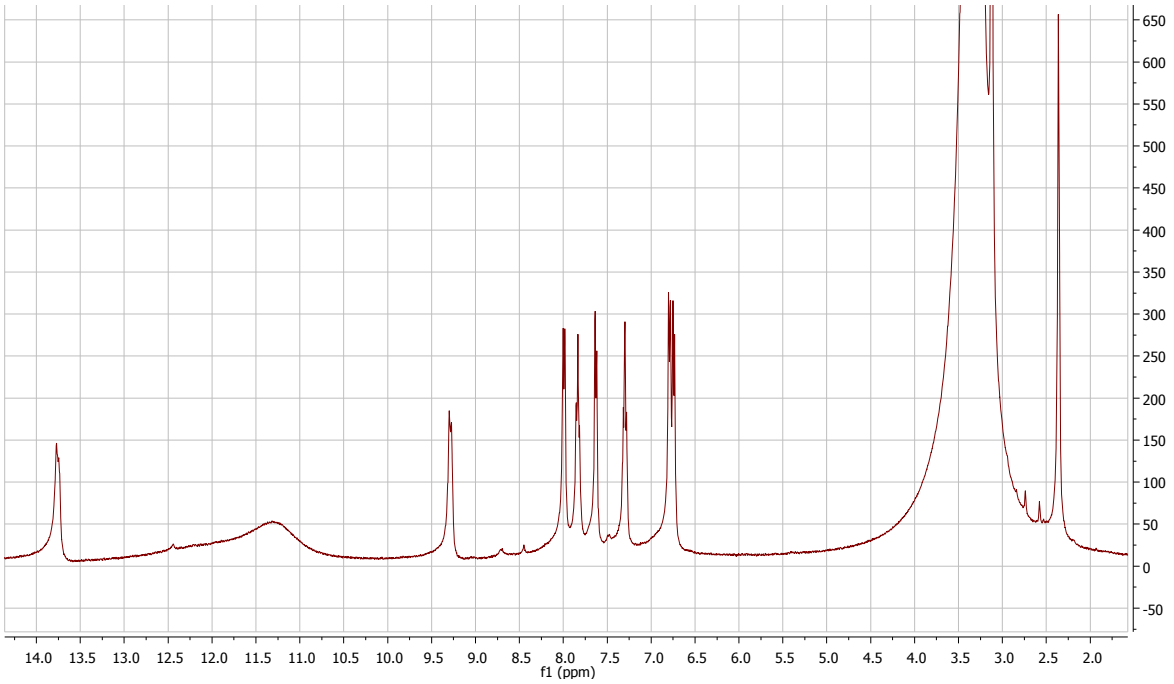

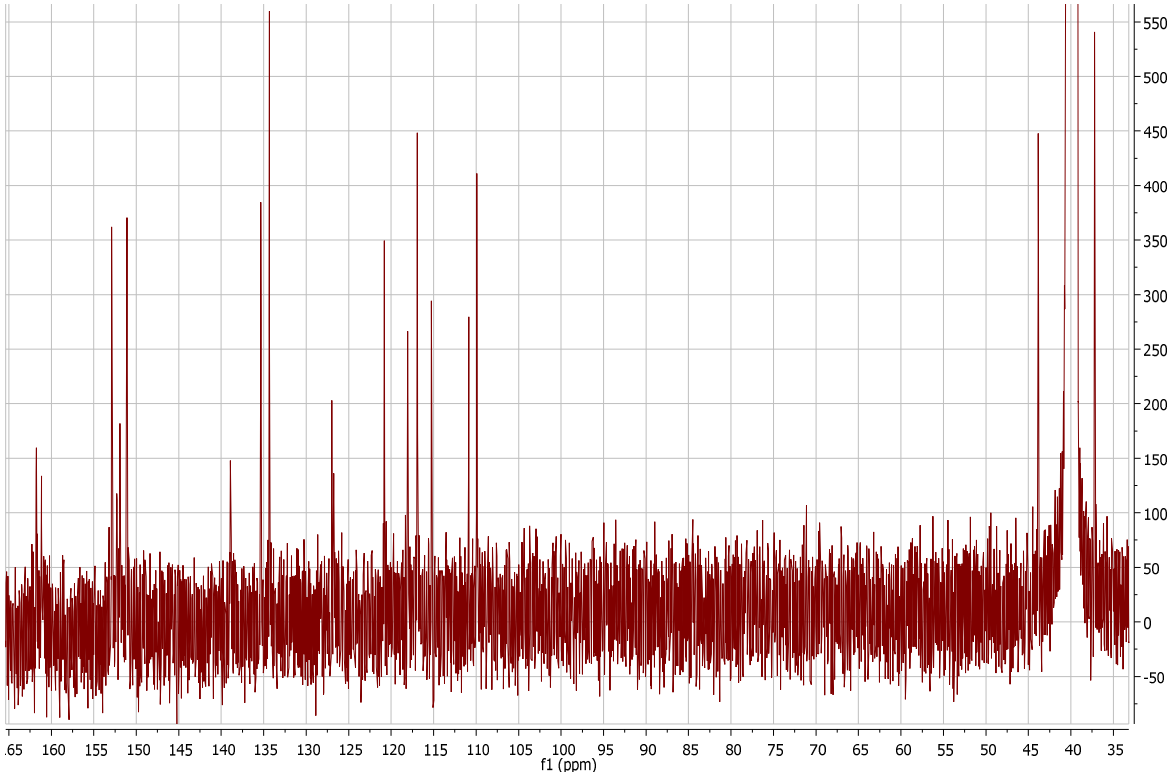
550
500
450
400
350
300
250
200
150
100
50
0
-50
.65 160 155 150 145 140 135 130 125 120 115 110 105 100 95 90 85 80 75 70 65 60 55 50 45 40 35
f1 (ppm)

Annex 5 - Tautomer B optimized geometries

Tables with bond distances (in Å) for all geometry optimizations performed and for averaged experimental (solid state determined geometry) bond distances. Atom labelling respects Figure 5.2.

Bond (A)	Experimental	PBE1PBE			B3LYP		
		6-31G**	6-311++G**	cc-pVTZ	6-31G**	6-311++G**	cc-pVTZ
C1-H1	0.950	1.087	1.086	1.084	1.087	1.085	1.083
C1-C2	1.372	1.387	1.385	1.381	1.390	1.388	1.384
C1-C6	1.398	1.407	1.405	1.402	1.410	1.408	1.405
C2-H2	0.950	1.086	1.085	1.084	1.086	1.084	1.082
C2-C3	1.377	1.391	1.389	1.386	1.394	1.392	1.388
C3-H3	0.949	1.083	1.082	1.080	1.082	1.081	1.078
C3-C4	1.396	1.394	1.392	1.390	1.398	1.396	1.393
C4-C7	1.442	1.447	1.445	1.443	1.451	1.450	1.447
C4-C5	1.415	1.412	1.411	1.407	1.418	1.417	1.413
C5-C8	1.451	1.458	1.457	1.455	1.464	1.463	1.460
C5-C6	1.413	1.423	1.421	1.419	1.427	1.425	1.423
C6-N2	1.366	1.351	1.353	1.348	1.360	1.361	1.356
N2-H6	0.976	1.003	1.004	1.001	1.006	1.005	1.002
N2-H7	1.085	1.015	1.014	1.012	1.016	1.014	1.011
C7-O2	1.338	1.346	1.346	1.345	1.355	1.356	1.354
C7-N1	1.289	1.288	1.284	1.282	1.292	1.287	1.284
O2-H5	0.937	0.967	0.964	0.964	0.970	0.967	0.966
N1-N3	1.372	1.353	1.351	1.349	1.366	1.363	1.361
N3-H4	0.878	1.009	1.009	1.007	1.011	1.010	1.007
N3-C8	1.339	1.370	1.369	1.365	1.378	1.377	1.372
C8-O1	1.263	1.238	1.233	1.232	1.242	1.237	1.236

Bond (A)	Experimental	HF			MP2	
		6-31G**	6-311++G**	cc-pVTZ	6-31G**	6-311++G**
C1-H1	0.950	1.076	1.076	1.074	1.084	1.088
C1-C2	1.372	1.377	1.377	1.373	1.395	1.399
C1-C6	1.398	1.401	1.400	1.397	1.404	1.406
C2-H2	0.950	1.076	1.076	1.074	1.083	1.087
C2-C3	1.377	1.387	1.387	1.383	1.389	1.393
C3-H3	0.949	1.071	1.071	1.069	1.080	1.084
C3-C4	1.396	1.382	1.381	1.379	1.402	1.406
C4-C7	1.442	1.463	1.463	1.461	1.441	1.442
C4-C5	1.415	1.403	1.402	1.398	1.416	1.420
C5-C8	1.451	1.471	1.471	1.469	1.465	1.467
C5-C6	1.413	1.411	1.410	1.408	1.422	1.424
C6-N2	1.366	1.357	1.361	1.357	1.375	1.378
N2-H6	0.976	0.991	0.992	0.989	1.007	1.010
N2-H7	1.085	0.995	0.995	0.992	1.013	1.016
C7-O2	1.338	1.336	1.335	1.334	1.360	1.356
C7-N1	1.289	1.258	1.255	1.253	1.304	1.302
O2-H5	0.937	0.946	0.944	0.944	0.970	0.967
N1-N3	1.372	1.359	1.357	1.355	1.366	1.361
N3-H4	0.878	0.993	0.993	0.990	1.010	1.013
N3-C8	1.339	1.352	1.352	1.349	1.376	1.378
C8-O1	1.263	1.213	1.208	1.208	1.246	1.239

Annex 6 - Energetic differences between luminol's tautomers

The difference in electronic energy between luminol's tautomers is presented in the following table. Values in kcal/mol (like in enthalpies table) and the nomenclature is analogous to the one presented in section 5.3 (like all tables presented in this second annex). OPT stands for geometry optimizations on MP2/6-31G** level of theory and SPE calculations (Gas, SCRF, DMSO or H_2O) for MP2/aug-cc-pVTZ level of theory

	MP2	Gas	DMSO	H_2O
A/B	4.89	6.83	-1.02	-1.14
A/C	1.03	2.69	-3.54	-3.48
A/D	-6.05	-3.33	-15.00	-14.93
A/E1	-45.62	-43.23	-44.06	-43.54
A/F	-40.40	-35.42	-45.21	-44.80
B/C	-3.87	-4.14	-2.52	-2.34
B/D	-10.94	-10.16	-13.98	-13.79
B/E1	-50.51	-50.05	-43.04	-42.40
B/F	-45.30	-42.25	-44.19	-43.66
C/D	-7.07	-6.01	-11.46	-11.45
C/E1	-46.65	-45.91	-40.52	-40.06
C/F	-41.43	-38.11	-41.67	-35.45
D/E1	-39.57	-39.90	-29.06	-28.61
D/F	-34.36	-32.09	-30.21	-29.87
E1/F	5.22	7.80	-1.15	-1.26

The enthalpy difference between all luminol's tautomers is given below.

	OPT	SPE
A/B	5.37	7.30
A/C	1.53	3.19
A/D	-5.01	-2.29
A/E1	-44.76	-42.36
A/F	-39.07	-34.09
B/C	-3.84	-4.11
B/D	-10.38	-9.59
B/E1	-50.12	-49.66
B/F	-44.44	-41.39
C/D	-6.54	-5.48
C/E1	-46.28	-45.55
C/F	-40.60	-37.28
D/E1	-39.74	-40.07
D/F	-34.06	-31.80
E1/F	5.68	8.27

The entropy difference between luminol's tautomers is given in the following table. Values in kcal.K^{-1}.mol^{-1}. These values come from geometry optimization calculations using 6-31G** basis set.

	MP2
A/B	0.192
A/C	-0.693
A/D	0.151
A/E1	-0.042
A/F	0.355
B/C	-0.885
B/D	-0.041
B/E1	-0.234

	MP2
B/F	0.163
C/D	0.844
C/E1	0.651
C/F	1.048
D/E1	-0.193
D/F	0.204
E1/F	0.397
---	---

Annex 7 - Luminol Acidity

The relationship between the ΔG and pK was deduced according to their definitions:

$$\Delta G = -RT\ log(K) = -RT\ log\left(10^{log_{10}(K)}\right) = -RT\ log(10)\ log_{10}(K) = RT\ pK\ log(10) \Leftrightarrow$$

$$\Leftrightarrow pK = \frac{\Delta G}{RT\ log(10)}$$

The next two tables present the result for acid-base parameters obtained by the calculations with 6-31G** as basis set using MP2.

MP2/6-31G**				
Structures In Equilibrium	$\Delta G_{tbutoxide}$ (kcal.mol^{-1})	$\Delta G_{hydroxide}$ (kcal.mol^{-1})	$pK_{hydroxide}$	$pK_{tbutoxide}$
Aα	-50.69	-85.86	-62.94	-37.15
Aδ	-53.19	-88.36	-64.77	-38.99
αε	58.01	22.84	16.74	42.52
αβ	59.20	24.02	17.61	43.39
βγ	154.04	118.87	87.13	112.91
δε	61.70	26.52	19.44	45.22
εγ	152.86	117.68	86.26	112.05
δζ	63.97	28.79	21.10	46.89
ζγ	150.59	115.42	84.60	110.38
Aη	-30.23	-65.40	-47.94	-22.16
ηβ	37.55	2.38	1.74	27.53
ηζ	41.01	5.83	4.28	30.06
Bα	-45.38	-80.55	-59.04	-33.26
Bν	49.93	14.76	10.82	36.60
νε	51.12	15.94	11.69	37.47
νξ	64.51	29.34	21.51	47.29
ξγ	139.46	104.29	76.44	102.23
Bo	-25.67	-60.84	-44.60	-18.81
oβ	38.30	3.13	2.29	28.08
oξ	52.89	17.71	12.98	38.76

Annex 8 – Excited State pK

$$(1) \qquad \Delta G_j^i = \Delta H_j^i - T\Delta S_j^i$$

Where i designates the electronic state considered, in the case, $i = 0{,}1$ and j is the species in analysis, HA or A^-. If $\Delta S_j^1 = \Delta S_j^0 = \Delta S_j$ and $\Delta H_j^1 = \Delta H_j^0 + \Delta E_j$, because $\Delta E_j = \frac{hc}{\lambda}$, then

$$(2) \qquad \Delta G^1 = \Delta G^* = \Delta G + \frac{hc\Delta\lambda}{\lambda_{HA}.\lambda_{A-}}$$

Here, $\Delta G^1 = \Delta G^*$ is the variation of Gibbs free energy of the acid-base reaction in the excited state, ΔG the same parameter for ground state acid-base reaction, h is Planck's constant, c the speed of light, λ_{HA} the wavelength associated with transition from ground to first excited state of the acid, λ_{A-} the wavelength associated with the transition from ground to first excited state of the base compound and $\Delta\lambda$ the difference of the gaps of the first excited state and ground state for the base and the acid species in wavelength $(\lambda_{A-} - \lambda_{HA})$.

Because

$$(3) \qquad \Delta G = -RTlog(K)$$

then

$$(4) \qquad pK^* = pK + \frac{hc\Delta\lambda}{\lambda_{HA}.\lambda_{A-}} \frac{1}{k_B T log(10)}$$

where k_B is Boltzmann's constant, T the absolute temperature (Kelvin) and $log(10)$ the natural logarithm.

Annex 9 - TD HF and TD DFT in Gas Phase

Tables with information regarding luminol's tautomers and conjugate bases for the first three electronic transitions using TD HF calculations and TD DFT in gas phase. Sp stands for species. Once again, TN stands for transition nature and Cont. for contamination of transition with other character.

Transition 1

Sp	Method	Phase	λ_{max} (nm)	F	TN	Orbitals
A	PBE1PBE	Gas	332.0	0.11	ππ* (Ring1) Cont.	43 - 48 46 - 47
	HF	Gas	273.8	0.17	πσ* (Ring1)	45 - 56,60 46 - 50,51
		DMSO	279.7	0.24	πσ* (Ring1)	46 - 47,48,54,55,57,64
B	HF	Gas	271.6	0.21	πσ*	44 - 56,61 46 - 52,56
		DMSO	277.2	0.30	πσ*	44 - 56,61 46 - 52,56
α	PBE1PBE	Gas	427.0	2.9×10^{-3}	ππ* (Ring1)	45 - 47
	HF	Gas	300.5	8.0×10^{-4}	ππ* (Ring2) Cont.	46 - 47,49,50,51,62,68
		DMSO	267.6	0.29	ππ* Cont.	44 - 61 45 - 53,54 46 - 53,54,55,56,57,58
δ	PBE1PBE	Gas	410.2	1.6×10^{-2}	ππ* (Ring2)	46 - 47,48
	HF	Gas	296.2	4.1×10^{-3}	½ πσ* ½ ππ*	45 - 47 46 - 47,49,50,51,63
		DMSO	273.6	0.28	πσ*	44 - 61 45 - 54 46 - 53,54,55,56,57
β	PBE1PBE	Gas	1100.4	0.0	ππ*	46 - 47
ε	PBE1PBE	Gas	1413.9	2.0×10^{-4}	ππ*	46 - 47
ζ	PBE1PBE	Gas	1332.6	1.0×10^{-4}	ππ* (Ring1)	46 - 47

Transition 2

Sp	Method	Phase	λ_{max} (nm)	f	TN	Orbitals
A	PBE1PBE	Gas	288.15	7.9×10^{-3}	ππ* Contaminated	42,43,44,45 - 47
	HF	Gas	241.75	1.5×10^{-3}	πσ* (Ring1)	45 - 50,51 46 - 54,56,57,60
		DMSO	244.6	4.6×10^{-3}	πσ* (Ring1)	45 - 50,51 46 - 54,56,57,58,60,61,81
B	HF	Gas	248.8	3.9×10^{-2}	πσ*	44 - 52 45 - 52 46 - 56,57,60,61
		DMSO	251.35	7.2×10^{-2}	πσ*	44 - 52 45 - 52 46 - 56,57,58,60,61
α	PBE1PBE	Gas	410.98	6.0×10^{-2}	ππ* (Ring1) Cont.	45 - 48,49
	HF	Gas	285.87	6.2×10^{-3}	ππ* Cont.	45 - 47 46 - 47,50
		DMSO	244.61	9.4×10^{-2}	ππ* Cont.	44 - 53,54,56,57 45 - 57,61 46 - 53,57,58,59,61,67
δ	PBE1PBE	Gas	399.07	5.25×10^{-2}	ππ* (Ring2) Cont.	46 - 47,48,49
	HF	Gas	287.94	4.2×10^{-3}	½ ππ* ½ πσ*	45 - 47 46 - 47,48,50,51
		DMSO	247.84	9.7×10^{-2}	πσ*	44 - 53,54,57 45 - 61 46 - 53,55,57,58,59,61,67
β	PBE1PBE	Gas	849.82	2.0×10^{-4}	ππ*	46 - 48
ε	PBE1PBE	Gas	1125.01	2.0×10^{-4}	ππ*	46 - 48
ζ	PBE1PBE	Gas	981.5	1.2×10^{-3}	ππ* (Ring1) Cont. πσ*	46 - 48,49

Transition 3

Sp	Method	Phase	λ_{max} (nm)	F	Nature Transition	Orbitals
A	PBE1PBE	Gas	276.7	1.5×10^{-2}	ππ* Cont.	43,44,45 - 47 43,44,45,46 - 48
	HF	Gas	212.1	7.0×10^{-4}	σσ*	42 - 50,51,56,60 43 - 50,51,56,60
		DMSO	210.6	1.1×10^{-2}	½ ππ* ½ πσ*	46 - 50,51,52,56
B	HF	Gas	217.2	7.0×10^{-4}	ππ* Cont.	46 - 47,49,57,59,63,64
		DMSO	217.8	2.2×10^{-3}	ππ* Cont.	46 - 47,48,53,55,56,57,59,64
α	PBE1PBE	Gas	383.8	6.2×10^{-3}	ππ* (Ring1) Cont.	45 - 48,49,50,51
	HF	Gas	276.5	0.17	ππ* (Ring2) Cont.	44 - 69 45 - 60 46 - 47,55,56,57,58,60,64,65,66,69
		DMSO	235.2	4.0×10^{-4}	ππ* Cont.	45 - 49 46 - 47,49,51,56,64
δ	PBE1PBE	Gas	368.4	2.5×10^{-3}	ππ* (Ring2) Cont.	46 - 48,49
	HF	Gas	279.1	0.18	πσ*	45 - 60 46 - 47,55,56,60,64,65,66
		DMSO	236.5	3.4×10^{-3}	πσ* Cont. ππ*	45 - 48,49 46 - 47,48,49,54,56,64
β	PBE1PBE	Gas	777.9	5.0×10^{-4}	πσ*	45 – 49 46 - 49
ε	PBE1PBE	Gas	827.5	2.0×10^{-3}	πσ*	46 - 49
ζ	PBE1PBE	Gas	891.2	3.0×10^{-4}	πσ* (Ring1) Cont. ππ*	46 - 48,49

Annex 10 - Molecular Orbitals involved in tautomer B transitions

The molecular orbitals of tautomer B involved in the three electronic transitions studied are presented below. The orbitals presented are named with their number and name (towards HOMO or LUMO). As a title of example, HOMO-1 (45) is the molecular orbital energetically below the HOMO having the number 45. The molecular orbitals are divided in two rows. The first row presents solely occupied molecular orbitals. The second row presents in the edges the two unoccupied molecular orbitals involved in tautomer's A transitions. All molecular orbitals are presented in the same view of luminol. The molecule representation (without any molecular orbital representation) is also presented in the second row of picture in the middle.

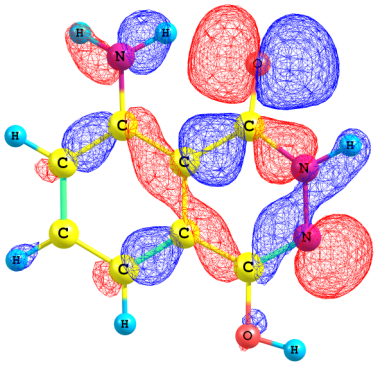

HOMO-3 (43)

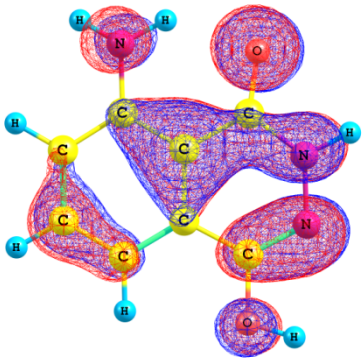

HOMO-1 (45)

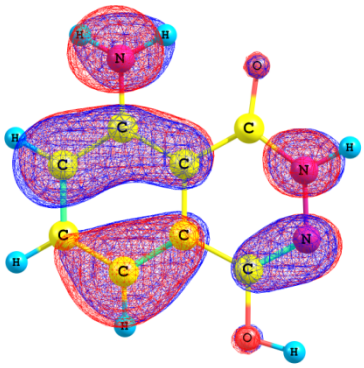

HOMO (46)

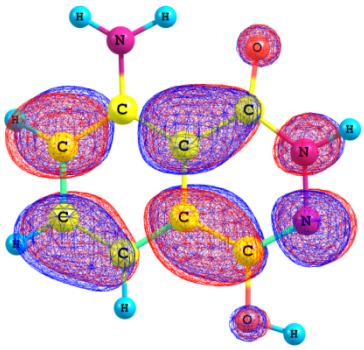

LUMO (47)

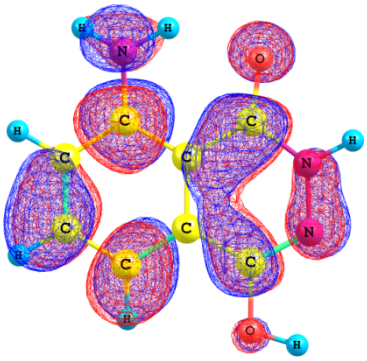

LUMO+1 (48)